

**ESTABLISHMENT OF HUMAN UMBILICAL CORD-DERIVED
MESENCHYMAL STROMAL CELLS EXPRESSING
INTERLEUKIN-12 AND ASSESSMENT OF THEIR EFFECT ON
LUNG ADENOCARCINOMA CELLS**

GOH JIUNN JYE

A dissertation submitted to the Department of Pre-clinical Sciences,

M. Kandiah Faculty of Medicine and Health Sciences,

UNIVERSITI TUNKU ABDUL RAHMAN,

In partial fulfilment of the requirements for the degree of

MASTER OF MEDICAL SCIENCE

2023

ABSTRACT

ESTABLISHMENT OF HUMAN UMBILICAL CORD-DERIVED MESENCHYMAL STROMAL CELLS EXPRESSING INTERLEUKIN-12 AND ASSESSMENT OF THEIR EFFECT ON LUNG ADENOCARCINOMA CELLS

Goh Jiunn Jye

Mesenchymal stromal cells (MSCs) are promising vehicles for cancer therapy due to their homing ability. They can be genetically manipulated through either non-viral or viral methods to express anti-cancer genes for cancer therapy. Interleukin-12 (IL-12) is one of the key immunomodulatory cytokines which has potential in antitumour effect. However, systemic administration of the cytokine at therapeutic dosage can lead to serious toxicity in the host system due to the high systemic level of interferon- γ (IFN- γ) induced by this strategy. In this study, we investigated the *in vitro* growth inhibition of genetically engineered human umbilical cord-derived mesenchymal stromal cells (hUCMSC) expressing IL-12 on human lung adenocarcinoma cells. The hUCMSC-IL12 were generated via adenoviral and electroporation method. Based on the results between the two methods, adenoviral method showed superior results in transfection efficiency (63.6%), post-transfection cell viability (82.6%) and hIL-12 protein expression (1.2×10^7 pg/ml). Thus, adenoviral vector was selected for the downstream experiments. Subsequently, hUCMSC-IL12 showed significant inhibition effect

on H1975 lung adenocarcinoma cells after 5 days of co-culture. No significant difference was observed for all other co-culture groups, indicating that the inhibition effect was because of hIL-12. Interestingly, cell viability of MRC-5 cells was significantly increased on day 5 after co-cultured with untransduced hUCMSC but not hUCMSC-IL12. The hIL-12 mRNA was upregulated significantly in hUCMSC-IL12 compared with untransduced hUCMSC leading to the exogenous expression of hIL-12 protein in the supernatant of hUCMSC-IL12. The hIL-12 protein expressed by hUCMSC-IL12 was 1.2 µg/ml on day 3 and increased to 2.2 µg/ml on day 5. Lastly, the integrity of hUCMSC-IL12 remained unaffected by the transduction through examination of their surface markers and differentiation properties. In conclusion, this study provided the proof of concept that hUCMSC can be genetically engineered to express hIL-12 and exert growth inhibition effect on human lung adenocarcinoma cells.

ACKNOWLEDGEMENT

First and foremost, I would like to express my sincere gratitude to my supervisor, Dr. Teoh Hoon Koon for her continuous support of my master study and research, for her patience, motivation and immense knowledge. Her valuable guidance helped me in all the time of research and writing of this dissertation.

Besides, I would also like to extend my gratitude to my co-supervisors, Associate Professor Dr. Ong Hooi Tin and Clinical Associate Professor Dr. Lee Bee Sun, for their insightful comments and motivation along the way of my research journey. In addition, I owe my deepest gratitude to Emeritus Prof. Dr. Cheong Soon Keng for his valuable comments and providing the inspiration for the completion of this project. Without his encouragement, guidance and support, this project would not be materialised.

I am extremely grateful to my parents, mother-in-law and siblings for their moral and emotional support. To my caring and super supportive husband, Mr. Jerry Pang Chong Yee, my deepest gratitude for your unconditional love, understanding and continuing support, letting me focus on my study and got through the hurdles. My sincere thanks and appreciation also go to my son and my daughter for their presence in my life. They are the greatest gifts of my life.

I am also very much thankful to Cryocord Sdn Bhd, for providing the funding and hUCMSC of this study.

Last but not least, I would like to convey my heartfelt appreciation to my seniors and labmates, Dr. Tan Yuen Fen, Ms. Lee Soke Sun, Ms. Lim Yee Ching, Dr. Erica Choong Pei Feng, Ms. Tai Lihui, Ms. Teh Hui Xin, Ms. Nalini, Mr. Looi Hong Keat, and everyone else in the postgraduate laboratories of M.

Kandiah Faculty of Medicine and Health Sciences, UTAR, for their guidance, assistance and stimulating discussions.

APPROVAL SHEET

This dissertation entitled “**ESTABLISHMENT OF HUMAN UMBILICAL CORD-DERIVED MESENCHYMAL STROMAL CELLS EXPRESSING INTERLEUKIN-12 AND ASSESSMENT OF THEIR EFFECT ON LUNG ADENOCARCINOMA CELLS**” was prepared by GOH JIUNN JYE and submitted as partial fulfilment of the requirements for the degree of Master of Medical Science at Universiti Tunku Abdul Rahman.

Approved by:

(Dr. Teoh Hoon Koon)

Date:

Assistant Professor / Supervisor

Department of Pre-clinical Sciences

M. Kandiah Faculty of Medicine and Health Sciences

Universiti Tunku Abdul Rahman

(Dr. Ong Hooi Tin)

Date:

Associate Professor / Co-supervisor

Department of Pre-clinical Sciences

M. Kandiah Faculty of Medicine and Health Sciences

Universiti Tunku Abdul Rahman

(Dr. Lee Bee Sun)

Date:

Clinical Associate Professor / Co-supervisor

Department of Medicine

M. Kandiah Faculty of Medicine and Health Sciences

Universiti Tunku Abdul Rahman

M. KANDIAH FACULTY OF MEDICINE AND HEALTH SCIENCES

UNIVERSITI TUNKU ABDUL RAHMAN

Date: _____

SUBMISSION OF DISSERTATION

It is hereby certified that Goh Jiunn Jye (ID no: 19UMM06154) has completed this dissertation entitled “ESTABLISHMENT OF HUMAN UMBILICAL CORD-DERIVED MESENCHYMAL STROMAL CELLS EXPRESSING INTERLEUKIN-12 AND ASSESSMENT OF THEIR EFFECT ON LUNG ADENOCARCINOMA CELLS” under the supervision of Dr. Teoh Hoon Koon (Supervisor), Associate Professor Dr Ong Hooi Tin (Co-supervisor) from the Department of Pre-clinical Sciences, M. Kandiah Faculty Medicine and Health Sciences and Clinical Associate Professor Dr Lee Bee Sun (Co-supervisor) from Department of Medicine, M. Kandiah Faculty Medicine and Health Sciences, Universiti Tunku Abdul Rahman.

I understand that university will upload softcopy of my dissertation in pdf format into UTAR Institutional Repository, which may be made accessible to UTAR community and public.

Yours truly,

(Goh Jiunn Jye)

DECLARATION

I, Goh Jiunn Jye hereby declare that the dissertation is based on my original work except for quotations and citations which have been duly acknowledged. I also declare that it has not been previously or concurrently submitted for any other degree at UTAR or any other institutions.

(GOH JIUNN JYE)

Date: _____

TABLE OF CONTENTS

ABSTRACT	ii
ACKNOWLEDGEMENT	iv
APPROVAL SHEET	vi
SUBMISSION OF DISSERTATION	viii
DECLARATION	x
LIST OF TABLES	xv
LIST OF FIGURES	xvi
LIST OF ABBREVIATIONS	xix
1.0 INTRODUCTION	1
1.1 General Objectives	4
1.2 Specific Objectives	4
2.0 LITERATURE REVIEW	5
2.1 Mesenchymal Stromal Cells (MSC).....	5
2.1.1 Historical Overview and Nomenclature of MSC	5
2.1.2 Sources of MSC.....	7
2.1.3 Homing ability	8
2.1.4 Factors Affecting MSC Homing Ability	10
2.1.5 MSC as Cellular Vehicles of Cytokines	12
2.1.6 Clinical Trials of Genetically Engineered MSC.....	15
2.2 Gene Delivery Systems	17
2.2.1 Viral Vectors	17
2.2.2 Non-viral Vectors	22
2.3 Interleukin-12 (IL-12).....	25
2.3.1 Discovery and Structures	25
2.3.2 Expression and Biological Function.....	26
2.3.3 Mechanisms of Action.....	27
2.3.4 Antitumour Effect.....	29
2.4 Cancer.....	33
2.4.1 Lung Cancer	35
2.4.2 Epidemiology of Lung Cancer	36

2.4.3 Risk Factors	41
3.0 MATERIALS AND METHODS	42
3.1 Experimental Design	42
3.2 Cell Culture	44
3.2.1 Human Umbilical Cord-derived Mesenchymal Stromal Cells (hUCMSC)	44
3.2.2 Human Embryonic Kidney 293 Cell Line (HEK 293)	45
3.2.3 Human Lung Adenocarcinoma Cell Line (H1975)	45
3.2.4 Human Lung Fibroblast Cell Line (MRC-5) (ATCC ® CCL-171™)	46
3.3 Characterisation of human Umbilical Cord-Derived Mesenchymal Stromal Cells (hUCMSC)	47
3.3.1 Immunophenotyping	47
3.3.2 Trilineage Differentiation	47
3.4 Plasmids	51
3.4.1 Plasmid Encoding hIL-12 Gene	51
3.4.2 Plasmid Encoding Green Fluorescence Protein (GFP)	54
3.5 Generation of Genetically Engineered Human Umbilical Cord-Derived Mesenchymal Stromal Cells Expressing Human Interleukin-12 (hUCMSC-IL12)	58
3.5.1 Adenoviral Method	58
3.5.2 Electroporation Method	77
3.6 Determination of Inhibition Effect of hUCMSC Expressing hIL-12 on Human Lung Cell Lines	78
3.7 Determination of hIL-12 mRNA Expression of Transduced hUCMSC	80
3.7.1 Total Ribonucleic Acid (RNA) Extraction	80
3.7.2 DNase I Treatment of RNA and Reverse Transcription of RNA to cDNA	81
3.7.3 Quantitative Real-Time PCR	82
3.8 Statistical Analysis	83
4.0 RESULTS	84
4.1 Characterisation of hUCMSC	84
4.1.1 Immunophenotyping	84
4.1.2 Trilineage Differentiation	85

4.2 Generation of Genetically Engineered Human Umbilical Cord-Derived Mesenchymal Stromal Cells Expressing Human Interleukin-12 (hUCMSC-IL12) Using Adenoviral Method	90
4.2.1 Amplification of hIL-12 gene	90
4.2.2 Screening of clones using PCR.....	91
4.2.3 Restriction Analysis of Recombinant Plasmids.....	93
4.2.4 Sequencing Analysis of Recombinant Plasmids.....	95
4.2.5 Digestion of Recombinant Plasmids with PacI Restriction Enzyme	95
4.2.6 Packaging of AdenoX Recombinant Viruses	96
4.2.7 Primary Amplification of AdenoX Recombinant Viruses....	100
4.2.8 Titration of Recombinant Adenovirus	102
4.2.9 High Titer Amplification of AdenoX Recombinant Viruses	107
4.2.10 Verification of Recombinant Adenovirus Construct	110
4.2.11 Functional Titer of AdhIL-12 and AdlacZ	111
4.3 Comparison between Viral and Non-viral Method in Generation of hUCMSC Expressing hIL-12	114
4.3.1 Transfection Efficiency	114
4.3.2 Expression of hIL-12 Protein.....	115
4.3.3 Cell Viability of hUCMSC Post-transfection	116
4.4 Determination of Inhibition Effect of hUCMSC Expressing hIL-12 on Human Lung Cell Lines	117
4.5 Determination of hIL-12 Protein Expression Level in Co-culture Experiment	119
4.6 Determination of hIL-12 mRNA Expression Level of hUCMSC-IL12	121

5.0 DISCUSSION..... 123

5.1 Comparison of viral and non-viral method in generation of hUCMSC-IL12	123
5.2 Characterisation of hUCMSC and hUCMSC-IL12.....	126
5.3 The Direct Inhibition Effect of hUCMSC-IL12 on H1975 Human Lung Adenocarcinoma Cells	128
5.4 Co-culture of hUCMSC and Genetically Engineered hUCMSC with MRC-5 Human Lung Fibroblasts.....	133

6.0 CONCLUSIONS..... 136

6.1 CONCLUSION	136
----------------------	-----

6.2 RECOMMENDATIONS OF FUTURE RESEARCH.....	138
REFERENCES	140
APPENDIX A.....	156
APPENDIX B	162

LIST OF TABLES

3.1	PCR mixture components.....	59
3.2	PCR cycle profile	59
3.3	PCR primer sequences	59
3.4	In-Fusion cloning reaction	61
3.5	PCR mixture components.....	62
3.6	PCR Thermal cycling	62
3.7	Expected results of PCR colony screening analysis.....	63
3.8	Primer sequence for Sanger sequencing.....	64
3.9	Digestion set-up for restriction enzyme PacI	65
3.10	Components of solution A and B	67
3.11	Control and sample dilutions for qPCR	68
3.12	Thermal cycling conditions for qPCR using ABI StepOnePlus Real-Time PCR System	69
3.13	PCR mixture components for recombinant adenovirus construct verification	71
3.14	PCR Thermal cycling	71
3.15	Expected band sizes of PCR products.....	71
3.16	Experimental groups of co-culture experiment.....	79
3.17	Reaction components of qPCR for mRNA expression.....	82
3.18	Primers of qPCR for mRNA expression	83
3.19	Thermal cycler parameters for mRNA expression.....	83
4.1	Concentration and purity of the extracted DNA	91
4.2	Concentration and purity of the extracted recombinant plasmid DNA... 93	
4.3	Expected fragment sizes in recombinant pAdenoX vectors digested with NheI or XhoI	94
4.4	Concentration and purity of the extracted plasmid DNA.....	96
4.5	Ct value for control dilutions	103
4.6	Ct value and copy number of samples with different dilutions.....	104
4.7	Ct value for control dilutions	105
4.8	Ct value and copy number of samples with different dilutions.....	107
4.9	Size of gene of interest	111
4.10	Functional titer of AdhIL-12 and AdlacZ	114

LIST OF FIGURES

Figure	Page
2.1 Mesenchymal stem cells sources.....	7
2.2 The homing mechanisms of MSC.....	10
2.3 Three generations of adenoviral vectors.	19
2.4 Cellular sources and responders of IL-12 along with their respective functions.	27
2.5 Mechanism of actions of IL-12.....	29
2.6 Overview of the biological functions of IL-12 contributing to its antitumour effects.....	30
2.7 National Ranking of Cancer as a Cause of Death at Ages <70 years in 2019.....	34
2.8 Histologic classification of lung cancer.....	36
2.9 Distribution of Cases and Deaths for the Top 10 Most Common Cancers in 2020 for (A) Both Sexes, (B) Men, and (C) Women.....	38
2.10 Region-Specific Incidence Age-Standardised Rates by Sex for Lung Cancer Among Men and Women in 2020.....	38
2.11 Ten most common cancers, all residents, Malaysia, year 2012-2016.....	39
2.12 Trachea, bronchus and lung: Comparison of age-standardised rate by year, major ethnic group and sex in Malaysia.....	40
2.13 Trachea, bronchus and lung: Staging percentage by sex, Malaysia, year 2012-2016.....	40
3.1 Experimental design flow chart of this study.....	43
3.2 Restriction map of pUNO1-hIL12 plasmid.....	52
3.3 Restriction map of pCMV-GFP plasmid.....	55
3.4 Process of recombinant adenovirus production.	58
3.5 Layout of the 6-well plate for plaque forming assay.	72
3.6 Layout of the 96-well plate for MOI optimisation assay.....	74
3.7 Timeline for co-culture experiment.....	78
4.1 Immunophenotyping of UCMSC.....	85
4.2 AdhIL-12 transduced UCMSC maintained cell surface markers similar to untransduced UCMSC. PerCP-Cy5.5 included CD90 and CD105 while APC included CD34 and CD45.....	85
4.3 Adipogenesis of hUCMSC.....	87
4.4 Osteogenic differentiation of hUCMSC.....	88
4.5 Chondrogenic differentiation of hUCMSC.....	89
4.6 Agarose gel electrophoresis image of PCR product of hIL-12 gene amplification.....	91
4.7 Agarose gel electrophoresis image of hIL-12 gene amplification.	92
4.8 Agarose gel electrophoresis of the recombinant pAdenoX digested with NhoI or XhoI restriction enzymes.....	94

4.9	Agarose gel electrophoresis of the recombinant pAdenoX digested with PacI restriction enzyme.....	96
4.10	HEK 293 cells transfected with pAdenoX-hIL12 observed under inverted microscope..	97
4.11	HEK 293 cells transfected with linearised pAdenoX-hIL12 observed under fluorescence microscope	98
4.12	HEK 293 cells transfected with pAdenoX-hIL12 observed under inverted microscope.	99
4.13	HEK 293 cells transfected with linearised pAdenoX-lacZ observed under fluorescence microscope.....	99
4.14	HEK 293 cells showed cytopathic effect after transduction with AdhIL-12.....	100
4.15	HEK 293 cells showed green fluorescence after transduction with AdhIL-12.....	101
4.16	HEK 293 cells showed cytopathic effect after transduction with AdlacZ.....	101
4.17	HEK 293 cells showed green fluorescence after transduction with AdlacZ.....	102
4.18	Standard curve of Adeno-X control titration.....	104
4.19	Standard curve of Adeno-X control titration.....	106
4.20	HEK 293 cells showed cytopathic effect after transduction with AdhIL-12.....	108
4.21	HEK 293 cells showed green fluorescence after transduction with AdhIL-12.....	108
4.22	HEK 293 cells showed cytopathic effect after transduction with AdlacZ (control).....	109
4.23	HEK 293 cells showed green fluorescence after transduction with AdlacZ (control).....	110
4.24	Agarose gel electrophoresis of PCR products of AdhIL-12 and AdlacZ.....	111
4.25	Functional titration of AdhIL-12.....	112
4.26	Functional titration of AdlacZ.....	113
4.27	Comparison of transfection efficiency between hUCMSC-IL12 generated by adenoviral vector and electroporation	115
4.28	Comparison of hIL-12 protein expression between hUCMSC-IL12 generated by adenoviral vector and electroporation	116
4.29	Comparison of hUCMSC viability post transfection between hUCMSC-IL12 generated by adenoviral vector and electroporation ...	117
4.30	Inhibition effect of hUCMSC-IL12 on H1975 lung adenocarcinoma cells.....	118
4.31	Inhibition effect of hUCMSC-IL12 on MRC-5 human normal lung fibroblast cells	119
4.32	Protein expression of hIL-12 in untransduced and hUCMSC-IL12 when co-cultured with H1975 cells.....	120

4.33	Protein expression of hIL-12 in untransduced and hUCMSC-IL12 when co-cultured with MRC-5 cells	120
4.34	<i>In vitro</i> mRNA expression of hIL-12 in hUCMSC-IL12 relative to untransduced hUCMSC.....	122

LIST OF ABBREVIATIONS

AAH	Atypical adenomatous hyperplasia
AAV	Adeno-associated viruses
ADCC	Antibody-dependent cellular cytotoxicity
Ad	Adenovirus
AIM	Adipogenic induction medium
AIS	Adenocarcinoma in situ
ATCC	American Type Culture Collection
BLAST	Basic local alignment search tool
CaCl ₂	Calcium Chloride
CaCl ₂ .2H ₂ O	Calcium chloride dihydrate
CAR	Chimeric antigen receptor
CCK-8	Cell Counting Kit-8
CD	Cluster of differentiation
cDNA	Complementary DNA
CFDA	China Food and Drug Administration
CLMF	Cytotoxic lymphocyte maturation factor
CNS	Central nervous system
CO ₂	Carbon Dioxide
COPD	Chronic obstructive pulmonary disease
COVID-19	Coronavirus disease 2019
CPE	Cytopathic effect
DAPI	4',6-diamidino-2-phenylindole
DC	Dendritic cells
DMEM	Dulbecco's Modified Eagle Medium
DMSO	Dimethyl sulfoxide
DNA	Deoxyribonucleic acid
EF-1 α	Elongation Factor-1 α
ELISA	Enzyme-linked immunosorbent assay
EMEM	Eagle's Minimum Essential Medium
FBS	Fetal Bovine Serum
FDA	Food and Drug Administration
G-CSF	Granulocyte colony-stimulating factor
GFP	Green Fluorescence Protein
GIT	Gastrointestinal tract
GM-CSF	Granulocyte-macrophage colony-stimulating factor
GMP	Good Manufacturing Practice
hAD-MSC	Human adipose-derived MSC
HBS	HEPES-buffered saline
HCl	Hydrochloric acid
HEPES	N-2-hydroxyethylpiperazine-N-2-ethane sulfonic acid
HGF	Hepatocyte growth factor
hIL-12	Human interleukin-12
HLA	Human leukocyte antigen
HNSCC	Head and neck squamous cell carcinoma
HSC	Haematopoietic stem cells
HSV-TK	Herpes simplex virus thymidine kinase
HTLV	Human T-Cell Leukaemia Virus

hUCMSC	Human umbilical cord-derived mesenchymal stromal cells
hUCMSC-IL12	Human umbilical cord-derived mesenchymal stromal expressing human IL-12
IEI	Inborn errors of immunity
IFN- γ	Interferon- γ
IFN- β	Interferon-beta
ifu	Infectious unit
IL-10	Interleukin-10
IL-12	Interleukin-12
IL-17	Interleukin-17
IL-18	Interleukin-18
IL-1 β	Interleukin 1 β
IL-2	Interleukin-2
IL-3	Interleukin-3
IL-35	Interleukin-35
IL-6	Interleukin-6
IL-7	Interleukin-7
IPF	Idiopathic pulmonary fibrosis
ISCT	International Society for Cellular Therapy
ITRs	Inverted terminal repeats
IT-tavo-EP	Intratumoral tavokinogene telseplasmid electroporation
IV	Intravenous
lacZ	β -galactosidase
LB	Luria-Bertani
MHC I	Major histocompatibility I
MIA	Minimally invasive adenocarcinoma
miRNA	Micro-RNA
MMPs	Matrix metalloproteinases
MOI	Multiplicity of Infection
mRNA	Messenger RNA
MSCs	Mesenchymal stromal cells
MSCs-GUSB	MSC to express therapeutic level of lysosomal enzyme β -glucuronidase
MTD	Maximum Tolerated Dosage
MTT bromide	3- [4,5-dimethylthiazol-2-yl]-2,5 diphenyl tetrazolium bromide
MV-NIS	Oncolytic measles viruses expressing thyroidal sodium iodide symporter
Na ₂ HSO ₄	Sodium Sulfate
NaCl	Sodium Chloride
NF- κ B cells	Nuclear factor kappa-light-chain-enhancer of activated B cells
NH ₄ OAc	Ammonium acetate
NK	Natural killer
NKSF	Natural killer cell stimulatory factor
NOD-SCID MPSVII	Non-obese diabetic severe combined immunodeficient mucopolysaccharidosis type VII
NSCLC	Non-small cell lung cancer
OIM	Osteogenic Induction Medium
OTC	Ornithine transcarbamylase

PAH	Pulmonary arterial hypertension
PBAE	Polymeric nanoparticles, β -amino esters
PBS	Phosphate-buffered saline
PCR	Polymerase chain reaction
PDGFB	Platelet-derived growth factor subunit B
PEG-3	Progression elevated gene 3
PEI	Polyethyleneimine
qPCR	Quantitative PCR
rhIL-12	Recombinant hIL-12
RNA	Ribonucleic Acid
ROS	Reactive oxygen species
RPMI	Roswell Park Memorial Institute
SADR	Severe adverse drug reaction
saRNA	Self-amplifying RNA
SCF	Stem cell factor
SD	Standard deviation
SDF-1	Stromal-derived factor-1
SOC	Super Optimal Broth
STAT1	Signal transducer and activator of transcription 1
TGF	Transforming growth factor
TGF- β	Transforming growth factor β 1
Th1	T helper type 1
TNF	Tumour necrosis factor
TNF- α	Tumour necrosis factor-alpha
TRAIL	Tumour necrosis factor (TNF)-related apoptosis-inducing ligand
WHO	World Health Organization
XSCID	X-linked severe combined immune deficiency

CHAPTER 1

INTRODUCTION

Mesenchymal stromal cells (MSCs), also known as mesenchymal stem cells, can be isolated from bone marrow, adipose tissues, umbilical cord and other tissues. MSCs are multipotent cells that can differentiate into multilineages. They are also self-renewable and culturally expandable *in vitro* with fewer ethical issues in comparison with embryonic stem cells, marking its suitability in cell therapy, regenerative medicine and tissue repairment (Ullah, Subbarao and Rho, 2015). There is still a lack of a single definition or quantitative assay to assist in the identification of MSCs in a mixed population of cells. However, the International Society for Cellular Therapy (ISCT) has recommended the minimum criteria to define MSCs. First, MSCs should exhibit plastic adherence. Second, MSCs must possess specific set of cell surface markers, e.g. cluster of differentiation (CD)73, CD90, CD105 and lack expression of CD14, CD34, CD45, CD19 and human leucocyte antigen-DR (HLA-DR). Third, MSCs must have the ability to differentiate *in vitro* into adipocytes, chondroblasts and osteoblasts (Dominici et al., 2006). These characteristics are valid for all MSCs although there might be some differences that exist in MSCs isolated from different tissue origins (Ullah, Subbarao and Rho, 2015).

Interleukin-12 (IL-12) is one of the key immunomodulatory cytokines which has potential in antitumour effect through a combination of immunostimulatory and anti-angiogenic mechanisms. It is a heterodimeric

cytokine comprising two different disulfide-linked subunits, namely p35 and p40 (Choi et al., 2011). IL-12 is naturally produced by activated macrophages and dendritic cells (DCs) (Choi et al., 2011). It induces interferon-gamma (IFN- γ) production by natural killer (NK) cells, T cells, dendritic cells (DCs) and activated macrophages which consequently triggers the release of anti-angiogenic chemokines CXCL9, CXCL10 and CXCL 11 (Airoldi et al., 2009). The anti-angiogenic effect of IL-12 is further enhanced by its ability to down-regulate the production of the pro-angiogenic molecules fibroblast growth factor 2 and vascular endothelial growth factor (Airoldi et al., 2009). In addition, IL-12 also stimulates the proliferation of NK cells and T cells and enhances the cytotoxic effects of NK cells and cytotoxic T cells by promoting the T helper type 1 (Th1) differentiation (Gambotto et al., 1999).

Previous studies have shown the promising antitumour effect of IL-12 either *in vitro* or *in vivo*. However, it is important to note that the systemic administration of the cytokine at therapeutic dosage can lead to serious toxicity in human cancer-bearing patients as well as in animal models due to the extremely high systemic level of interferon- γ (IFN- γ) induced by this strategy (Choi et al., 2011). A phase I clinical trial with dose escalation of human recombinant IL-12 administered intravenously into patients with advanced malignancies showed acceptable level of safety at Maximum Tolerated Dosage (MTD). In marked contrast to the phase I trial, patients in phase II trial suffered from severe toxicities following continuous multiple treatment of human recombinant IL-12 at MTD (Leonard et al., 1997).

Lung cancer is the leading cause of cancer worldwide and it accounts for one third of all the cancer-related deaths (Kolluri, Laurent and Janes, 2013). Non-small cell lung cancer (NSCLC) accounts for the majority of all the lung cancer cases and can be further classified into three types: squamous cell carcinoma, adenocarcinoma and large cell carcinoma (Zappa and Mousa, 2016). Out of the three types, adenocarcinoma is the most common type of lung cancer as it constitutes around 40% of all lung cancers.

In order to enhance the therapeutic application of IL-12, there is a need to overcome the associated systemic toxicities. Studies have shown that MSCs preferentially migrate to tumour microenvironment (Yuan, Kolluri, Sage, Gowers, & Janes, 2015). This study aimed to employ genetically engineered hUCMSC-IL12 as a cancer treatment without causing severe toxicities as compared to the systemic administrative approach. This study focused on the initial stage which is the proof of concept using *in vitro* setting. Therefore, the hypothesis of this study is the MSCs can be genetically engineered to provide paracrine secretion of IL-12 for *in vitro* growth inhibition of human lung adenocarcinoma cells. In this study, human umbilical cord-derived mesenchymal stromal cells (hUCMSC) were utilised as cellular vehicles to deliver IL-12 to lung adenocarcinoma cells. The hUCMSC were modified using both viral and non-viral vectors in order to determine the most efficient vector for IL-12 expression in hUCMSC. Lastly, the integrity of hUCMSC after the modification was also determined by examining their surface markers and trilineage differentiation properties.

1.1 General Objectives

The general objective of this study is to investigate the *in vitro* growth inhibition of human umbilical cord-derived mesenchymal stromal cells (hUCMSC) expressing human interleukin-12 (hIL-12) on human lung adenocarcinoma cell line.

1.2 Specific Objectives

The specific objectives of this study are as follows:

- (a) To generate hUCMSC expressing hIL-12 using non-viral method (electroporation) and viral method (adenoviral vector).
- (b) To compare the transfection efficiency, post-transfection cell viability and hIL-12 protein expression level of the hUCMSC-IL12 generated using the viral and non-viral methods.
- (c) To determine the surface markers and differentiation properties of genetically engineered hUCMSC-12.
- (d) To determine the *in vitro* growth inhibition of genetically engineered hUCMSC on H1975 lung adenocarcinoma cell line.

CHAPTER 2

LITERATURE REVIEW

2.1 Mesenchymal Stromal Cells (MSC)

2.1.1 Historical Overview and Nomenclature of MSC

Mesenchymal stromal cells (MSC) were first discovered in 1970s by Friedenstein and his colleagues (Friedenstein, Chailakhjan and Lalykina, 1970). In their pioneer studies, a subpopulation of adherent, fibroblast-like, clonogenic bone marrow-derived non-hematopoietic cells was isolated from mice and guinea pigs with potential in osteogenic, chondrogenic and adipogenic differentiation (Afanasyev, Elstner and Zander, 2009).

In the early 90s, Caplan coined the term "mesenchymal stem cells" due to the *in vitro* multipotency and self-renewal characteristics of these cells (Caplan, 1991). However, about 20 years later, Caplan proposed to change the name of MSC to "medicinal signalling cells" because he found that the cells homed to sites of injury or disease and performed secretory function of biofactors that showed immunomodulatory or regenerative effects rather than differentiation into regenerating tissue-producing cells. He further elaborated that the new tissue was in fact generated by patient's own site-specific or tissue-

specific resident stem cells as the results of stimulation by the biofactors secreted by MSC (Caplan, 2017).

There was no single definition to define MSC which led to confusion and difficulty in results comparison between clinical and non-clinical studies in the 1990s and 2000s (Mizukami and Swiech, 2018). Hence, a set of minimum criteria for MSC classification was proposed by the International Society of Cell and Gene Therapy (ISCT) in the year 2006 (Dominici et al., 2006). According to this widely adopted definition, MSC have to be able to 1) adhere to plastic; 2) differentiate into adipocytes, osteoblasts and chondrocytes when culture *in vitro*; 3) positive for CD105, CD73, and CD90 and negative for the expression of CD45, CD34, CD14 or CD11b, CD79 or CD19, and human leukocyte antigen class II (HLA class II). MSC of different origins have been shown to fulfill these minimal criteria though they often exhibited variation in their transcriptomic profiles (Kern et al., 2006a).

In 2019, ISCT updated the nomenclature with suggestion that the fibroblast-like plastic-adherent cells, regardless of their origins, be termed as multipotent mesenchymal stromal cells, while the term mesenchymal stem cells is only used for cells that meet specified stem cell criteria (Viswanathan et al., 2019). The three main criteria are as listed below:

- tissue of origins
- rigorous functional evidence *in vitro* and *in vivo* to demonstrate self-renewal and differentiation properties

- matrix of functional assays to demonstrate secretion of trophic factors, modulation of immune cells and other relevant properties including promoting angiogenesis

However, the acronym, MSC, is still commonly used for both cell populations under current practice.

2.1.2 Sources of MSC

Studies have shown that MSC can be extracted from various tissues such as bone marrow, umbilical cord Wharton's jelly, umbilical cord blood, placenta, amniotic fluid, breastmilk, dental pulp, adipose tissues, synovial membrane and many others as illustrated in Figure 2.1 (Musiał-Wysocka, Kot and Majka, 2019).

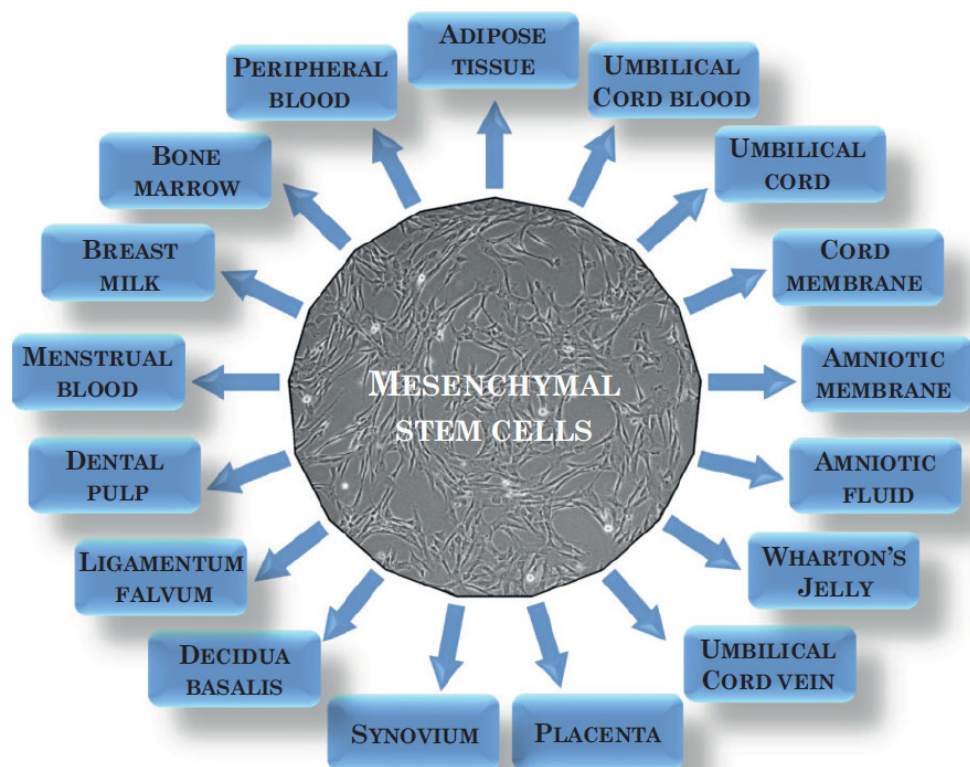


Figure 2.1 Mesenchymal stem cells sources. (Musiał-Wysocka et al., 2019)

Bone marrow was the first type of tissue used for the isolation of MSC. It is also known as the gold standard of MSC as it is the most used source of MSC (Musial-Wysocka et al., 2019). However, the collection method for bone marrow MSC is highly invasive and can cause pain to the donor. Bone marrow collection also requires advanced planning and scheduling as the procedure can only be conducted by a skillful medical officer. This increases the chances of last-minute consent withdrawal by the donor. Moreover, there is also risk of viral exposure due to donor's morbidity. Because of all these factors, alternative sources to isolate MSC are required.

In recent years, umbilical-cord derived MSC (UCMSC) have emerged as a promising source for MSC in research as well as in clinical applications. There are no ethical issues involved for UCMSC collection as the umbilical cord is treated as a biological waste. UCMSC are also readily available as they can be cryopreserved in advance (Ao et al., 2017). Studies have shown that UCMSC have higher proliferation rate compared to BMMSC (Kern et al., 2006b).

2.1.3 Homing ability

The most prominent feature of MSC is their homing ability. However, the exact mechanism has yet to be fully elucidated. In 2009, Karp and Teo defined MSC homing as the capture of MSC within the vasculature of a tissue followed by transmigration across the endothelium (Karp and Teo, 2009). In order to achieve therapeutic effect, MSC can be administered either systemically or directly to specific site, therefore it is essential to extend the definition of MSC

homing to encompass the mechanism. Nitzsche and his colleagues classified MSC homing into two categories, namely systemic and non-systemic homing. Non-systemic homing involves the interstitial migration of the locally transplanted MSC towards the site of injury/inflammatory which is guided by chemokine gradient released from the injured/inflamed tissues. On the other hand, systemic homing is a multistep process. First, MSC will be administered into the bloodstream, then continues with extravasation and chemokine guided interstitial migration to the injury/inflammatory site. Endogenous MSC can be recruited as well to the site of injury/inflammatory with an additional active intravasation step into the blood circulation (Nitzsche et al., 2017).

It was suggested that the mechanism of leucocyte homing can be the conceptual role model of MSC homing as the two cell populations shared many similarities (Henschler, Deak and Seifried, 2008). Hence, the mechanism of systemic homing of MSC can be further split into 5 steps: (1) tethering and rolling, (2) activation, (3) arrest, (4) transmigration or diapedesis, and (5) migration as illustrated in Figure 2.2 (Ullah, Liu and Thakor, 2019). The tethering step is initiated by the recognition and binding of MSC with the selectins expressed by the endothelial cells which subsequently caused the rolling of the cells along the vasculature wall (Sackstein et al., 2008). The second step, activation, is mediated by the chemokine receptors. This step plays an important role in increasing the affinity of integrins which is crucial for cell arrest (Constantin et al., 2000). The binding of integrins and its ligands on the endothelial cells occurs in the third step. In the transmigration step, MSC secrete matrix metalloproteinases (MMPs) to degrade the endothelial basement membrane thereby facilitates transcellular penetration of MSC through the

endothelial cells and basement membrane (Steingen et al., 2008). Finally, MSC can migrate to the site of injury/inflammation following the chemoattractive signals released by the injured/inflammatory tissues. It is noteworthy that tumours are considered as chronic inflammation (Peta, Ambele and Pepper, 2021). Therefore, the tropism of MSC to injured/inflammatory sites should include tumour sites as well.

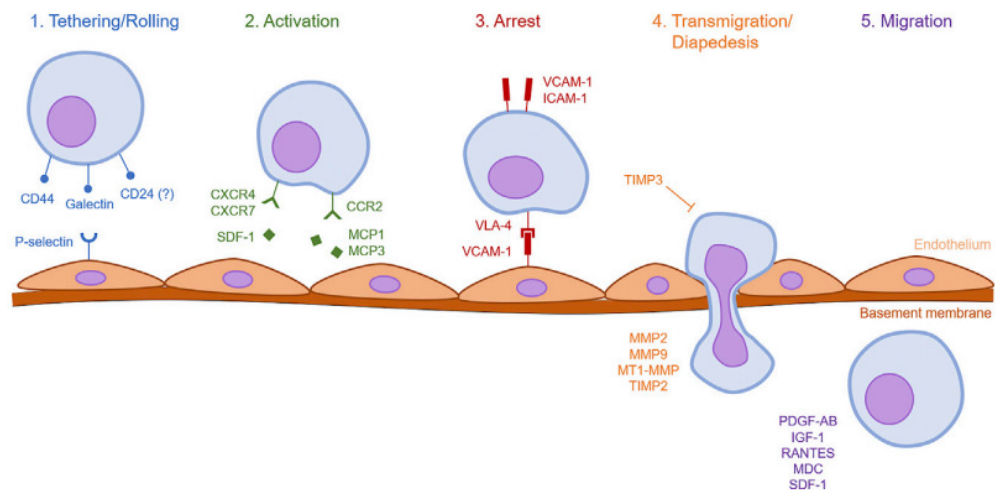


Figure 2.2 The homing mechanisms of MSC. (Ullah, Liu and Thakor, 2019)

2.1.4 Factors Affecting MSC Homing Ability

Numerous factors such as passage number of MSC, culture conditions, source of MSC, age of the donor and administration method can affect MSC homing capability. Rombouts *et al.* demonstrated that *in vitro* culture of MSC greatly reduced the homing efficiency of the cells in a syngeneic mouse model (Rombouts and Ploemacher, 2003). The study showed that the percentage of injected MSC found in the lymphohaematopoietic organs was reduced from 55-

65% for primary MSC to 10% for MSC that were cultured for 24 hours and further decreased to 0% when the cells were cultured for 48 hours prior to injection.

In vitro culture has been shown to cause MSC in either gaining or losing certain surface receptors which affect their homing ability. For example, the expression of CXCR4, a chemokine receptor for stromal-derived factor-1 (SDF-1) is lost during *in vitro* culture (Wynn et al., 2004). Interestingly, modification of culture condition by adding in a cocktail of cytokines such as interleukin-6 (IL-6), interleukin-3 (IL-3), stem cell factor (SCF), hepatocyte growth factor (HGF) (Shi et al., 2007) and under hypoxic (Schioppa et al., 2003) condition, can effectively restore the expression of CXCR4. In addition, the activity of matrix metalloproteinases (MMPs) which involved in transmigration step of MSC homing, can be upregulated by the presence of inflammatory cytokines such as transforming growth factor β 1 (TGF- β 1), interleukin 1 β (IL-1 β) and tumour necrosis factor-alpha (TNF- α) (Ries et al., 2007). Yu *et al.* demonstrated that combination of erythropoietin and granulocyte colony-stimulating factor (G-CSF) enhances the expression of MMP-2 and therefore promotes MSC homing capability (Yu et al., 2011).

Studies have shown that MSC derived from different sources exhibit phenotypic variation although they fulfill the minimal criteria of MSC definition under the ISCT guidelines. Furthermore, Kilpinen *et al.* have demonstrated that MSC isolated from older donors showed changes in the membrane glycerophospholipid composition which eventually diminished the functionality

of the MSC (Kilpinen et al., 2013). All these aspects influence the capability of MSC to migrate to the site of injury.

The next critical factor which affects MSC homing is the administration method. There are multiple routes of MSC administration and can be classified into two main categories, namely systemically or locally at the injury sites. Intravenous (IV) injection is the most common administration route (Kabat et al., 2020) because it is least invasive, convenient and easily reproducible. However, as the average size of MSC is bigger than pulmonary capillaries, a vast majority of the IV-injected MSC will get trapped within the capillaries in the lung (Schrepfer et al., 2007). Therefore, direct administration of MSC into the injury site or near to the injury site might achieve higher effectiveness. The types of local injection into tissue which have been reported in clinical trials included intra-cardiac, intra-articular, intra-muscular and intra-osseous injections (Kabat et al., 2020).

2.1.5 MSC as Cellular Vehicles of Cytokines

With traits such as migration to the sites of injury, immune evasion, wide availability and easy *in vitro* expansion, MSC have become suitable trojan horses for a variety of therapeutic agents (Niess et al., 2016). Generally, modification of MSC can be classified into 4 categories: 1) genetically modified to express cytokines or suicide genes; 2) loaded with oncolytic viruses; 3) primed with therapeutic drugs and 4) micro-RNA (miRNA) modified to produce MSC-derived microvesicles containing miRNA (Chulpanova et al., 2018).

Interleukin-12 (IL-12) is one of the key immunomodulatory cytokines which exert potential antitumour effect (Weiss et al., 2007). However, it is important to note that the systemic administration of this cytokine at therapeutic dosage can lead to serious toxicity in human cancer patients as well as in animal cancer models due to the extremely high systemic level of interferon- γ (IFN- γ) induced by this strategy (Choi et al., 2011). Hence, different groups of researchers investigated the effectiveness of MSC as the cellular vehicle for IL-12 in various cancer models.

MSC engineered to secrete IL-12 using lentiviral vector, showed they can inhibit lung adenocarcinoma cell migration and invasion *in vitro* (Li et al., 2015a). In contrast to our current study, Li *et al.* utilised adipose-derived MSC (AD-MSC) as the cell source for MSC. However, umbilical cord-derived MSC which was utilised in our study may be a better choice due to their non-invasive collection method, and higher proliferation rate compared to AD-MSC. As compared to lentiviral vector, the usage of adenoviral vector in our study may be a safer and less risky option as it is not integrated into the host genome.

In addition, Han *et al.* demonstrated the effectiveness of genetically modified MSC by lentivirus-mediated IL-12 in the inhibition of the growth of malignant ascites in mice (Han et al., 2014). When MSC co-expressed high levels of IL-12 and interleukin-7 (IL-7) simultaneously, they exhibited

efficiency in modulating the immunosuppressive microenvironment of glioblastoma (Mohme et al., 2020).

Interleukin-18 (IL-18) was reported to enhance the antitumour effect of NK cells (Ni et al., 2012). Liu *et al.* generated MSC expressing IL-18 by transducing the cells with lentiviral vectors containing human IL-18 genes. These cells were reported to suppress the growth of the breast cancer cells *in vitro* (Liu et al., 2015) and *in vivo* (Liu et al., 2018).

Studený *et al.* investigated the antitumour effect of MSC expressing interferon-beta (IFN- β). IFN- β stimulates tumour regression by its indirect immunomodulatory and antiangiogenic properties or inhibits the proliferation of malignant cells directly. They successfully demonstrated that MSC expressing IFN- β inhibited the proliferation of melanoma cells (Studený et al., 2002). Subsequent study showed that MSC expressing IFN- β eradicated ovarian cancer cells and prolonged the survival of ovarian cancer cells-bearing mice (Dembinski et al., 2013). Moreover, human umbilical cord-derived MSC transduced with adenoviral vector to express IFN- β have also been reported to inhibit the growth of breast cancer cells through apoptosis (Shen et al., 2016).

Apart from therapy in cancer, genetically engineered MSC also showed promising results in other disease models. Yan *et al.* demonstrated that MSC expressing interleukin-35 (IL-35) using lentiviral vector can ameliorate ulcerative colitis by down-regulating the expression of proinflammatory

cytokines which included tumour necrosis factor- α (TNF- α), interferon- γ (IFN- γ) and interleukin-17 (IL-17) (Yan et al., 2018). In addition, platelet-derived growth factor subunit B (PDGFB)-expressing MSC also showed efficacy in improving human haematopoietic stem cells (HSC) engraftment in immunodeficient mice by providing a better humanised microenvironment for HSC proliferation (Yin et al., 2020).

2.1.6 Clinical Trials of Genetically Engineered MSC

With the encouraging results evidenced by the pre-clinical data in MSC-based studies, many of the studies have further extended to the translation from the bench to the bedside. To date, there are many MSC-based clinical trials reported according to U.S National Institute of Health (<http://www.clinicaltrials.gov>) with the objectives to investigate the therapeutic potential of MSC in various clinical disorders, such as graft-versus-host disease, cancer, neurological disease, cardiovascular disease, autoimmune disease as well as diseases related to joint.

According to the U.S. Food and Drug Administration (FDA), the status of a clinical trial can be categorised into 4 phases. Phase I mainly focuses on the drug's safety and any major adverse effects related to the drug; phase II gathers preliminary data on the effectiveness; phase III involves the comparison of the experimental drug to the commonly used treatments and lastly, phase IV encompasses additional information of the FDA-approved drug such as risks, benefits, and optimal usage.

The first clinical trial of genetically modified MSC was conducted in year 2017 to determine the safety and efficacy of genetically modified autologous MSC expressing Herpes-simplex-virus thymidine kinase (HSV-TK) for the treatment of advanced gastrointestinal cancer (ClinicalTrials.gov: NCT02008539) (Einem et al., 2017). The modified MSC was named as MSC_apceth_101. In this study, six patients were injected intravenously with MSC_apceth_101 followed by the infusion of prodrug ganciclovir. A total dose of 1.5×10^6 cells/kg was given to three of the six patients. One patient only received two doses of 1×10^6 cells/kg due to a severe adverse drug reaction (SADR), whereas the other two patients each received three doses of 1×10^6 cells/kg. This strategy is considered as suicide gene therapy whereby the HSV-TK delivered by the MSC catalysed the phosphorylation of the ganciclovir and subsequently led to the apoptosis of the cancer cells. The trial successfully demonstrated that MSC_apceth_101 was safe and well tolerated by the patients.

Since then, several clinical trials related to genetically modified MSC have been reported. One of the actively explored cytokine in recent years is the tumour necrosis factor (TNF)-related apoptosis-inducing ligand (TRAIL). A phase I/II trial using genetically modified MSC expressing TRAIL (MSCTRAIL) in combination with chemotherapy for metastatic lung adenocarcinoma was initiated two years ago and still in progress currently (ClinicalTrials.gov: NCT03298763). Patients will receive cisplatin and pemetrexed followed by MSCTRAIL on the next day. This trial aims to evaluate the tolerability and preliminary efficacy of this combined treatment strategy.

Ruano *et al.* also successfully showed the safety of MSC as cellular vehicle for oncolytic adenovirus Icovir-5 in the first-in-human, first-in-child clinical trial of relapsed and refractory solid tumours in adults and children (ClinicalTrials.gov: NCT01844661) (Ruano *et al.*, 2020). Icovir-5 is a conditionally replicative oncolytic adenovirus whereby it only replicates in cancerous cells. Autologous bone marrow-derived MSC were infected with oncolytic adenovirus, Icovir-5 and the resulting product was named as Celyvir. Results indicated that MSC can successfully prevent Icovir-5 from being detected and attacked by the immune system, leading to the conclusion that Celyvir is safe even when repeatedly injected with several dosages. With this positive outcome, the Ruano group plans to further investigate the efficacy of Celyvir in combination with other antitumoural agents that might exhibit synergistic effects in cancer therapy.

2.2 Gene Delivery Systems

2.2.1 Viral Vectors

Adenovirus, adeno-associated virus, retrovirus and lentivirus are examples of viral vectors which are commonly used to transduce MSC in pre-clinical as well as in clinical studies. Globally, around 70% of the clinical gene therapy trials have used viral vectors (Lundstrom, 2018). Typically, viral vectors showed higher transduction efficiency and some of them also allowed long-term stable transgene expression (Sage, Thakrar and Janes, 2016). However, the utilisation of viral vectors always triggers the safety concern such as strong

immune response, insertional mutagenesis and cytotoxicity when translated clinically although the advancement in vectors design helped in mitigating this issue (Lee et al., 2017a).

2.2.1.1 Adenovirus

Adenoviruses (Ads) are non-enveloped, icosahedral DNA viruses with virion size ranging from 70 to 90 nm (Singh, Kumar and Agrawal, 2019). The viral genome is flanked on both ends by hairpin like inverted terminal repeats (ITRs) which possess a variety of functions (Lee et al., 2017). These viruses have the ability to replicate inside the nuclei of both dividing and non-dividing cells episomally. Therefore, they are considered as non-integrating viral vector. Serotype 2 and 5 are the most extensively studied human adenovirus serotype. By eliminating specific genome sequences, adenoviruses are modified to make them effective and safe for use as human vaccination, gene, and cancer therapy vectors. The first generation of adenovirus vectors are designed without the regulatory genes E1a and E1b to produce replication-deficient adenoviruses. In the second generation adenovirus vectors non-structural genes E2, E3 and E4 were deleted in addition to the absence of the E1 gene. The third generation of adenovirus vectors are named as gutless or helper-dependent adenovirus in which all the viral coding sequences were removed, leaving only the ITRs and packaging signal (Lee et al., 2017). The three generations of adenoviral vectors are illustrated in Figure 2.3.

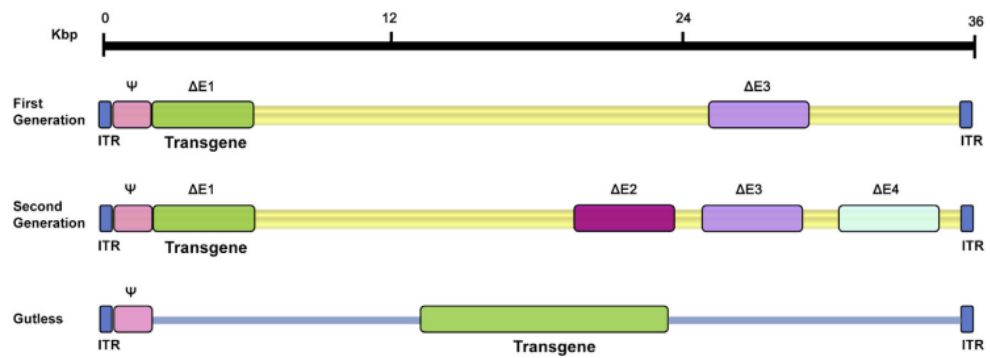


Figure 2.3 Three generations of adenoviral vectors. (Lee et al., 2017)

Muhammad *et al.* have demonstrated that MSC expressing tumour suppressor genes p14 and p53 generated by adenoviral vectors can inhibit prostate tumour growth *in vitro* and in xenograft mouse models (Muhammad et al., 2019). In year 2003, the first commercially available gene therapy vector in the world was approved by State Food and Drug Administration of China for the treatment of head and neck squamous cell carcinoma (HNSCC) (Lee et al., 2017). Since then, many clinical trials were conducted for various types of cancers such as head and neck cancers, hepatic cell carcinoma, NSCLC, malignant glioma and epithelial ovarian carcinoma (Li et al., 2015). Generally, these clinical trials showed satisfying results with better survival rates and response rates compared to the control groups (Li et al., 2015).

Besides, human IL-12 has also been encoded in the replication-deficient adenoviral vector, Ad-RTS-hIL-12 (Sato-Dahlman et al., 2020). This is an inducible system controlled by the oral activator, veledimex (Barrett et al., 2018). In year 2019, the safety of Ad-RTS-hIL-12 in combination with veledimex was

demonstrated in a clinical trial conducted for the treatment of recurrent high-grade glioma (Chiocca et al., 2019).

2.2.1.2 Lentivirus

Another common and widely investigated viral vector is lentivirus. Lentiviruses are categorised as a subclass of retroviruses. Unlike other retroviruses which can only infect dividing cells, lentiviruses are naturally integrating vector that can infect non-dividing cells (Nayerossadat, Ali and Maedeh, 2012). Lentiviruses have high cloning capacity that allows up to 8kb of transgene delivery into target cells. Meyerrose et al. utilised lentiviral-transduced human MSC to express therapeutic level of lysosomal enzyme β -glucuronidase (MSCs-GUSB) in a xenotransplantation model of human disease (non-obese diabetic severe combined immunodeficient mucopolysaccharidosis type VII [NOD-SCID MPSVII]). The study demonstrated that MSCs-GUSB were able to increase the serum level of GUSB to about 40% of normal level and the transduced human MSC retained their homing ability while persisted for at least 4 months in delivering the therapeutic level of GUSB in the xenotransplantation model (Meyerrose et al., 2008).

In recent years, several clinical trials have used third generation self-inactivating lentiviral vectors to insert genes into haematopoietic stem cells to treat primary immunodeficiencies and haemoglobinopathies (Milone and O'Doherty, 2018). Moreover, lentiviral vectors also have been used to carry

genes into mature T cells to generate immunity via the delivery of chimeric antigen receptor (CAR) in the CAR-T therapy (Milone and O'Doherty, 2018).

2.2.1.3 Adeno-associated Virus

Adeno-associated viruses (AAV) are tiny, non-enveloped, icosahedral viruses that are members of the Dependovirus genus, Parvoviridae family (Vannucci et al., 2013). AAV contains only two genes, namely rep and cap, which is necessary for viral genome replication and structural proteins encoding respectively (Vannucci et al., 2013). These vectors are a desirable option for gene therapy applications due to their high transduction efficiency in a variety of target cells and tissues, outstanding safety profiles, and low inflammatory toxicity (Naso et al., 2017). However, the AAV has a relatively low cloning capacity at 4kb when compared to the lentivirus. Nonetheless, AAV are still the popular choice of viral vector in clinical applications (Hirsch, Wolf and Samulski, 2016).

The transduction of interleukin-10 (IL-10) gene into MSC using AAV improved the neuroprotective effects of the MSC in an acute ischaemic stroke rat model (Nakajima et al., 2017). Nakajima et al. 2017 suggested the neuroprotective effect was due to anti-inflammation modulation and reduction in neuronal degeneration. Gabriel et al. also showed that AAV-transduced mesenchymal stromal cells (MSCs) can be the vehicle for hepatic gene transfer in a murine liver injury model (Gabriel, Samuel and Jayandharan, 2017).

2.2.2 Non-viral Vectors

Despite having lower transfection efficiency, non-viral gene delivery methods are safer, able to load with larger transgene and more feasible in large scale production in comparison with viral-based methods (Schaffert and Wagner, 2008). Generally, non-viral gene delivery method in MSC can be classified into physical method and chemical method.

2.2.2.1 Physical Method

Physical gene delivery method includes microinjection, electroporation, and sonoporation (Wang et al., 2014). Microinjection deliver genes directly into the nucleus of the target cell. However, microinjection is not suitable for transfection of high number of cells or precious cell sources as this technique requires single manipulation of each cell and very low injection rate (Han et al., 2008). In comparison with microinjection, electroporation has higher throughput as it utilises transient electrical pulse to create nanometer-scale pores on the cell membranes of a population of cells and thus allowing the nucleic acid to enter into the cells (Hamann, Nguyen and Pannier, 2019a). Instead of using conventional electroporation cuvettes, the micro-electroporation system reduces pH variations and enables the cost-effective use of small gold electrodes that are more electrolytically inert (Kim et al., 2008). Study has shown that electroporation conducted using micro-electroporation system exhibited higher transfection efficiency on human adipose-derived MSC (hAD-MSCs) compared

to other transfection method, without affecting the differentiation properties of hAD-MSCs (Halim et al., 2014). Canton et al. demonstrated that the intratumoural tavokinogene telseplasmid electroporation (IT-tavo-EP) monotherapy is safe and well tolerated by melanoma patients in a phase I/II clinical trial (Algazi et al., 2020).

Nucleofection is a transfection method which works efficiently for primary cells or hard-to-transfect cell lines. Plasmid DNA, oligonucleotides, and siRNA can be delivered directly into the cell nucleus via nucleofection, which combines electrical parameters and cell-type solutions (Aluigi et al., 2006). Fakiruddin et al. showed that nucleofection was an efficient method to deliver TRAIL gene into adipose-derived MSC for its antitumour effects on LN18 glioblastoma cells, A549 lung cancer cells, HepG2 hepatocellular carcinoma cells and REH acute lymphocytic leukemia cells (Fakiruddin et al., 2014). Moreover, nucleofection was shown to be a non-viral transfection method which is in tune with Good Manufacturing Practice (GMP) guidelines (Agostini et al., 2021). When comparing with chemical transfection method using polyethyleneimine (PEI) to transfect the mouse pancreatic α TC1-6 cells, nucleofection showed much higher transfection efficiency (Đorđević et al., 2022).

2.2.2.2 Chemical Method

Unlike physical methods, chemical methods use chemical carriers to form complex and carry nucleic acid materials into the cells. Various chemical carriers have been developed and thoroughly studied over the past few decades in an effort to achieve high transfection performance, including low toxicity, high efficiency, biodegradability, and targeting specificity. These chemical nanocarriers are electrostatically condensing or encapsulating nucleic acids to form complexes that bind with cell membranes through surface receptor binding or charge interactions. The complexes then enter the target cells via micropinocytosis, clathrin-mediated endocytosis or caveolae-mediated endocytosis, depending on the nanoparticle size and charge (Xiang et al., 2012). Mangraviti *et al.* demonstrated that MSC transfected with biodegradable polymeric nanoparticles, β -amino esters (PBAE) containing bone morphogenetic protein 4 (BMP4) can secrete BMP4 while maintaining their multipotency and homing ability simultaneously (Mangraviti et al., 2016). The study also showed significant improvement in survival for athymic rat bearing human brain tumours when treated with the modified MSC intranasally. According to this study, the nanocarrier used, PBAE showed transfection efficiency (75%) similar to and viability (71%) higher than electroporation (Hamann, Nguyen and Pannier, 2019). Even though these nanocarriers can achieve high transfection efficiency, it should be emphasised that a wide range of transfection results have been reported, likely because of variation in the species, tissue source, passage, and donor of the MSC (Hamann, Nguyen and Pannier, 2019). Madeira et al. demonstrated that the transfection efficacy of

hBMSCs through Lipofectamine 2000 (LF2000) at passage one varies amongst donors by 5 to 20% and declines with increasing passage number (Madeira et al., 2010). Hence, donor heterogeneity may account for the variations in transfection efficiency reported by several researchers utilising the same MSC nonviral delivery methods, and direct comparisons of various ways on the same donor(s) are necessary to properly determine the best performing nanocarriers.

2.3 Interleukin-12 (IL-12)

Cytokines have been utilised in cell and gene therapies for various types of cancer as have been outlined in section 2.1.5. In this study, interleukin-12 (IL-12) was selected due to its immunostimulatory effects which mediate both innate and adaptive immune system.

2.3.1 Discovery and Structures

Interleukin-12 (IL-12) was first discovered as a natural killer cell stimulatory factor (NKSF) in the year 1989 (Kobayashi et al., 1989). The following year, Stern and his colleagues identified cytotoxic lymphocyte maturation factor (CLMF) from a human B-lymphoblastoid cell line (Stern et al., 1990). Thereafter, the term IL-12 was proposed as NKSF and CLMF were found to be identical (Gubler U et al., 1991).

IL-12 is a heterodimeric cytokine comprised two different disulfide-linked subunits, namely p35 and p40 with molecular masses of 35 and 40 kDa respectively (Gately et al., 1996). In human, the genes encoding p35 and p40 are located at the chromosome 3 and 5 respectively. Hence, the protein expression is regulated individually (Watford et al., 2003). When the cell co-expresses the two genes, the biological active p70 heterodimer will be formed (Gubler U et al., 1991).

Study showed that IL-12p40 can be produced in free p40 monomer or disulfide-linked p40 homodimer (Gately et al., 1996). In mice, the p40 homodimer was found to inhibit the murine IL-12 signalling *in vivo* (Gately et al., 1996). In contrast, p35 is not secreted in monomeric form.

2.3.2 Expression and Biological Function

Interleukin-12 (IL-12) is one of the key immunomodulatory cytokines which has potential in antitumour effect. IL-12 is naturally produced by phagocytes such as activated macrophages and dendritic cells (DCs) (Watford et al., 2003). It induces interferon-gamma (IFN- γ) production by NK cells, T cells, DCs and activated macrophages. It also stimulates the proliferation of NK cells and T cells and enhances the cytotoxic effects of NK cells and cytotoxic T cells (Watford et al., 2003). Moreover, IL-12 is also the key cytokine in polarisation of T cells towards T helper type I differentiation (Del Vecchio et al., 2007). This indicates the bridging of innate and adaptive immunity by IL-12. Figure 2.4

shows the cellular sources and responders of IL-12 along with their respective functions.

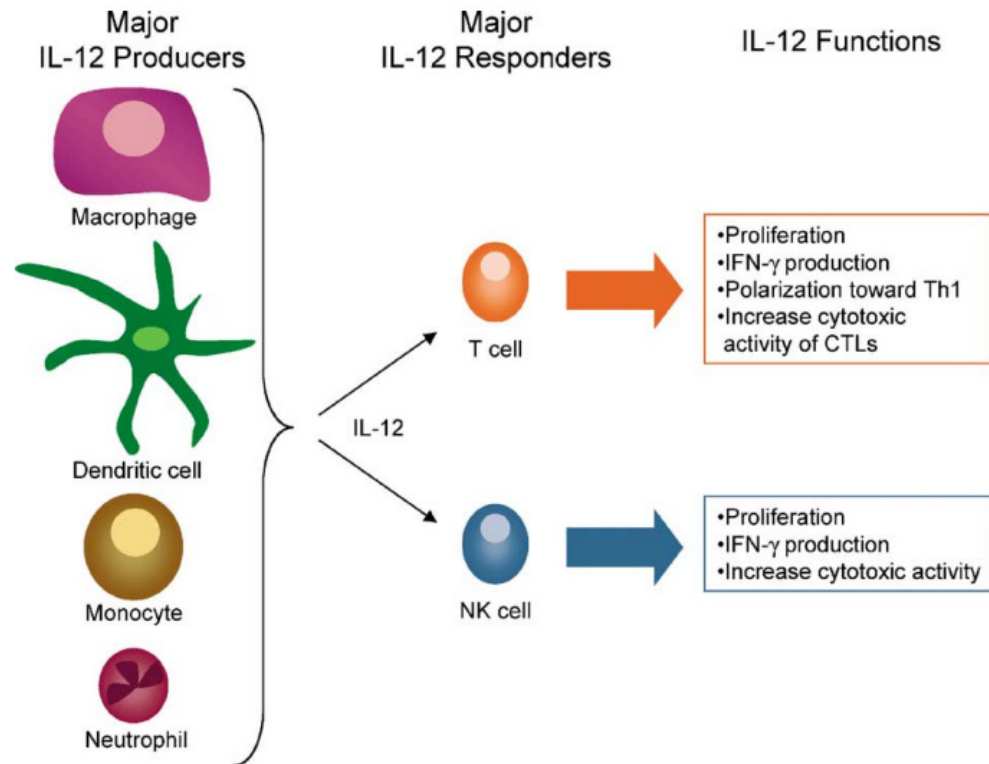


Figure 2.4 Cellular sources and responders of IL-12 along with their respective functions. (Watford et al., 2003)

2.3.3 Mechanisms of Action

The remarkable function of IL-12 is in its capability to stimulate the production of IFN- γ by NK cells, CD4⁺ T cells and CD8⁺ T cells. The IFN- γ in turn mediates the immunostimulatory properties of IL-12 that modifies the tumour microenvironment (Berraondo et al., 2018). The mechanisms include the following (Figure 2.5):

- i. Augmentation of major histocompatibility I (MHC I) antigen presentation in tumour cells.
- ii. Conversion of M2 macrophages into antitumour M1 macrophages.
- iii. Stimulation of chemokines expression to attract NK cells, Th1 cells and CD8⁺ T cells.
- iv. Regulation of antiangiogenesis in tumour microenvironment by acting on the endothelial cells while upregulating the expression of homing receptors for T cell recruitment to the tumour.

IL-12 stimulates the production of IFN- γ by phagocytes which in turn induces or increases the secretion of IL-12, forming a positive feedback loop (Tugues et al., 2015). Moreover, IL-12 and IFN- γ also enhance cytotoxic effects by NK cells and CD8⁺ T cells by producing cytolytic factors such as perforin, granzymes and Fas ligand (FasL)(Tugues et al., 2015). Besides the IFN- γ production, IL-12 also stimulates the secretion of tumour necrosis factor-alpha (TNF- α), granulocyte-macrophage colony-stimulating factor (GM-CSF) and interleukin-2 (IL-2) (Trinchieri, 2003). TNF- α is an inflammatory cytokine that is produced by macrophages and monocytes during acute inflammation that triggers a wide variety of cellular signalling pathways resulting in necrosis or apoptosis (Idriss and Naismith, 2000). On the other hand, in response to stress, infections, and malignancies, GM-CSF stimulates the creation of myeloid cell subsets like dendritic cells, macrophages, monocytes, and neutrophils. Under pathologic settings, GMCSF has a broad impact on host immune surveillance by regulating the activities of innate immune cells that operate as a bridge to trigger adaptive immune responses (Kumar et al., 2022). Similarly, IL-2 also serves critical roles in controlling immune activation and homeostasis with the major

function to induce proliferation of CD4⁺ and CD8⁺ T cells (Gaffen and Liu, 2004).

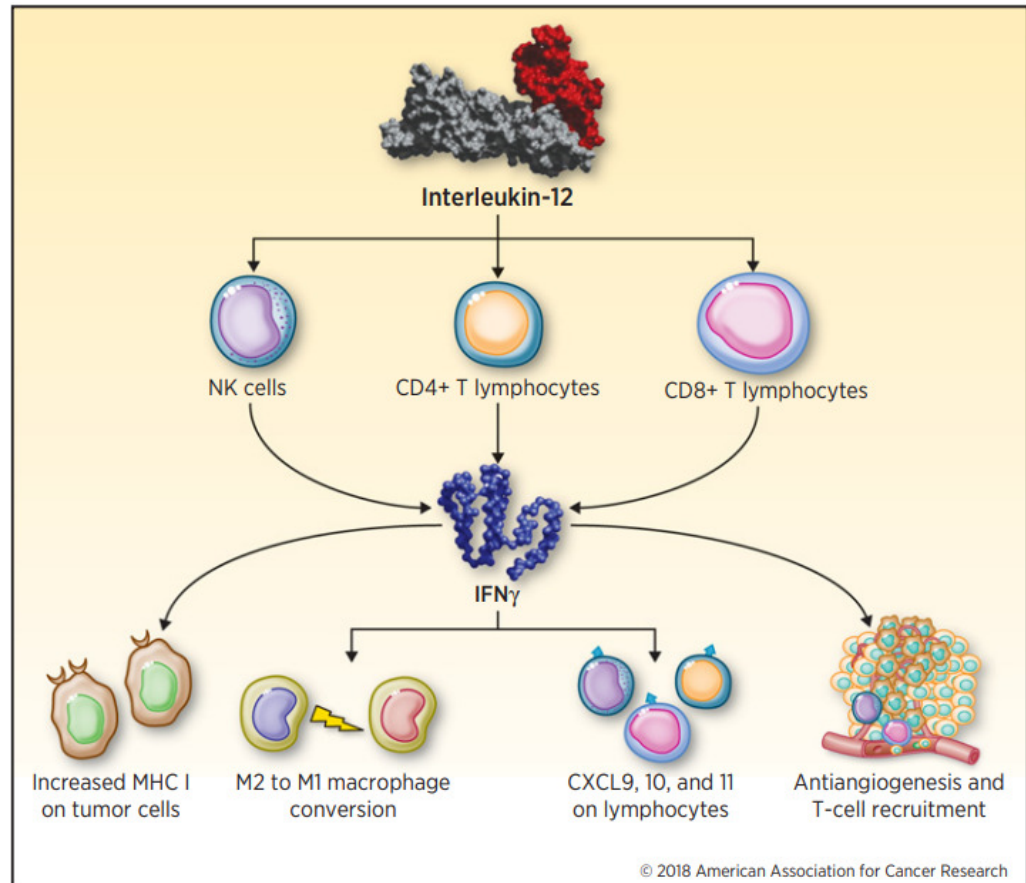


Figure 2.5 Mechanism of actions of IL-12. (Berraondo et al., 2018)

2.3.4 Antitumour Effect

IL-12 has shown to be highly efficient in animal models of tumour therapy due to its capacity to induce a variety of direct and indirect anticancer actions related to innate immunity, adaptive immunity, and non-immune mechanism (Lasek, Zagożdżon and Jakobisiak, 2014). The main IL-12 actions are as follows (Figure 2.6): increasing the IFN- γ production from NK and T cells, which is the most effective mediator of IL-12 actions; stimulating the growth

and cytotoxicity of activated NK cells, CD8⁺ and CD4⁺ T cells; shifting CD4⁺ Th0 cell differentiation towards the Th1 phenotype; enhancing antibody-dependent cellular cytotoxicity (ADCC) against tumour cells; and inducing IgG and suppressing IgE production from B cells. Furthermore, the IFN- γ produced can stimulate the reprogramming myeloid-derived suppressor cells and induces the expression of antiangiogenic cytokine and chemokine. Studies have also shown that IL-12 induces the expression of Fc receptors of macrophages and NK cells and thereby enhances the antibody-dependent cellular cytotoxicity (ADCC) (Liu et al., 2002). The Fc receptors on NK cells are triggered to attack the tumour cells when IgG1 antibody attaches to the surface of a tumour cells (Shiokawa et al., 2010).

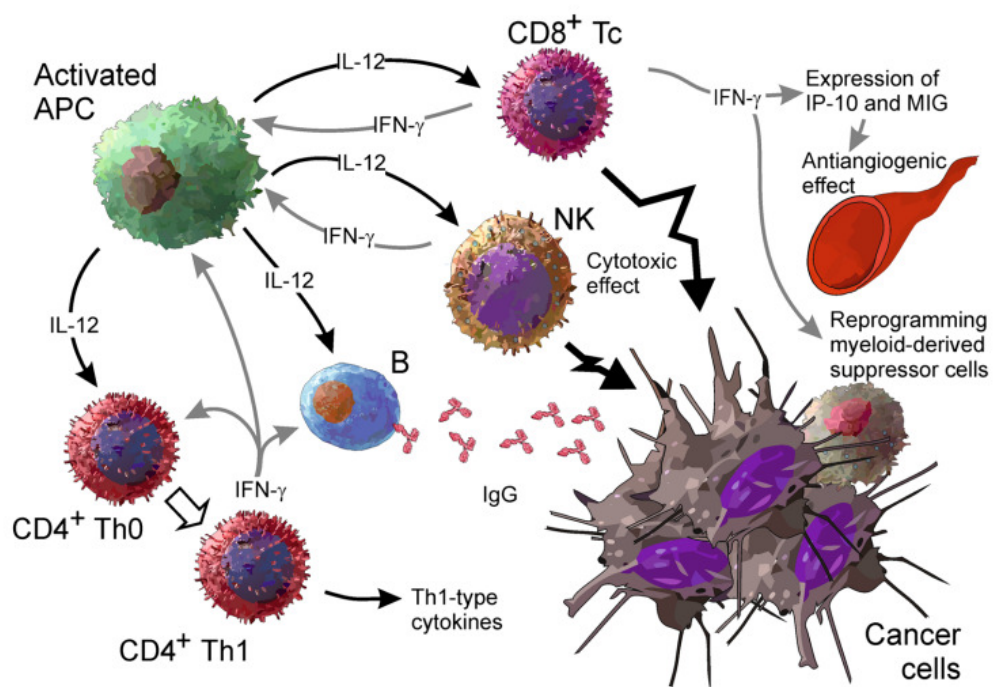


Figure 2.6 Overview of the biological functions of IL-12 contributing to its antitumour effects. (Lasek, Zagożdżon and Jakobisiak, 2014)

In the 1990s, there were some clinical trials which used IL-12 to treat Hepatitis B, Hepatitis C and renal cell carcinoma. Among these clinical trials, there were some common adverse effects reported such as flu-like symptoms, rapid transient leukopenia, increased liver enzymes, gastrointestinal tract (GIT) toxicity and liver dysfunction (Car et al., 1999). In the year 1997, a phase I dose escalation clinical trial was conducted to assess the safety and tolerance of recombinant hIL-12 (rhIL-12) administered intravenously (Leonard et al., 1997). In the trial, a single test dose of rhIL-12 was administered 14 days prior to the 5 days consecutive daily dose for every 3 weeks. The results demonstrated safety at maximum tolerated dose (MTD) of 500 ng/kg with this schedule of administration. However, a phase II clinical trial conducted using the same dosage to treat patients with renal cell carcinoma was reported to cause severe toxicities. The patients in the phase II clinical trial were not administered with the single priming dose prior to the multiple-dose regimen resulting in the differences in toxicities between the phase I and phase II trial. The IL-12 induced IFN- γ was believed to be the main culprit of the toxicities. Interferon- γ produced by T cells and NK cells causes myelosuppression, which is linked to macrophage activation and upregulation of MHC class I and II antigens in various epithelial cells (Car et al., 1995). Subsequently, enlargement or oedema occurred in multiple organs such as liver, spleen and lungs.

With the evidence of systemic toxicities resulting from the high level of interferon- γ produced from the direct administration of IL-12 at therapeutic dosage, novel therapeutic modalities that localised IL-12 within the tumour were extensively explored. For instance, Sangro and colleagues investigated the

feasibility and safety of the intratumoural injection of adenoviral vector encoding human IL-12 gene (Ad.IL12) on advanced digestive tumour-bearing patients (Sangro et al., 2004). The study demonstrated that the intratumoural injection of Ad.IL12 up to 3×10^{12} viral particles was feasible and well tolerated by the patients despite the low antitumour effect.

Another phase I clinical trial was conducted to treat patients of metastatic solid tumours with the tumour-targeted immunocytokine (NHS-IL12) (Strauss et al., 2019). The immunocytokine combined the IL-12 heterodimers with the NHS76 antibody. The antibody can bind to histones on free DNA fragments in tumour necrosis area which resulted in the tumour-targeting effect of this method. The study reported positive results on the tolerability of the NHS-IL12 in patients with metastatic or locally advanced solid epithelial or mesenchymal tumours.

Furthermore, IL-12 gene therapy was exploited in a phase I clinical trial as the treatment for patients with metastatic pancreatic cancer (Barton et al., 2021). In this trial, the replication-competent adenovirus carrying IL-12 gene (Ad5-yCD/mutTKSR39rep-hIL-12) was intratumourally injected into 12 patients followed by the standard-of-care chemotherapy. Although the outcome of the study showed acceptable safety profile, but it failed to demonstrate significant antitumour effects. Similarly, another adenoviral vector encoding IL-12 gene (Ad-RTS-hIL-12) was used in a phase I clinical trial to treat recurrent high-grade glioma patients (Chiocca et al., 2019). However, instead of a suicide gene, this trial utilised the veledimex, an oral IL-12 activator, as a switch to

regulate the IL-12 activation. Results showed that the optimal dose of 20mg veledimex led to an encouraging median overall survival of 12.7 months.

More recently, Komel et al. demonstrated high antitumour efficacy of combined IL-2 and IL-12 gene electrotransfer in murine B16.F10 melanoma models (Komel et al., 2021). The combined treatment with these immunomodulatory cytokines successfully increased the accumulation of dendritic cells, macrophages, CD4⁺ and CD8⁺ T-lymphocytes in the mice and resulted in significant tumour delay. Another preclinical study that also showed successful antitumour effects on a murine colorectal tumour model was conducted by Silva-Pilipich et al. using intratumoural electroporation of a self-amplifying RNA (saRNA) encoding IL-12 (SFV-IL-12) (Silva-Pilipich et al., 2022). This result was reproduced in a hepatocellular carcinoma tumour model as well.

2.4 Cancer

In every country in the world, cancer is the main cause of death and a major impediment to increase life expectancy. According to estimations from the World Health Organization (WHO) for 2019, cancer is the first or second top cause of death before the age of 70 in 112 of 183 countries and the third or fourth in the remaining 23 countries in the world (Figure 2.7). Globally, the burden of cancer incidence and death is rising rapidly which is due to the population's aging and expansion as well as changes in the prevalence and distribution of the key risk factors for cancer, some of which are related to socioeconomic development

(Sung et al., 2021). In the year 2020, the coronavirus disease 2019 (COVID-19) pandemic had negatively impacted the detection and treatment of cancer (Siegel et al., 2022). Delays in diagnosis and treatment due to health care facility closures and concern over COVID-19 exposure led to decreased access to care, which could cause a temporary decrease in cancer incidence followed by an increase in advanced-stage of disease and, eventually, higher mortality (Yabroff et al., 2022). The population-based statistics used in this analysis indicate significant declines in cancer pathology reports in 2020, which suggests significant delays in cancer diagnosis and treatment as indirectly contributed by the COVID-19 pandemic.

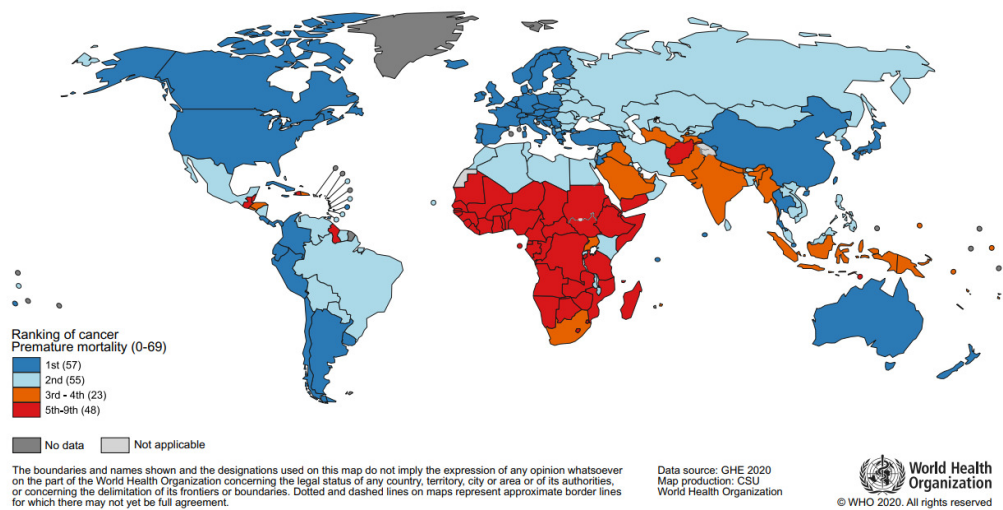


Figure 2.7 National Ranking of Cancer as a Cause of Death at Ages <70 years in 2019. (WHO, 2020)

2.4.1 Lung Cancer

Lung cancer is the leading cause of cancer worldwide and it accounts for one third of all the cancer-related deaths (Kolluri, Laurent and Janes, 2013). According to Globocan 2020 from the World Health Organization, lung cancer is shown to be the second most common cancer worldwide and also the highest mortality rate cancer among all the cancer types (Sung et al., 2021). Non-small cell lung cancer (NSCLC) accounts for the majority of all the lung cancer cases (Zappa and Mousa, 2016). NSCLC can be further classified into squamous cell carcinoma, adenocarcinoma and large-cell carcinoma. Adenocarcinoma is the most common type of lung cancer as it constitutes around 40% of all lung cancers (Schabath and Cote, 2019). Figure 2.8 shows the histologic classification of lung cancer.

Lung adenocarcinoma is the most common subtype to be diagnosed in non-smoker. It is also strongly correlated with one's past smoking experience (DJ M. and JM W., 2022). The understanding of lung adenocarcinoma and its subtypes has substantially expanded recently as a result of advances in oncology, imaging, and molecular biology, which have improved the paradigm for clinical management of the disease (Tang, Schreiner and Pua, 2014). A multidisciplinary consensus of the International Association for the Study of Lung Cancer, American Thoracic Society, and European Respiratory Society (IASLC/ATS/ERS) has endeavoured to address these growing challenges with a new classification system exclusively for lung adenocarcinoma (Tang, Schreiner and Pua, 2014). In this new system, lung adenocarcinoma is further classified

into atypical adenomatous hyperplasia (AAH), adenocarcinoma in situ (AIS), minimally invasive adenocarcinoma (MIA), invasive adenocarcinoma, and variants of invasive adenocarcinoma.

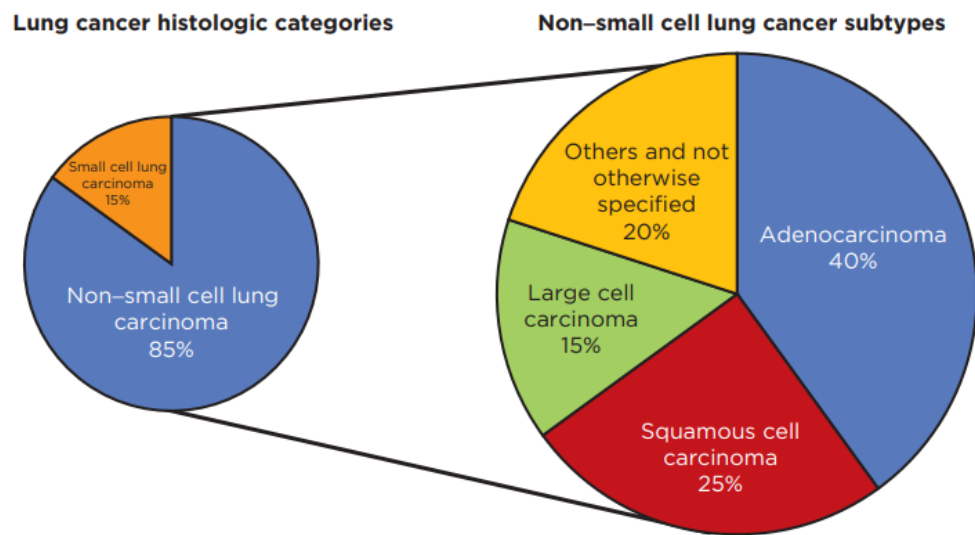


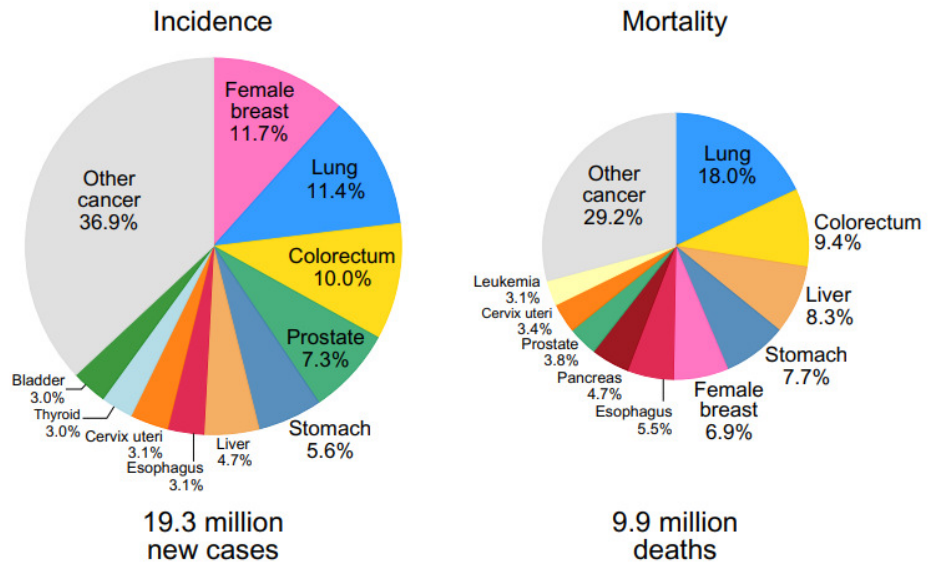
Figure 2.8 Histologic classification of lung cancer. (Schabath and Cote, 2019)

2.4.2 Epidemiology of Lung Cancer

Based on Globocan 2020, about 2.2 million of lung cancer cases were diagnosed worldwide, which covers 11.4% of the total cases (Figure 2.9 A). From the data of mortality rate in both sexes, lung cancer was the leading cause of cancer death worldwide (18% of total deaths) (Figure 2.9 A). When comparing the data of each gender, men showed nearly 2 times higher incidence and mortality rates than women (Figure 2.9 B and C). There is significant difference in the male-to-female ratio of lung cancer incidence across the regions (Figure 2.10). In terms of country-specific rates, Turkey had the greatest incidence rates among men while Hungary had the highest rates among women.

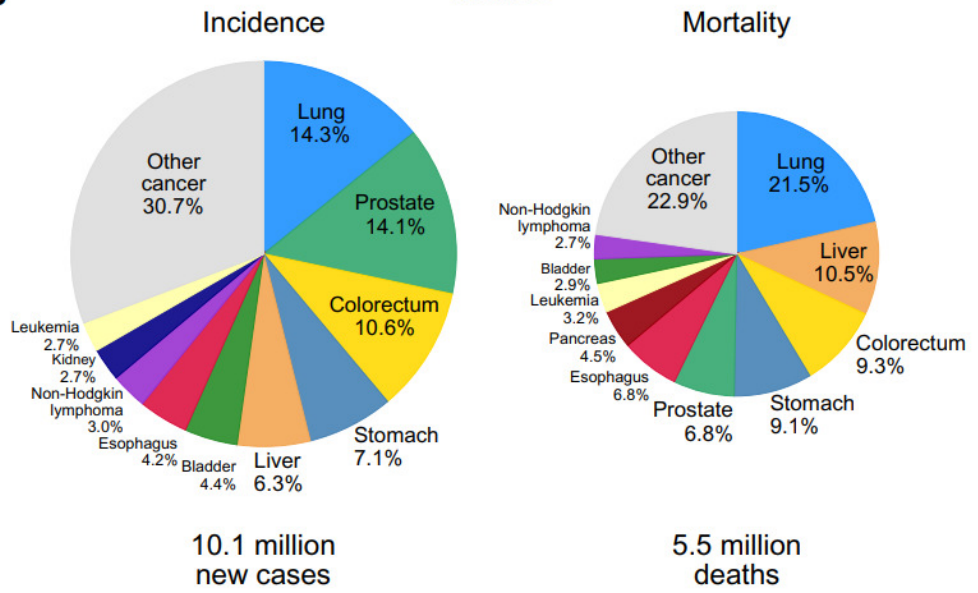
A

Both sexes



B

Males



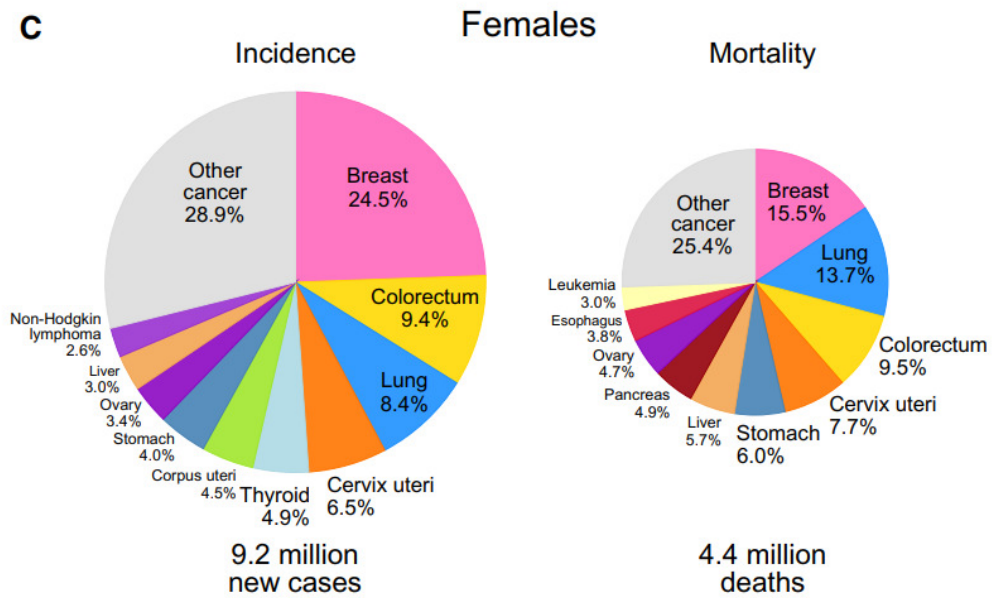


Figure 2.9 Distribution of Cases and Deaths for the Top 10 Most Common Cancers in 2020 for (A) Both Sexes, (B) Men, and (C) Women. (Sung et al., 2021)

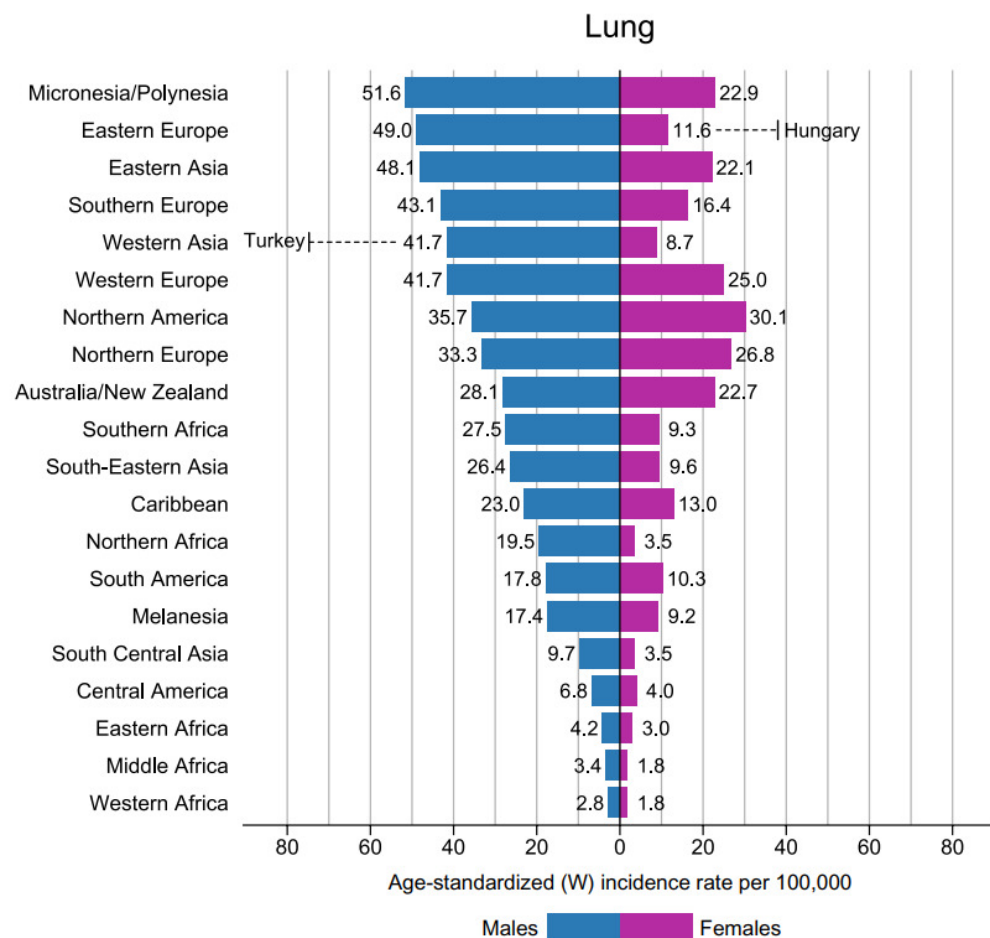


Figure 2.10 Region-Specific Incidence Age-Standardised Rates by Sex for Lung Cancer Among Men and Women in 2020. (Sung et al., 2021)

In Malaysia, trachea, bronchus and lung cancer was the third most common cancer during the period of 2012 to 2016, which accounts for 9.8% of all the cancer cases (Figure 2.11). During the same period, there were a total of 11,256 cases reported to the Malaysia National Cancer Registry with 68.3% among the males and 31.7% among the females. According to the Registry, the lifetime risk of male is higher than female which was reported as 1 in 60 and 1 in 138 respectively. The incidence of trachea, bronchus and lung cancer were highest among the Chinese in both genders (Figure 2.12). However, incidence rate among the Malays is increasing when compared with the rates among the Chinese and Indians from the period of 2007-2011 to the period of 2012-2016. Over 90% of lung cancer cases were diagnosed at very late stage (stage III or IV) for both genders (Figure 2.13).

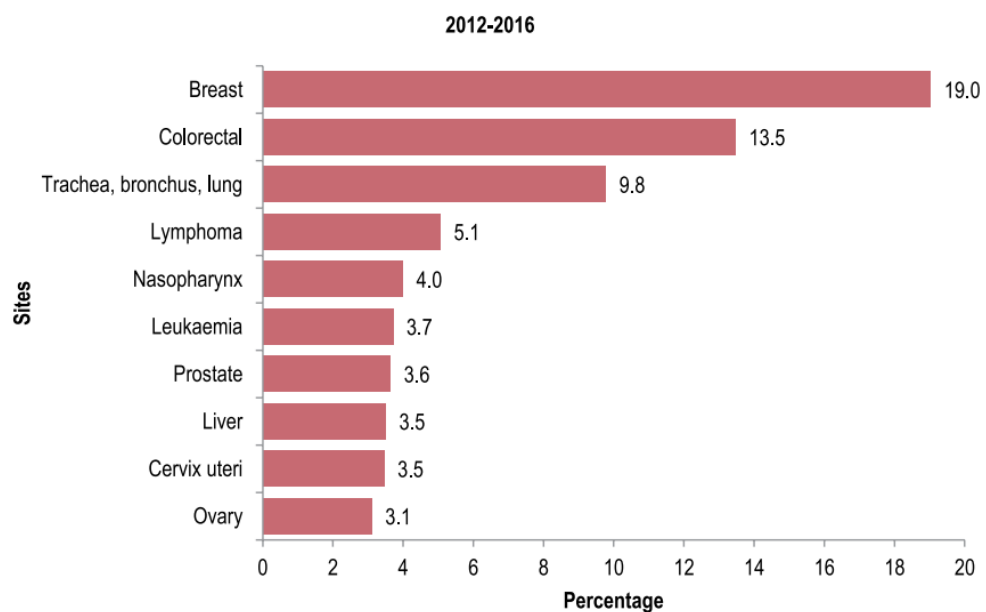


Figure 2.11 Ten most common cancers, all residents, Malaysia, year 2012-2016. (Sung et al., 2021)

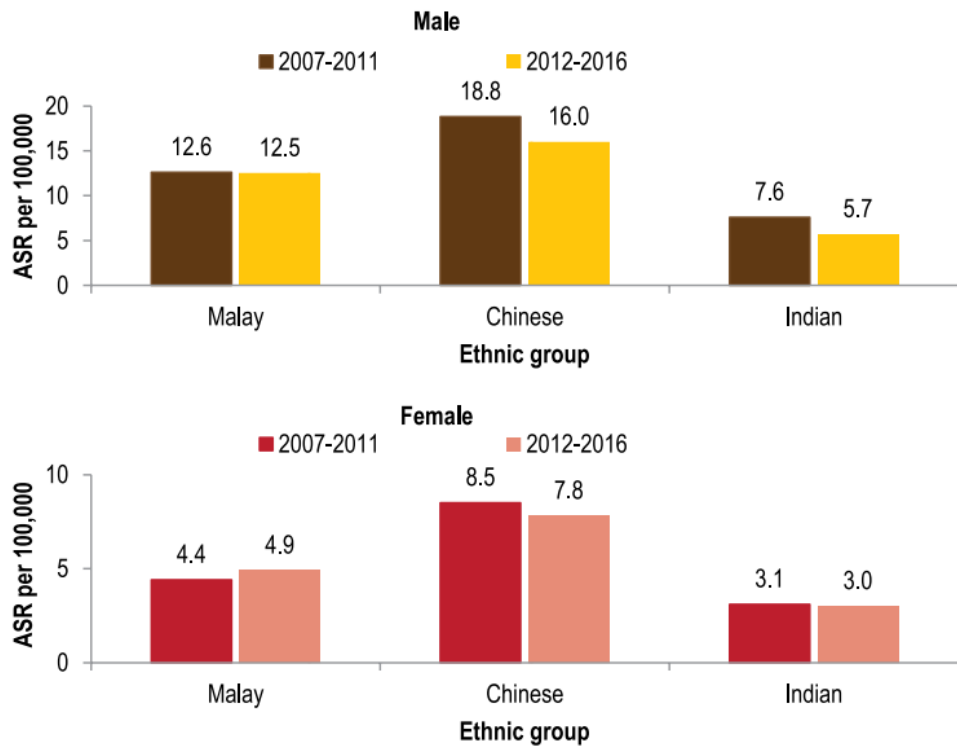


Figure 2.12 Trachea, bronchus and lung: Comparison of age-standardised rate by year, major ethnic group and sex in Malaysia. (Sung et al., 2021)

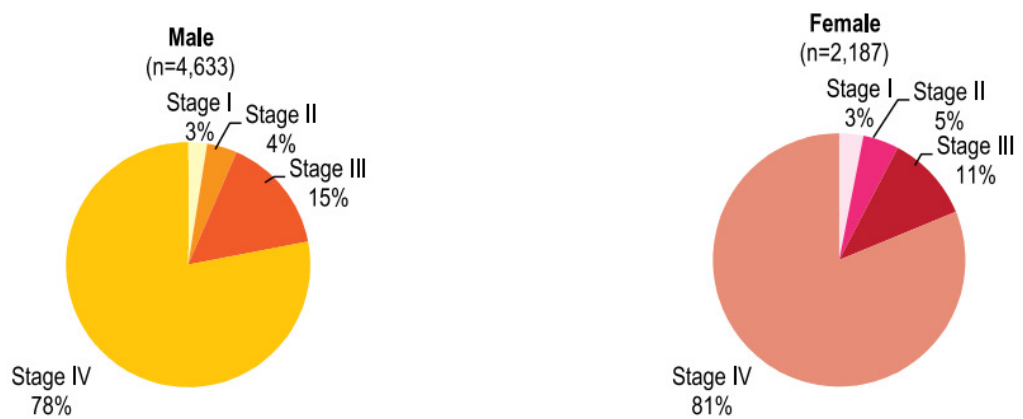


Figure 2.13 Trachea, bronchus and lung: Staging percentage by sex, Malaysia, year 2012-2016. (Sung et al., 2021)

2.4.3 Risk Factors

Smoking, exposure to passive smoke inhalation, residential radon, occupational exposures, infection and genetic susceptibility are all risk factors for lung cancer (de Groot et al., 2018). Up to 90% of lung cancer cases are attributable to smoking, making it the single major risk factor for the disease.

Smoking was first popularised among men in several high-income countries (Parkin, Bray and Devesa, 2001). Contrarily, the tobacco epidemic is less severe and progressed among women (Thun et al., 2012). The quantity of cigarettes smoked each day, the intensity of inhalation, and the age at which smoking first began are all directly correlated with the chance of developing lung cancer. The risk for a lifetime smoker is roughly 20–30 times higher than for a non-smoker. Filter and reduced tar cigarettes reduce the risk of cancers and the increased use of these products has helped recent generations of smokers to lower both the risk and the prevalence of smoking (Parkin, Bray and Devesa, 2001).

Lung cancer develops following a series of mutational events (Sato et al., 2007). The three main established pathways of cigarette smoking induced cancer are (1) the exposure to carcinogens, (2) the formation of covalent bonds between the carcinogens and DNA and (3) accumulating somatic mutations that are persistent in critical genes (United States. Public Health Service. Office of the Surgeon General., 2010).

CHAPTER 3

MATERIALS AND METHODS

3.1 Experimental Design

The workflow of this study is illustrated in Figure 3.1. Briefly, the human umbilical cord-derived mesenchymal stromal cells (hUCMSC) were obtained from Cryocord Sdn Bhd. The expanded hUCMSC were then characterised by cell surface markers and trilineage differentiation assays. Subsequently, the hUCMSC were genetically engineered to express human interleukin-12 (hIL-12) by using adenoviral method and electroporation. The cell viability, transduction/transfection efficiency and hIL-12 protein expression of the hUCMSC expressing hIL-12 (hUCMSC-IL12) generated by the two methods were compared and the method with better results was selected. The hUCMSC-IL12 were then generated by using the selected method and co-culture with H1975 human lung adenocarcinoma cells and MRC-5 human lung fibroblasts in order to study its cytotoxic effects on the cell lines. The viability of the cell lines was determined by CCK-8 assay. The *in vitro* expression of hIL-12 mRNA and protein in hUCMSC were analysed via quantitative real-time PCR and enzyme-linked immunosorbent assay (ELISA) respectively. Lastly, the hUCMSC-IL12 were characterised by cell surface markers and trilineage differentiation assays to confirm their integrity.

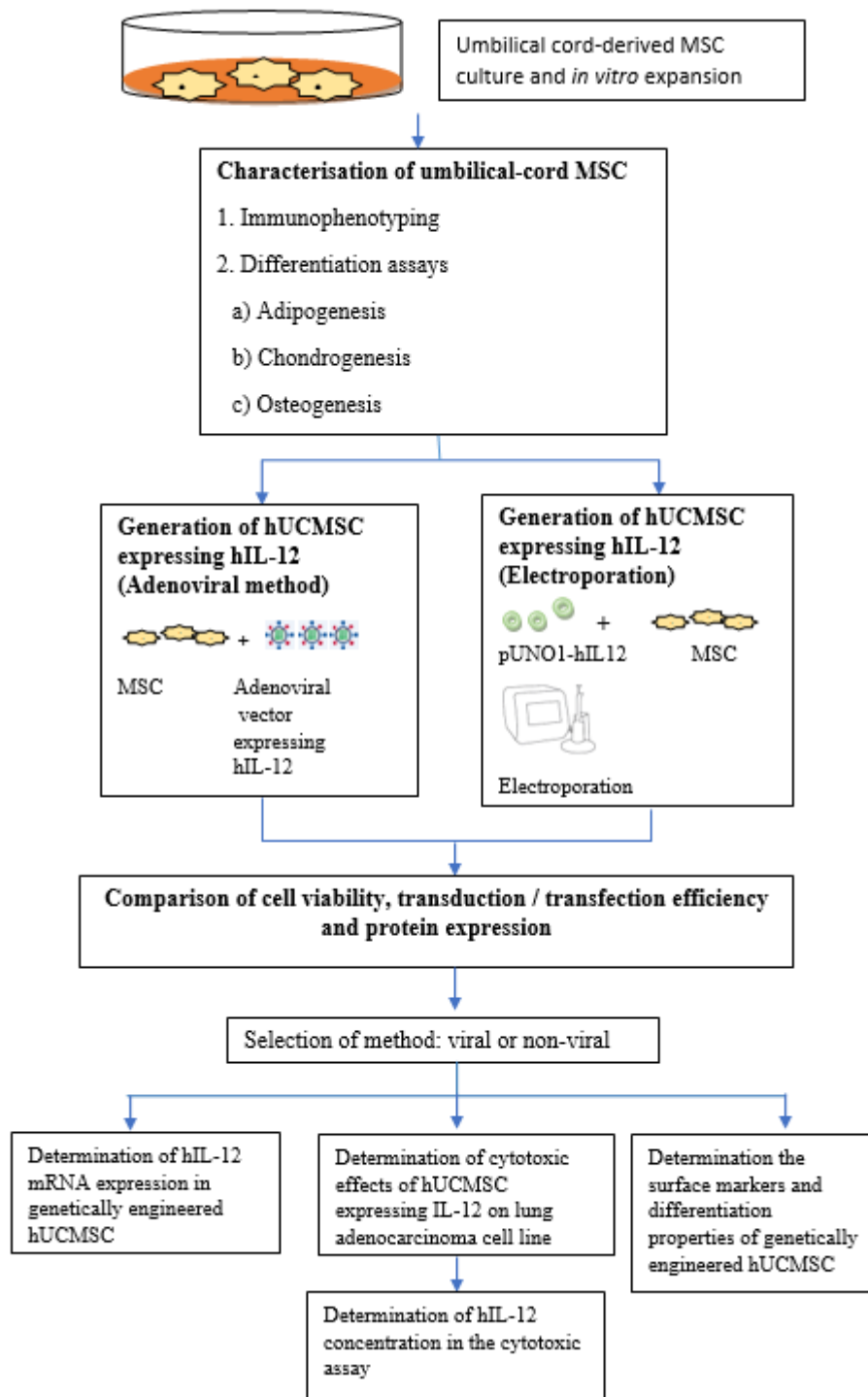


Figure 3.1 Experimental design flow chart of this study.

3.2 Cell Culture

3.2.1 Human Umbilical Cord-derived Mesenchymal Stromal Cells (hUCMSC)

The hUCMSC from three different donors (passage 3 to 5) were obtained from Cryocord Sdn. Bhd. The cells were cultured in complete medium that was made up of low glucose Dulbecco's Modified Eagle Medium (DMEM) supplemented with 10% Fetal Bovine Serum (FBS) (Gibco, Invitrogen, USA), 1% Penicillin-Streptomycin (Gibco, Invitrogen, USA) and 1% L-Glutamine (Gibco, Invitrogen, USA) at 37°C in a humidified 5% CO₂ incubator. Seeding density of the cells ranged from 7 X 10³ cells to 1 X 10⁴ cells per cm² of surface size of the culture vessel. The cells were expanded and medium was changed every 3-4 days. The cells were sub-cultured when they reached 70-80% confluency. For cryopreservation, cells were harvested and cryopreserved using hUCMSC freezing medium which composed of 90% FBS and 10% CryoSure-DMSO (WAK-Chemie, Germany). Cryovials were immediately placed into a Cool Cell and kept in -80°C freezer overnight prior to being transferred into a liquid nitrogen storage tank at -196°C. Cells from third to fifth passage were used for subsequent studies.

3.2.2 Human Embryonic Kidney 293 Cell Line (HEK 293)

The HEK 293 cell line was a kind gift from Professor Dr Leong Chee Onn (International Medical University, Malaysia). The cells were originally purchased from the American Type Culture Collection (ATCC). The complete growth medium of the cells consists of high glucose Dulbecco's Modified Eagle Medium (DMEM) supplemented with 10% Fetal Bovine Serum (FBS) (Gibco, Invitrogen, USA), 1% Penicillin-Streptomycin (Gibco, Invitrogen, USA) and 1% Sodium Pyruvate (Gibco, Invitrogen, USA) at 37°C in a humidified 5% CO₂ incubator. The seeding density for the cells ranged from 1 X 10⁴ cells/cm² to 4 X 10⁴ cells/cm². The cells were sub-cultured when the concentration is between 6 and 7 X 10⁴ cells/cm². During culture, the medium was replaced every 3 to 4 days. HEK 293 cells were cryopreserved in freezing medium which was made up of 95% complete growth medium and 5% DMSO. The cells were kept overnight at -80°C and then transferred into a -196°C liquid nitrogen storage tank on the next day.

3.2.3 Human Lung Adenocarcinoma Cell Line (H1975)

H1975, a cell line established from a non-smoking female with adenocarcinoma, non-small cell lung cancer, was purchased from the ATCC. The H1975 cells were cultured in growth medium containing Roswell Park Memorial Institute (RPMI) 1640 medium (Gibco, Invitrogen, USA) supplemented with 10% FBS (Gibco, Invitrogen, USA) at 37°C in a humidified 5% CO₂ incubator. The cells

were cultured in a T75 flask at seeding density 1×10^4 cells/cm² upon received and were maintained by replacement of fresh medium for every 2 to 3 days. The H1975 cells were sub-cultured when the confluency reached 70-80%. The cells were cryopreserved in freezing medium containing 95% complete growth medium and 5% DMSO. The cryovial was stored in -80°C freezer overnight before being moved into a -196°C liquid nitrogen storage tank.

3.2.4 Human Lung Fibroblast Cell Line (MRC-5) (ATCC ® CCL-171™)

MRC-5, a human normal lung fibroblast cell line was purchased from the ATCC. The cells were cultured in growth medium composing of Eagle's Minimum Essential Medium (EMEM) (ATCC, USA) supplemented with 10% FBS (Gibco, Invitrogen, USA) at 37°C in a humidified 5% CO₂ incubator. The cells were cultured at seeding density of 1×10^4 cells/ml upon received and were maintained by replacement of fresh medium every 3 to 4 days. When the confluency reached 70-80%, the cells were sub-cultured. MRC-5 cells were cryopreserved with freezing medium containing 95% complete growth medium and 5% DMSO. The cryovial was kept in -80°C freezer for one night prior to being stored in a liquid nitrogen tank at -196°C.

3.3 Characterisation of human Umbilical Cord-Derived Mesenchymal Stromal Cells (hUCMSC)

3.3.1 Immunophenotyping

Umbilical cord-derived MSC at passage three to six were used for the analysis of their phenotypic properties. Cryopreserved MSC were thawed and washed twice with 1X phosphate-buffered saline (PBS) (Gibco, USA). Aliquots of MSC (5×10^5 cells in 100 μ l PBS) were prepared in each flow tube. Analysis was carried out using BD Stemflow™ hMSC Analysis Kit (Becton Dickinson, USA). Briefly, cells in the tubes were stained with fluorochrome conjugated monoclonal antibodies accordingly and incubated on ice for 30 minutes. The antibodies used were CD73, CD90, CD105, CD34, CD11b, CD19, CD45, HLA-DR and CD44. Mouse isotype antibodies served as control. After incubation, the cells were washed twice with 1X PBS in order to remove excess antibodies. The supernatant was discarded and the cells were resuspended in 300 μ l of 1X PBS and subjected to flow cytometric analysis using FACSDIVA Software (Becton Dickinson, USA).

3.3.2 Trilineage Differentiation

3.3.2.1 Adipogenic Differentiation

Aliquots of 1.0×10^5 cells from early passage (P3-P6) were seeded into each of the wells in a 6-well plate. Cells were cultured in complete medium (90% DMEM

+ 10% FBS + 1% Glutamax + 1% Penicillin-Streptomycin) at 37°C, 5% CO₂ until they were approximately 90-95% confluent. Adipogenic induction medium (AIM) was prepared from DMEM/F12 medium (Gibco, Invitrogen, USA) supplemented with 10% FBS, 1% L-Glutamine, 1% Penicillin-Streptomycin, 1.0µM dexamethasone (Stemcell Technologies, Canada), 100µM indomethacine (Sigma-Aldrich, USA) and 0.25mM 3-isobutyl-1-methylxantine (Sigma-Aldrich, USA). AIM was filtered with 0.2 µm filter unit (Sartorius, Germany) prior to usage. The growth medium was then replaced with 2ml of AIM per well. The medium was changed every alternate day for 21-28 days and monitored daily using microscope for the presence of lipid droplets. Cells maintained in regular growth medium served as negative control.

After 21-28 days of induction, the cells were stained with Oil Red O to observe any lipid droplets formed. The working solution for Oil Red O was prepared by mixing 3 volumes of Oil Red O solution (Sigma Adrich, USA) with 2 volumes of deionised water (Millipore, USA). The working solution was allowed to settle down in room temperature for 10 minutes and were to be used within 2 hours. In order to eliminate the sediment, the working solution was filtered with filter paper or syringe filter before use. The culture medium was discarded and the cells were washed twice with 1X PBS followed by fixation with 4% paraformaldehyde (Sigma Adrich, Germany) for 30 minutes at room temperature. Then, the 4% paraformaldehyde was discarded and the cells were washed thrice with deionised water followed by incubation with 60% isopropanol (Nacalai tesque, Japan) for 5 minutes. One millilitre of Oil Red O working solution was added into each well of the 6-well plate to stain the cells for 30 minutes. After

incubation, the excessive staining was washed with deionised water. Staining results were evaluated and images were captured using Nikon eclipse TS100 microscope.

3.3.2.2 Osteogenic Differentiation

The hUCMSC cultures at passage three to six were used for osteogenesis. The experiments were carried out using the MesenCult[®] Stimulatory Kit, Human (Stemcell Technologies, Canada) with some modification on the manufacturer's protocol. Briefly, 3×10^4 to 4×10^4 cells were seeded in a well of a 6-well plate and cultured at 37°C, 5% CO₂ with $\geq 95\%$ humidity until the cells were approximately 90-98% confluent. This took about 1-5 days. The medium was then replaced with 2ml of complete Osteogenic Induction Medium (OIM) per well. The OIM consisted of Mesencult[®] MSC Basal Medium supplemented with Osteogenic Supplements, 10^{-4} M dexamethasone, 10mg/ml ascorbic acid (Stemcell Technologies, Canada) and 1M β -Glycerophosphate (Stemcell Technologies, Canada). The medium was changed every 3-4 days until bone matrix formation occurs (approximately 10-15 days). Cells cultured in regular growth medium served as negative control.

At the end of the experiment, Alizarin Red S was used to stain the matrix mineralisation associated with osteoblasts. The medium from each well was removed carefully and the cells were washed twice with 1X PBS. The cells were then fixed with 10% formalin (Nacalai tesque, Japan) and incubated for 15 minutes at room temperature. Next, the fixative was removed and the cells were

rinsed with excess of distilled water. Alizarin Red S solution (Millipore, USA) was then added into the well and incubated for 20 minutes. The excessive staining solution was removed completely and the cells were washed four times with deionised water. During each wash, the plate was swirled gently for 5 minutes. Then, 1.5ml of water was added into each well to prevent cells from drying. Staining results were evaluated and images were captured using Nikon eclipse TS100 microscope.

3.3.2.3 Chondrogenic Differentiation

The hUCMSC cultures at passage three to six were used for chondrogenesis. The experiments were carried out using the MesenCult™-ACF Chondrogenic Differentiation Kit (Stemcell Technologies) with some modification on the manufacturer's protocol. Aliquots of 1×10^5 cells were resuspended in 10µl of complete medium (90% DMEM + 10% FBS + 1% Glutamax + 1% Penicillin-Streptomycin) and dropped into the center of a well on a 24-well plate. The cells were allowed to adhere for 2-3 hours at 37°C, 5% CO₂. The medium was then carefully aspirated without disturbing the pellet and replaced with 1ml of complete Mesencult™ -ACF Chondrogenic Differentiation Medium per well which composed of the Mesencult™ -ACF Chondrogenic Differentiation Basal Medium and Mesencult™ -ACF 20X Chondrogenic Differentiation Supplement. The medium was changed every 3-4 days for 2 weeks. Cells cultured in regular growth medium served as negative control. Chondrogenic differentiation medium was completely removed from each well and cell pellet was fixed for 15 minutes at room temperature with Kahle's fixative, which contained 150ml

of double distilled water, 65ml of 95% ethanol (Sigma-Aldrich, USA), 30ml of formalin (Sigma-Aldrich, USA) and 25ml of acetic acid (Merck, Germany). The cell pellet was then washed with 1X PBS for three times. Subsequently, Alcian Blue solution (Millipore, USA) was added to the fixed cells and incubated for 30 minutes in the dark. The excessive staining solution was removed by washing with 0.1M of HCl (Fisher Scientific, UK). The cells were observed using Nikon eclipse TS100 microscope and Nikon stereomicroscope SMZ445. Images were captured for analysis.

3.4 Plasmids

3.4.1 Plasmid Encoding hIL-12 Gene

One vial of lyophilised plasmid DNA containing 20 μ g of pUNO1 bearing the human IL-12 elasti (p40: p35) gene was purchased from InvivoGen (InvivoGen, USA). Plasmid pUNO1-hIL12 (Figure 3.2) is an expression vector containing human interleukin-12 (hIL-12) open reading frame. The size of the inserted hIL-12 gene is 1646 bp. This plasmid contained EF-1 α / HTLV hybrid promoter comprised the Elongation Factor-1 α (EF-1 α) promoter and 5' untranslated region of the Human T-Cell Leukaemia Virus (HTLV). It is expressed at high levels in all cell cycles and lower levels during the G0 phase. The promoter is also non-tissue specific. Hence, it is highly expressed in all cell types. This hybrid promoter not only increases steady state transcription, but also significantly increases translation efficiency possibly through mRNA stabilisation. The plasmid pUNO1-hIL12 also contained blasticidin-resistance

gene (bsr) driven by the CMV promoter/enhancer in tandem with the bacterial EM7 promoter. This allows the amplification of the plasmid in *E. coli*, as well as the selection of stable clones in mammalian cells using the same selective antibiotic. Other features of this plasmid are detailed in Appendix A1.

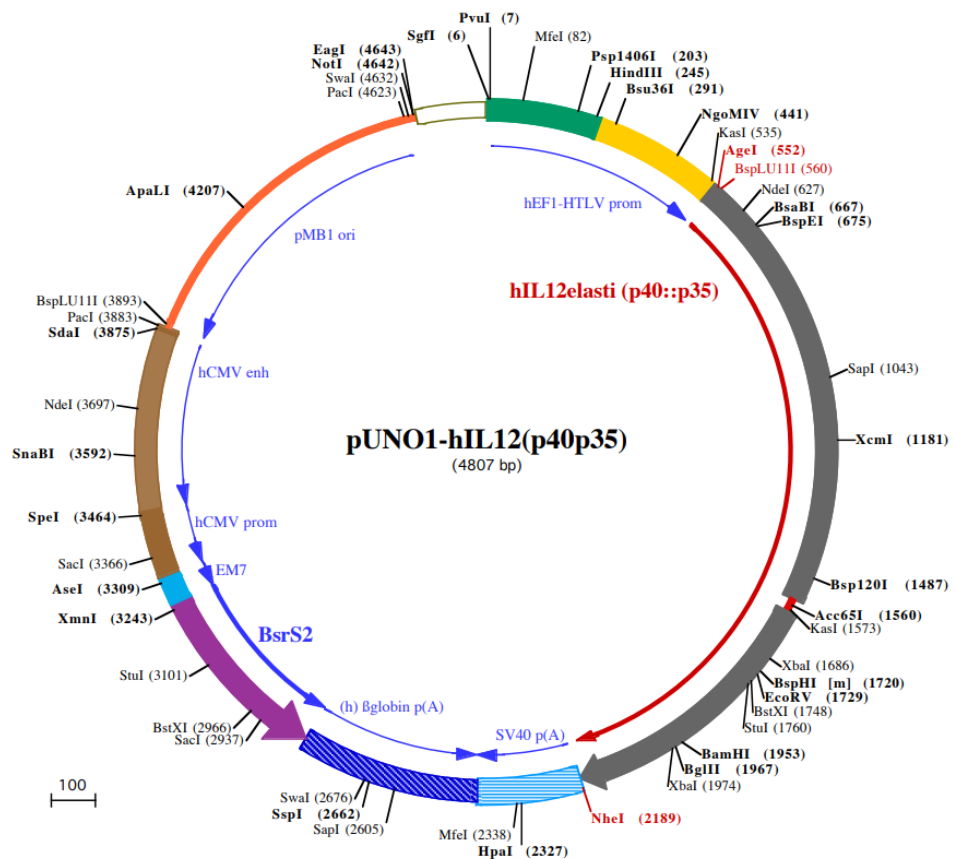


Figure 3.2 Restriction map of pUNO1-hIL12 plasmid.

3.4.1.1 Liquid Media

E. coli Fast-Media® Blas Terrific Broth (InvivoGen, USA) was used to prepare LB media with blasticidin (InvivoGen, USA). To prepare 200ml of liquid media containing blasticidin, one pouch of the Fast-Media® Blas Terrific Broth was

poured into a beaker and 200ml of double distilled water was added into it. The mixture was mixed by gently swirling the beaker. Then, the beaker containing the mixture was put into a microwave oven to heat up with medium power setting until the medium was completely dissolved. The medium was cool down to 37°C prior to use in the seeding of the bacteria.

3.4.1.2 Solid media

E.coli Fast-Media® Blas Agar (InvivoGen, USA) was used to prepare agar plates with blasticidin. To prepare 200ml of agar medium containing blasticidin, one pouch of the Fast-Media® Blas agar was poured into a beaker and 200ml of double distilled water was added into it. The mixture was mixed by gently swirling the beaker. Then, the beaker containing the mixture was put into a microwave oven to heat up with medium power setting until the medium was completely dissolved. The medium was cool down to 45°C before pouring on plates.

3.4.1.3 Growth and Storage of pUNO1-hIL12-transformed Bacteria

E.coli competent cells transformed with pUNO1-hIL12 was plated on Fast-Media® Blas agar plates and incubated at 37°C overnight. On the next day, single colony of the bacteria was isolated and allowed to culture overnight at 37°C in Fast-Media® Blas Terrific Broth containing blasticidin. For long term storage of pUNO1-hIL12-transformed *E.coli*, 500µl of pUNO1-hIL12-

transformed *E.coli* culture and 500µl of 50% sterilised glycerol (Biobasic, Germany) were added into a cryovial. The vial was vortex vigorously to ensure even mixing before freezing at -80°C. The Wizard® *Plus* SV Minipreps DNA Purification System (Promega, USA) was used to harvest and isolate pUNO1-hIL12 plasmid DNA from the overnight bacteria culture.

3.4.2 Plasmid Encoding Green Fluorescence Protein (GFP)

An agar stab containing the bacteria with mammalian expression vector for expression of GFP was purchased from Addgene (Addgene, USA). Plasmid pCMV-GFP (Figure 3.3) is a mammalian expression vector containing CMV promoter-EGFP gene. The size of this gene is 1400 bp. Plasmid pCMV-GFP has cytomegalovirus immediate early promoter. This plasmid also contained the ampicillin resistance gene which allows the selection of the plasmid from bacteria culture. Other features of this plasmid are detailed in Appendix A2.

3.4.2.2 Solid media

E.coli strains can be grown on LB agar (1st Base, Singapore) containing appropriate antibiotic. To prepare 10 LB agar plates, 4.4g of LB agar powder was dissolved in 120ml of double distilled water and autoclaved at 121°C for 30 minutes. The solution was allowed to cool to 55°C and antibiotic was then added into it. Then, the LB medium containing antibiotic were poured into sterile 90mm petri dishes in a laminar hood and allowed to solidify. The LB plates containing antibiotic were put in a sealed bag and stored at 4°C.

3.4.2.3 Antibiotic

E.coli containing pCMV-GFP plasmid were grown in medium containing ampicillin. A stock solution of 100 mg/ml ampicillin (GoldBio, USA) was made by dissolving 2.5g of ampicillin in 25 ml of sterile UltraPure™ DNase/RNase-Free Distilled Water (Invitrogen, USA), filtered and stored in -20°C. The working concentration of ampicillin used to culture pCMV-GFP transformed *E.coli* was 100µg/ml.

3.4.2.4 Growth and Storage of pCMV-GFP-transformed Bacteria

E.coli competent cells transformed with pCMV-GFP was plated on LB-ampicillin agar plates and incubated at 37°C overnight. On the next day, single colony of the bacteria was isolated and allowed to culture for 16 to 18 hours at

37°C in LB broth containing ampicillin with vigorous shaking. For long term storage of pCMV-GFP-transformed *E.coli*, 500µl of pCMV-GFP-transformed *E.coli* culture and 500µl of 50% sterilised glycerol were added into a cryovial. The vial was vortex vigorously to ensure even mixing before freezing at -80°C. The Wizard® Plus SV Minipreps DNA Purification System was used to harvest and isolate pCMV-GFP plasmid DNA from the overnight bacteria culture.

3.4.2.5 Verification of Plasmid using sequencing

The concentration and purity of the extracted plasmid DNA were measured using spectrophotometer, Nanodrop 2000 (Thermo Scientific, USA), prior to sequencing. The acceptable range for ratio of A260/A280 for pure DNA was 1.8 to 2.0. The extracted pCMV-GFP were sent for sequencing using the following primer:

5' sequencing primer: CGCAAATGGGCGGTAGGCGTG (CMV-F)

3.5 Generation of Genetically Engineered Human Umbilical Cord-Derived Mesenchymal Stromal Cells Expressing Human Interleukin-12 (hUCMSC-IL12)

3.5.1 Adenoviral Method

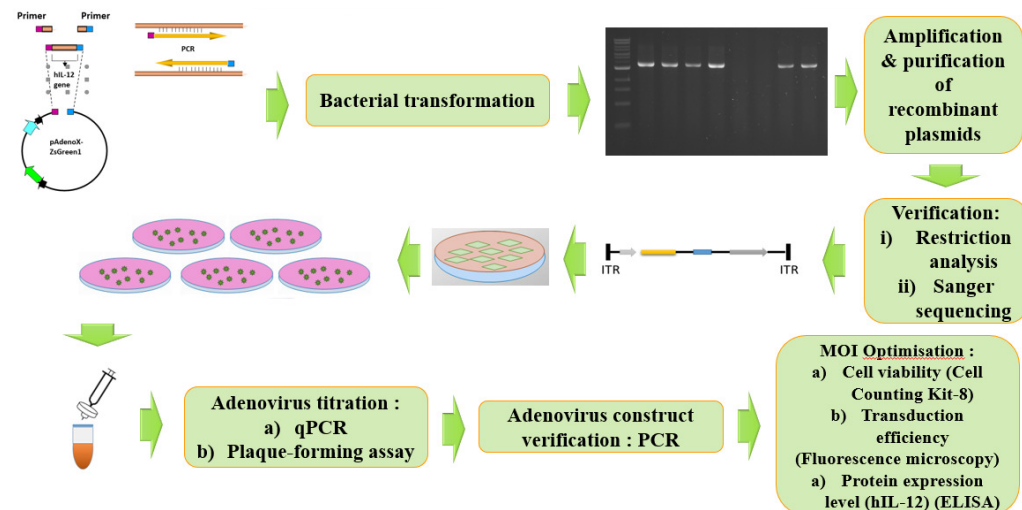


Figure 3.4 Production of recombinant adenovirus.

3.5.1.1 PCR Primer Design and Amplification

PCR primers to amplify the hIL-12 gene were designed and synthesised in such a way that each end of the PCR product generated shared 15 bp of homology with the one end of the linearised pAdenoX-ZsGreen1 vector. The amplification of hIL-12 gene was performed using CloneAmp HiFi Premix (Clontech, USA) in Applied Biosystems Veriti Thermal Cycler (Thermo Fisher Scientific, USA). PCR mixture, PCR cycle profile and PCR primers (Bioneer, Korea) used are summarised in the Tables 3.1, 3.2 and 3.3 respectively.

Table 3.1 PCR mixture components

Reagent	Volume	Final Concentration
CloneAmp HiFi PCR Premix	12.5 µl	1X
Primer 1	5 - 7.5 pmol	0.2 - 0.3 µM
Primer 2	5 - 7.5 pmol	0.2 - 0.3 µM
Template	< 100 ng	
DNase/RNase-free water	Up to 25 µl	
Total volume per reaction	25.0 µl	

Table 3.2 PCR cycle profile

Cycle Steps	Temperature	Time	Cycles
Initial denaturation	98°C	5 minutes	1
Denaturation	98°C	10 seconds	} 35
Annealing & Extension	72°C	35 seconds	
Final Elongation	72°C	5 minutes	1
	4°C	Hold	

Table 3.3 PCR primer sequences

Primer	Sequence	Length (bp)
hIL-12 forward	5'- GTA ACTATAACGGTC CTGAGATCACCGGTCAACATGTG-3'	38
hIL-12 reverse	5'- ATTACCTCTTTCTCC GAGGGACCTCGCTTTT TAG-3'	36

Note: Sequence highlighted in red indicates the 15 bp homology with the one end of the linearised pAdenoX-ZsGreen1 vector.

3.5.1.2 Purification of PCR Fragment

Agarose gel electrophoresis was conducted to analyse the PCR products and visualised under ultraviolet light. The DNA bands were excised and purified using Nucleospin Gel and PCR Clean-up kit (Macherey-Nagel, Germany) according to the manufacturer's protocol. Briefly, the weight of the excised DNA fragment was determined and the fragment was then transferred into a clean tube. 200 µl of Buffer NTI was added into the tube and incubated at 50°C for 5 to 10 minutes. The sample was vortexed briefly every 2 to 3 minutes until the gel slice was completely dissolved. Next, the sample was loaded into the NucleoSpin Gel and Clean-up Column and centrifuged at 11,000 xg, 30 seconds. After centrifugation, the sample was washed with Buffer NT3 and eluted using Buffer NE. The concentration and purity of the extracted DNA was determined using Nanophotometer (Implen, Germany). The ratio of A260/A280 for pure DNA was generally accepted to be in the range of 1.7-1.9.

3.5.1.3 In-Fusion Cloning of Purified PCR Fragments

In-Fusion reactions (Table 3.4) were set up in 0.2 ml PCR tubes and incubated at 50°C for 15 minutes, then placed on ice immediately. The tubes were stored in -20°C before the transformation step. The Adeno-X Control Fragment consisted of a complete *lacZ* gene flanked by 15 bp of sequence homologous to the ends of pAdenoX-ZsGreen 1 vector. It is designed as a cloning control, but

the gene will also be expressed in the CMV Systems so *lacZ* expression can be assayed in these systems.

Table 3.4 In-Fusion cloning reaction

Reagent	Reagent Volume (μl per sample)	
	Cloning reagent (hIL-12)	Cloning reagent (control)
Deionised water	6	5
Linearised pAdenoX-ZsGreen1	1	1
hIL-12 PCR insert (102 ng/ μl)	1	0
Control fragment, <i>lacZ</i> (50 ng/ μl)	0	2
5X In-Fusion HD Enzyme Premix	2	2
Total volume per reaction	10	10

3.5.1.4 Transformation Using StellarTM Competent Cells

The recombinant plasmids (pAdenoX-hIL12 and pAdenoX-lacZ) were transformed into Stellar Competent Cells. Briefly, 1.5 μl of In-Fusion reaction mixture was added into 100 μl of Stellar cells. The cells were incubated on ice for 30 minutes, followed by heat shock at 42°C for 45 seconds and incubated on ice again for 2 minutes. Subsequently, SOC medium (Invitrogen, USA) was added and the cells were incubated at 37°C and shaken at 250 rpm for 1 hour. Next, 100 μl of cell suspension was plated on LB ampicillin plate and incubated overnight at 37°C.

3.5.1.5 Screening of Clones Using PCR

On the next day, 5-8 single colonies were picked and transferred into 40 µl of deionised water. Twenty microlitres of the suspension was transferred into 5 ml of liquid LB medium containing 100 µg/ml ampicillin (LB/Amp) and incubated at 37°C with shaking for 6 to 8 hours. PCR colony screening was performed using Terra™ PCR kit (Takara Bio, USA). PCR master mix was set up by using 5 µl of each clone (Table 3.5) and proceeded for thermal cycling as follows:

Table 3.5 PCR mixture components

Reagent	Reagent Volume (µl per sample)
Deionised H ₂ O	7
Adeno-X Screening Primer Mix 3 (10 µM)	0.5
Template (bacterial culture)	5
Terra PCR Direct Red Dye Premix	12.5
Total volume per reaction	25

Table 3.6 PCR Thermal cycling

Cycle Steps	Temperature	Time	Cycles
Initial denaturation	98°C	2 minutes	1
Denaturation	98°C	10 seconds	} 35
Annealing & Extension	68°C	3 minutes	
Final Elongation	68°C	5 minutes	1
	4°C	Hold	

Next, 5 µl of each PCR reaction was analysed on a 1.0% agarose gel. The expected band sizes of the recombinant plasmids are shown in Table 3.7.

Table 3.7 Expected results of PCR colony screening analysis

Gene of interest	Expected Band Sizes When Cloning into pAdenoX-ZsGreen1 vector (1.9 kb)	
	Recombinant	Non-recombinant
hIL-12	3.5 kb	1.6 kb
lacZ (control fragment)	4.9 kb	3.0 kb

3.5.1.6 Verification of Recombinant Plasmid using Restriction Analysis

After the positive clones were identified by PCR, the clones were amplified by transferring the initial culture into 100 ml of liquid LB/Ampicillin medium and incubated overnight in a shaking incubator at 37°C with speed of 260 to 280 rpm. Next, the plasmids were purified using the NucleoBond Xtra Plasmid Midi Kit (Macherey-Nagel, Germany) according to the manufacturer's protocol. The identities of the purified recombinant plasmids were verified by individual digestions with XhoI (Promega, USA) and NheI (New England Biolabs, USA) restriction analysis. The digested products were separated on a 1% agarose gel and viewed using UVP Biospectrum AC Chemi HR410 Imaging System (Analytik Jena, Germany).

3.5.1.7 Verification of Recombinant Plasmid Using Sequencing

The purified recombinant plasmids were also sent for Sanger sequencing. For this purpose, 1 µg of each of the purified plasmids were sent to NHK Bioscience, Malaysia. Table 3.8 shows the primers used for the Sanger sequencing of each recombinant plasmid. Nucleotide sequence results were later analysed using

NCBI BLAST to confirm that the inserted gene of interest corresponded with the published sequence.

Table 3.8 Primer sequence for Sanger sequencing

Recombinant plasmid	Primers
pAdenoX-hIL-12	5' - tgcacaccacagaagtaaggtcc - 3'
	5' - tagtgtggcggaagtgtgatgttc - 3'
	5' - gggaacattcctgggtctg - 3'
	5' - gattgtcgtcagccaccag - 3'
pAdenoX-lacZ	5' - tgcacaccacagaagtaaggtcc - 3'
	5' - tagtgtggcggaagtgtgatgttc - 3'

3.5.1.8 Digestion of Recombinant Plasmids with PacI Restriction Enzyme

The recombinant plasmids (pAdenoX-hIL12 and pAdenoX-lacZ) were digested with PacI restriction enzyme (New England Biolabs, USA) before the adenovirus packaging can be performed. The purpose of this digestion is to expose the inverted terminal repeats (ITRs) located at either end of the adenoviral genome and release the adenoviral genome from the plasmid backbone. The ITRs contain the origins of adenoviral DNA replication and must be positioned at the termini of the linear Ad DNA molecule to support the formation of the replication complex. The PacI restriction enzyme digestion set-up is as shown in Table 3.9 below:

Table 3.9 Digestion set-up for restriction enzyme PacI

Component	Volume (µl)
pAdenoX-hIL12 or pAdenoX-lacZ (500ng/µl)	2 (1µg)
10X Neb buffer 2.1	5 (1X)
PacI	1
Nuclease-free water	42
Total	50

The above reaction was prepared in 5 tubes and incubated at 37°C for 15 minutes. The content for all the 5 tubes were combined into one tube and 5µl was taken to analyse on a 1% agarose gel. The plasmid portion of the recombinant pAdenoX vector will migrate at ~ 3 kb, while the adenoviral genome will not enter the gel, but will remain at the top of the lane. The remaining content from the digestion reaction was subjected to pAdenoX DNA extraction. In brief, 60 µl of 1X TE Buffer (pH 8.0) (Invitrogen, USA) was added into the reaction tube followed by 100 µl phenol: chloroform: isoamyl alcohol (25:24:1) (Amresco, USA) The mixture was vortexed and centrifuged at 14,000 rpm for 5 minutes at 4°C to separate phases. After centrifugation, the top aqueous layer was transferred into a clean sterile 1.5 ml microcentrifuge tube and 400 µl 95% ethanol, 25 µl of ammonium acetate (NH₄OAc) (Nacalai tesque, Japan), and 4 µl polyacrylamide (5 mg/ml) (Biorad, USA) were added. Then, the mixture was centrifuged again at 14,000 rpm and 4°C for 5 minutes. Supernatant was discarded and the pellet was washed with 300 µl 70% ethanol followed by centrifugation again at 14,000 rpm for 2 minutes. The extracted DNA was dissolved in TE buffer and kept in -20°C.

3.5.1.9 Transfecting HEK 293 Cells with PacI-Digested Recombinant Plasmids

One day before transfection, HEK 293 cells were plated on a 6-well plate with seeding density of 4.5×10^5 cells per well. The cells should be 50% to 70% confluent, display a flat morphology, and adhere well to the plate prior to transfection. The plates were incubated overnight at 37°C, 5% CO₂. On the following day, the transfection was performed using calcium phosphate method. The transfection reagents (2M CaCl₂ solution and 2X HBS) were prepared as follows:

- i) 2.94g of CaCl₂·2H₂O (MW=147.02 g/mol) (Amresco, USA) was dissolved in 10ml of deionised water and filtered sterilised. The solution was then kept in 4°C (shelf life: 1 week).
- ii) 100ml of 2X HBS was prepared with the following components added into 90ml of deionised water.

280mM NaCl (Amresco, USA)	1.636g
1.5mM Na ₂ HSO ₄ (Sigma-Aldrich, USA)	0.022g
50mM HEPES (Nacalai tesque, Japan)	1.192g

The pH of the solution was adjusted to 7.08-7.10 then topped up to 100ml with deionised water. The solution was filtered sterilised and aliquoted into smaller amount and kept in -20°C.

Solution A and B were then prepared as shown in Table 3.10 below:

Table 3.10 Components of solution A and B

Solution A	Solution B
1 - 3 µg plasmid DNA	2X HBS
Sterile water	
12.4 µl 2M CaCl ₂	
Total: 100 µl	Total: 100 µl

Solution A was vortexed slowly and carefully while adding in solution B dropwise. The transfection solution was incubated for 15 minutes. After incubation, the solution was vortexed gently and added drop by drop into the culture plate. The cells were incubated overnight at 37°C, 5% CO₂. On the next day, the calcium phosphate-containing medium was removed. The cells were washed with medium or 1X PBS and replaced with fresh complete culture medium and continue incubation at 37°C, 5% CO₂. The cytopathic effect (CPE) of the cells was checked frequently and the transfection efficiency was monitored using fluorescence microscopy. When the late CPE was observed, the cells were harvested by three freeze-thaw cycles and stored in -20°C. Primary amplification was performed by infecting HEK 293 cells in a 90mm culture plate with 250 µl of cell lysate (50% of the harvested lysate). Cells were incubated at 37°C, 5% CO₂ and the CPE was checked daily. When >50% of the cells have detached from the plate, “Primary Amplification” viral stock was prepared by harvesting the cells after three freeze-thaw cycles to lyse the cells. The cell lysate was aliquoted into multiple small volume and stored in -20°C.

3.5.1.10 Titration of Recombinant Adenovirus

Titration of the recombinant adenovirus was performed using Adeno-X qPCR Titration kit (TakaraBio, USA) according to the manufacturer's protocol. The Nucleospin Virus purification kit was used to purify the viral genomic DNA. Next, serial dilutions of the viral DNA sample (Table 3.11) were subjected to qPCR following the thermal cycling condition in Table 3.12 to determine the threshold cycle (Ct) for each dilution. The DNA copy number in a diluted sample is then determined from a standard curve generated by plotting the Ct values of the diluted Adeno-X DNA Control Template against their respective copy numbers.

Table 3.11 Control and sample dilutions for qPCR

Well	Strip 1	Strip 2	Strip 3
1	5×10^7	5×10^7	Sample (1X)
2	5×10^6	5×10^6	Sample (1X)
3	5×10^5	5×10^5	Sample (0.1X)
4	5×10^4	5×10^4	Sample (0.1X)
5	5×10^3	5×10^3	Sample (0.01X)
6	NTC	Sample (0.0001X)	Sample (0.01X)
7	NTC	Sample (0.0001X)	Sample (0.001X)
8	Sample (0.00001X)	Sample (0.00001X)	Sample (0.001X)

Table 3.12 Thermal cycling conditions for qPCR using ABI StepOnePlus Real-Time PCR System

Cycle Steps	Temperature	Time	Cycles
Initial denaturation	95°C	30 seconds	1
qPCR	95°C	3 seconds	40
	60°C	31 seconds	
Melting/Dissociation curve	95°C	15 seconds	1
	60°C	1 minute	
	95°C	15 seconds	

3.5.1.11 Amplification of Recombinant Adenovirus for High Titer Viral Stocks

One day before transduction, HEK 293 cells were seeded in five 150mm culture plates with cell density 12.5 to 14 million of cells per plate. The cell monolayer should be 50-70% confluent for optimal transduction. On the following day, the medium was replaced with 30ml of fresh growth medium containing recombinant adenovirus (AdhIL-12 or AdlacZ). For best results, the cells should be infected at a multiplicity of infection (M.O.I) ≥ 5 . The cells were incubated for 90 minutes at 37°C, 5% CO₂. Then, the flasks were added with 10ml of fresh growth medium and incubated for 3-4 days at 37°C, 5% CO₂. The CPE was checked daily. When >50% of the cells have detached from the surface of the flasks, they were lysed with three consecutive freeze-thaw and the lysate was collected for purification.

3.5.1.12 Purification of High Titer Recombinant Adenovirus Stocks

The purification of recombinant adenovirus (AdhIL-12 or AdlacZ) was carried out using Adeno-X Maxi Purification kit (TakaraBio, USA) according to the manufacturer's protocol. Briefly, 5µl of Benzonase Nuclease was added to the harvested cells which were resuspended in 5ml of culture media. The mixture was incubated at 37°C for 30 minutes. The sample was then diluted with equal volume of 1X Dilution Buffer and filtered through the 0.45µm syringe-tip pre-filter. Subsequently, the clarified lysate was purified using the equilibrated purification filter by pushing the lysate through the filter at a rate of ~3ml/min to allow the virus particles to bind to the filter membrane. The filter was washed with 20ml of 1X Wash Buffer and finally the recombinant virus particles were eluted with 3ml of 1X Elution Buffer. Eluted recombinant virus particles were aliquoted into multiple microcentrifuge tubes in small volume and stored in -80°C.

3.5.1.13 Verification of Recombinant Adenovirus Construct

The recombinant virus constructs were verified using PCR method. The PCR was performed using Terra™ PCR kit (Takara Bio, USA) with gene of interest-specific primers. The PCR master mix was set up by using 2.5 µl of purified recombinant adenovirus (Table 3.13) and proceeded for thermal cycling using parameters shown in Table 3.14.

Table 3.13 PCR mixture components for recombinant adenovirus construct verification

Reagent	AdhIL-12	AdlacZ
	Reagent Volume (μl per sample)	
Deionised H ₂ O	2.75	3.25
Adeno-X Screening Primer Mix 3 (10 μM)	-	0.5
Forward primer hIL12 (7.5 μM)	0.5	-
Reverse primer hIL12 (7.5 μM)	0.5	-
Template (Ad)	2.5	2.5
Terra PCR Direct Red Dye Premix	6.25	6.25
Total volume per reaction	12.5	12.5

Table 3.14 PCR Thermal cycling

Cycle Steps	Temperature	Time	Cycles
Initial denaturation	98°C	2 minutes	1
qPCR	98°C	10 seconds	30
	68°C	3 minutes	
Melting/Dissociation curve	68°C	5 minutes	1

Next, 5 μl of each PCR reaction was analysed on a 1.0% agarose gel. The expected band sizes of the PCR products are shown in Table 3.15.

Table 3.15 Expected band sizes of PCR products

Gene of interest	Size (bp)
hIL-12	1646
Recombinant AdlacZ	4900
lacZ	3000

3.5.1.14 Functional Titration of Recombinant Viruses

One day before infection, 1×10^6 of HEK 293 cells were plated in each well of a 6-well plate. On the day of infection, the cell confluency should be 80-100%. The cells in each well of the 6-well plate were infected with 100 μ l of 10-fold dilution of the recombinant adenoviruses (AdhIL-12 / AdlacZ), ranging from 10^4 to 10^8 (Figure 3.5). The plates were incubated at 37°C for 4-16 hours. After the incubation, the media containing viruses were removed. Two millilitre agarose overlay was applied into each well. The plates were incubated again at 37°C. Another 1 ml per well of agarose overlay was applied after 2-4 days following the initial overlay and continued to incubate at 37°C up to 7 days. The cells were stained with MTT solution (Sigma-Aldrich, USA) and the plaques were counted to determine the functional titer using the formula below:

Functional titer (ifu/ml)

= No. of plaques / (Volume of virus added to the well) x (dilution)

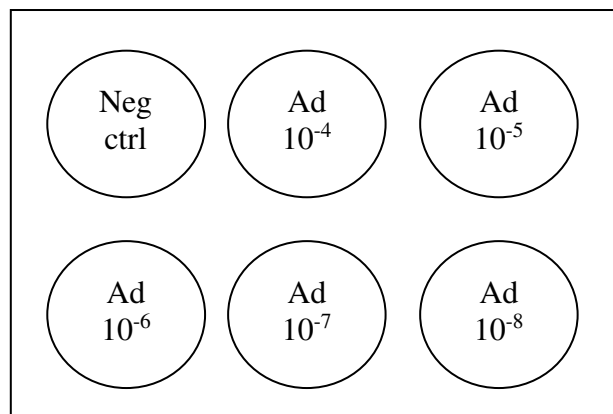


Figure 3.5 Layout of the 6-well plate for plaque forming assay.

3.5.1.15 Optimisation of Multiplicity of Infection (MOI) of Recombinant Adenoviruses

The hUCMSC (passage 3 to 5) were plated at the density of $4-5 \times 10^3$ cells per well of a 96-well plate in the presence of standard MSC growth media (Figure 3.6). After reaching 50%-80% confluency, the cells were transduced with AdhIL-12 or AdlacZ in 50 μ l of growth media per well at 0.5, 10, 20, and 50 MOI. After 4 hours incubation at 37°C, 5% CO₂, 50 μ l of fresh growth media was added to each of the well. On day 3 and 5 after transduction, the supernatant of the culture was collected for analysis of hIL-12 protein expression. The cells were analysed for GFP expression (transduction efficiency) and cell viability on day 3 and 5 post transduction.

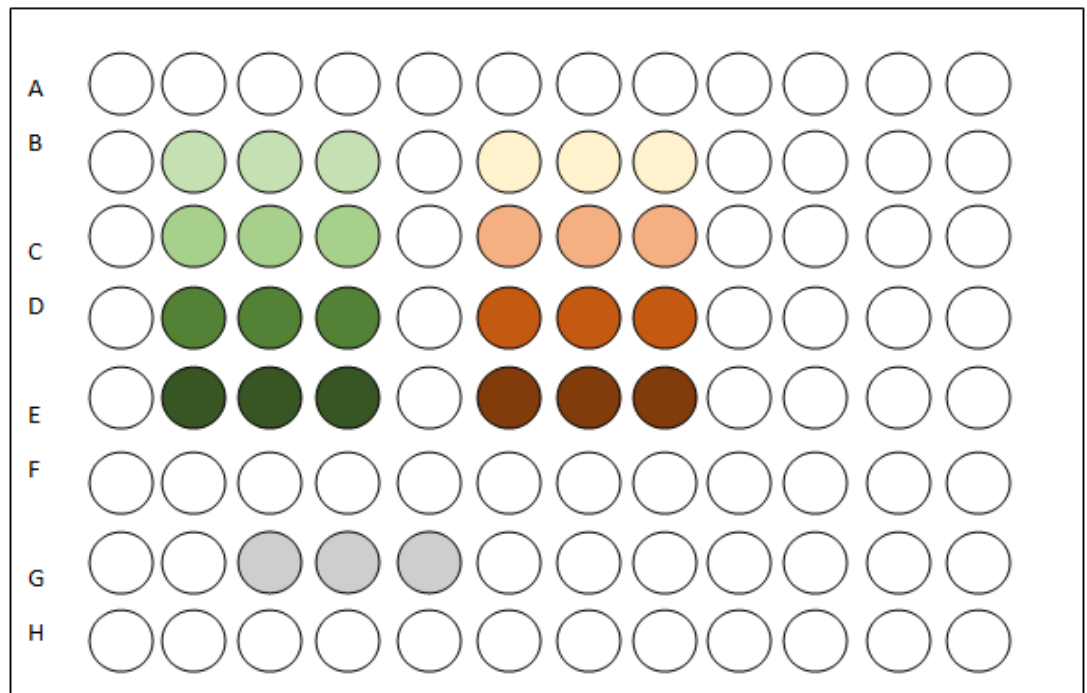




Figure 3.6 Layout of the 96-well plate for MOI optimisation assay

a) Determination of Transduction Efficiency

In order to check for transduction efficiency, the transduced hUCMSC were fixed with 4% paraformaldehyde for 10 minutes and followed by staining with 5µM DAPI (Abcam, UK) for 30 minutes. Then, the cells were viewed under fluorescence microscope (Carl Zeiss, Germany) and photos of each well were snapped for analysis. For quantification, at least 3 separate fields were counted in each transduced sample. The percentage of transduction efficiency was calculated using the formula as below:

$\frac{\text{DAPI + GFP positive cells}}{\text{DAPI positive cells}} \times 100\%$
--

b) Human Interleukin-12 (hIL-12) Protein Expression Level

On day 3 and 5 after transduction with AdhIL-12, the culture supernatant of each well was collected and centrifuged at 2,000 xg for 10 minutes to remove

the cell debris. After centrifugation, the supernatant was collected and stored in -20°C or below for ELISA assay later.

The hIL-12 level was measured using Human IL-12 (p70) ELISA Max Deluxe kit (Biolegend, USA) according to the manufacturer's protocol. Due to the wide range of hIL-12 concentration among the samples, different dilutions were used for the ELISA assay.

One day prior to the ELISA assay, the wells of a 96-well plate were coated with diluted capture antibody. The plate was sealed and incubated overnight (16-18 hours) at temperature 2°C to 8°C. On the next day, the plate was washed 4 times with at least 300 µl of wash buffer and tapped upside down on absorbent paper to remove the solution. Two hundred microlitres of assay diluent A was added into each well to block non-specific binding and to reduce background noise. Then, the plate was sealed and incubated at room temperature for 1 hour with shaking on a plate shaker followed by 4 times of washing using wash buffer. The wells were aspirated and washed 4 times again before addition of 100 µl per well of standards or samples. Serial dilutions of standard were performed by diluting 500 pg/ml of hIL-12 recombinant protein with assay diluent to make 7 standards (500, 250, 125, 62.5, 31.25, 15.63 and 7.81 pg/ml). All standards and samples were run in duplicate. Assay diluent was used as 0 pg/ml. The plate was sealed and incubated at room temperature for 2 hours with shaking. The wells were then aspirated and washed 4 times followed by addition of 100 µl per well of diluted detection antibody, sealed and incubated at room temperature for 1 hour with shaking. After the wells were aspirated and washed

for 4 times, 100 μ l of avidin-HRP was added into each well and incubated for 30 minutes at room temperature with shaking. The wells were finally washed for 5 times and 100 μ l of stop solution was added. The plate was read at 450 nm in a microplate reader (Tecan, USA). Data was analysed and standard curve was plotted with the absorbance of serial dilution of the standards against the concentration. Concentration of human IL12p70 from culture supernatant of hUCMSC expressing hIL12 was determined from the standard curve.

c) β -galactosidase Expression

On day 3 and 5 after transduction by AdlacZ, the expression of β -galactosidase was measured using the Luminescent Beta-galactosidase Reporter System 3 (Takara Bio, Japan) according to manufacturer's protocol. Briefly, the cells were harvested, resuspended in ice-cold lysate buffer and freeze-thawed for 3 cycles. After the freeze-thaw cycles, the cell lysate was collected and stored in -80°C until use. In order to perform the chemiluminescent β -galactosidase assay, 20-30 μ l of the individual cell lysates were aliquoted into wells of a white, opaque 96-wells flat-bottom microplate followed by 200 μ l of reaction buffer mixture added into each well. The plate was incubated at room temperature for 1 hour and luminescent measurement was carried out using the Infinite M200 Pro (Tecan, Switzerland).

d) Determination of Cell Viability

After the culture supernatant has been collected for ELISA assay, fresh medium was added into each well, followed by 10 µl of CCK-8 reagent (Dojindo, Japan). Wells with medium only were treated as blank. The culture plate was incubated at 37°C for 4 hours. After the incubation, the absorbance was measured at 450 nm with a microplate reader (Tecan, USA). The cell viability of the transduced UCMSC were calculated using the formula below:

$$\frac{\text{Absorbance of transduced hUCMSC} - \text{Absorbance of blank}}{\text{Absorbance of untransduced hUCMSC} - \text{Absorbance of blank}} \times 100\%$$

3.5.2 Electroporation Method

3.5.2.1 Electroporation Protocol

Early passage hUCMSC (P3-P5) were transfected with plasmids of interest using the Neon Transfection System (Thermo Fisher Scientific, USA). Prior to the electroporation, hUCMSC were harvested by trypsinisation and centrifugation for 5 minutes at 300 xg and the cell number was counted. The cells were washed with 1X PBS (without Ca²⁺ and Mg²⁺) by centrifugation again. Then, the cells were resuspended with Resuspension Buffer R at a final density of 2.0 X 10⁶ cells/ml. The Neon[®] Tube was set up by 3 ml of electrolytic buffer into the Neon[®] Pipette Station. As the size of Neon[®] Tip used was 100 µl, thus each

electroporation will be sufficient for plating of 10 wells in a 96-well plate setting. One hundred microlitres of cell suspension and 5 µg of plasmid DNA (pUNO1-hIL12 or pCMV-GFP, a positive control vector) were added into a 1.5 ml centrifuge tube and mix gently. The mixture was aspirated into the Neon® Tip which was installed on the Neon® Pipette. Following this, the Neon® Pipette was placed in the Neon® Pipette Station and electroporation was performed using the optimised setting of 1600V, 20ms, 1 pulse. Subsequently, 10 µl of transfected hUCMSC was transferred into each well of a prepared 96-well plate with 100 µl of pre-warmed fresh medium without antibiotics. The cells were incubated at 37°C in a humidified 5% CO₂ incubator. The transfection efficiency (refer to Section 3.5.1.15a), post-transfection cell viability (refer to Section 3.5.1.15d) and hIL-12 protein expression level (refer to Section 3.5.1.15b) were assessed on day 2 and day 4 after electroporation.

3.6 Determination of Inhibition Effect of hUCMSC Expressing hIL-12 on Human Lung Cell Lines



Figure 3.7 Timeline for co-culture experiment

Figure 3.7 outlined the timeline for co-culture experiment. The hUCMSC (passage 3 to 5) were plated at a density of 1.0×10^4 cells/well onto the transwell insert. During optimisation of effector cell and target cell ratio (E:T), target cells (H1975 human lung adenocarcinoma cells or MRC-5 human lung fibroblasts) were seeded in the bottom chamber of the transwell (24-well plate setting) in

500 µl of low glucose DMEM supplemented with 10% FBS and 1% Penicillin-Streptomycin, at different cell density with different effector (hUCMSC) to target ratio (E:T), namely 1:1, 2:1, 5:1 and 10:1. Upon the selection of the optimal E:T ratio, target cells were seeded in the bottom chamber of the transwell at the optimised E:T ratio. On the following day, the hUCMSC were transduced with AdhIL-12 and the transwell inserts were transferred onto the wells with target cells to initiate the co-culture on the same day. On day 3 and 5 after co-culture initiation, cell viability of target cells was determined using CCK-8 reagent (refer to Section 3.5.2.15d) while the culture supernatant was collected for analysis of hIL-12 protein expression (refer to Section 3.5.2.15b). The percentage of cell viability was calculated by averaging the optical density (O.D. absorbance) of duplicate wells of each experimental group using the following formula:

$\text{Percentage cell viability} = (A_{\text{treatment}} - A_{\text{blank}}) / (A_{\text{control}} - A_{\text{blank}}) \times 100\%$ <p>(where A=absorbance)</p>

The experiments were repeated for 3 hUCMSC biological replicates. Table 3.16 shows the experimental groups of the co-culture experiment.

Table 3.16 Experimental groups of co-culture experiment

	Transwell	Bottom chamber
Experiment 1	hUCMSC expressing hIL-12	H1975 cells or MRC-5 cells
Experiment 2	Transduced hUCMSC with lacZ control vector	H1975 cells or MRC-5 cells
Experiment 3	Untransduced hUCMSC	H1975 cells or MRC-5 cells
Control	H1975 cells or MRC-5 cells only	

3.7 Determination of hIL-12 mRNA Expression of Transduced hUCMSC

3.7.1 Total Ribonucleic Acid (RNA) Extraction

The hUCMSC (passage 3 to 5) were plated at 1.0×10^5 cells/well in a 6-well plate. Cells were cultured in complete medium (90% DMEM + 10% FBS + 1% Glutamax + 1% Penicillin-Streptomycin) at 37°C, 5% CO₂. On the next day, the hUCMSC were transduced with AdhIL-12 at selected MOI by replacing the culture medium with 1 ml/well of complete medium with AdhIL-12 and incubated for 3 hours. The medium was then discarded and replaced with fresh complete medium. Cells were cultured for 3 days. On day 3 post-transduction, the cells were harvested for RNA extraction using Qiagen RNeasy mini kit (Qiagen, Germany) according to the manufacturer's protocol. The hUCMSC were trypsinised and collected as a pellet in a microcentrifuge tube by centrifugation at 300 xg for 5 minutes prior to cell lysis. Supernatant was completely aspirated and remaining cells were disrupted by addition of 350 µl lysis buffer (Buffer RLT) and vortexed vigorously until no cell clumps were visible. The lysate was homogenised by loading directly into the QIAshredder spin column placed in a 2 ml collection tube (Qiagen, Germany) and centrifuged for 2 minutes at maximum speed. The flow-through was added with 350 µl of 70% ethanol and mixed well by pipetting. The sample was transferred to a RNeasy spin column placed in a collection tube and centrifuged for 15 seconds at maximum speed ($\geq 10,000$ rpm). Total RNA bound to the membrane of the column while the contaminants passed through the column and retained in the flow-through. The column was then washed with buffer RW1 (1 time) and buffer

RPE (2 times) by centrifugation for 15 seconds at maximum speed. The collection tube with flow-through was discarded and the RNeasy spin column was placed in a new collection tube and centrifuged at maximum speed for 1 minute to eliminate any remaining carry over of buffer RPE. Next, the RNA was eluted into a new 1.8 ml microcentrifuge tube by addition of 30 μ l of RNase-free water and centrifuged at maximum speed for 1 minute. The concentration and purity of the extracted DNA was determined using Nanodrop (Thermo Fisher Scientific, US). Untransduced hUCMSC were harvested for RNA extraction as well. The ratio of A260/A280 for pure RNA was generally accepted to be in the range of 1.8 - 2.1. Pure RNA was stored at -80°C.

3.7.2 DNase I Treatment of RNA and Reverse Transcription of RNA to cDNA

The DNase I treatment and reverse transcription of extracted RNA were performed using the ReverTra AceTM qPCR RT Master Mix with gDNA Remover (Toyobo, Japan) according to the manufacturer's protocol. RNA extracted from hUCMSC samples were subjected to denaturation by incubation at 65°C for 5 minutes and then kept on ice. Prior to use, a 1 in 50 volume of gDNA remover was added to the 4X DN Master Mix. A total of 0.5 μ g of RNA was resuspended with 2 μ l of 4X DN Master Mix diluted with nuclease-free water to a final volume of 8 μ l. The mixture was incubated at 37°C for 5 minutes. Then, the mixture was subjected to complementary DNA (cDNA) synthesis. Two microlitres of 5X RT Master Mix II was added into the mixture and incubated at 37°C for 15 minutes followed by 50°C at 5 minutes. Next, the

mixture solution was heated at 98°C for 5 minutes and stored in 4°C or -20°C for long term storage.

3.7.3 Quantitative Real-Time PCR

The hIL-12 mRNA expression in both transduced and untransduced hUCMSC were analysed via quantitative real-time polymerase chain reaction (qPCR). The qPCR was performed with StepOnePlus™ Real-Time PCR System (Thermo Fisher Scientific, USA). The PCR components for a single 10 µl reaction were prepared as shown in Table 3.17 and the primer sequences were listed in Table 3.18. The qPCR was performed according to the thermal cycler cycling parameters in Table 3.19. The hIL-12 mRNA expression was quantified using comparative C_T method ($\Delta\Delta C_t$) with GAPDH as the endogenous control. The qPCR was performed in triplicates for each sample. The experiment was carried out for samples of 3 biological replicates with 2 different passages samples from each biological replicate.

Table 3.17 Reaction components of qPCR for mRNA expression

Component	Volume (µl)/reaction
PowerUp™ SYBR™ Green Master Mix (2X)	5
Forward primer (10 µM)	0.2 (final concentration: 200 nM)
Reverse primer (10 µM)	0.2 (final concentration: 200 nM)
cDNA (10 ng/µl)	2 (final concentration: 20 ng)
Nuclease-free water	2.6
Total	10

Table 3.18 Primers of qPCR for mRNA expression

Primer	Sequence
hIL-12 primer (Forward)	CTGCAGTGTTCCTGGAGTAG
hIL-12 primer (Reverse)	GAACATTCCTGGGTCTGGAG

Table 3.19 Thermal cycler parameters for mRNA expression

Cycle Step	Temperature	Time	Cycle
Initial setup	50°C	2 minutes	1 (Holding stage)
Dual-lock™ DNA polymerase	95°C	2 minutes	1 (Holding stage)
Denature	95°C	15 seconds	} 40
Anneal/Extend	60°C	1 minutes	
Dissociation curve condition (melt curve stage)	95°C	15 seconds	Step & Hold
	60°C	1 minute	
	95°C	15 seconds	

3.8 Statistical Analysis

Data were expressed as mean \pm standard deviation (SD). Difference between two groups of data were compared using Student's T-tests while One-way ANOVA was used to analyse difference between more than two groups. Data for gene expression assay was analysed using Wilcoxon Signed Ranks Test. Differences were considered significant at $p < 0.05$. Statistical analyses were conducted using GraphPad Prism 7.0.

CHAPTER 4

RESULTS

4.1 Characterisation of hUCMSC

4.1.1 Immunophenotyping

A panel of surface markers were used in the immunophenotyping analysis of early passage (passage 3 to 5) hUCMSC. The results showed that the untransduced hUCMSC expressed typical MSC markers, including CD73, CD90, CD105 and negative for CD14, CD34, CD45, CD19 and human leucocyte antigen-DR (HLA-DR) (Figure 4.1). Due to the transduced hUCMSC expressing green fluorescent protein (GFP) which interfered with the fluorescence signal detection in the flow cytometry, a different set of fluorochrome antibodies was used for the immunophenotyping analysis for transduced hUCMSC. Results showed that the transduced hUCMSC expressed CD90 and CD105 positively and lacked expression of CD34 and CD45 similar to untransduced hUCMSC (Figure 4.2).

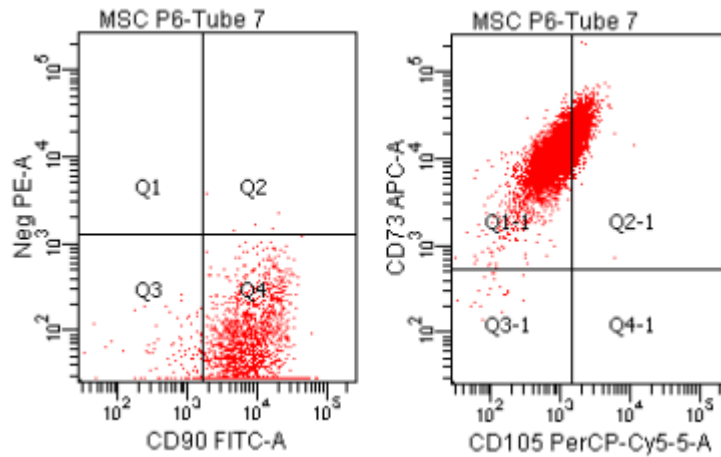


Figure 4.1 Immunophenotyping of UCMSC. Flow cytometry analysis showed the UCMSC were positive for cell surface markers CD73, CD90, CD105 and negative for CD34, CD45, CD11b, CD19 and HLA-DR. All the negative markers are conjugated with the same fluorochrome, PE. Representative images shown from 3 independent experiments.

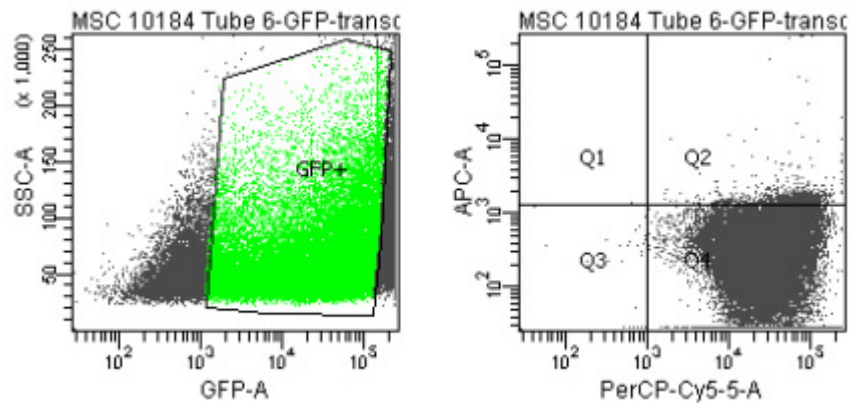


Figure 4.2 AdhIL-12 transduced UCMSC maintained cell surface markers similar to untransduced UCMSC. PerCP-Cy5.5 included CD90 and CD105 while APC included CD34 and CD45. Representative images shown from 3 independent experiments.

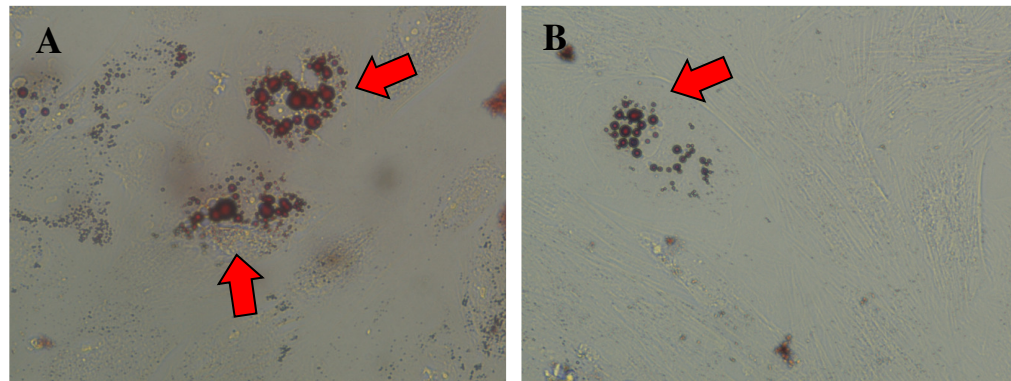
4.1.2 Trilineage Differentiation

Both untransduced and transduced hUCMSC from passage 3 to 5 were investigated for their differentiation capacity. The differentiation capacity was

defined by the ability to undergo trilineage differentiation which included adipogenesis, osteogenesis and chondrogenesis after culturing in appropriate induction media.

4.1.2.1 Adipogenic differentiation

After 3 to 4 weeks of incubation with adipogenic induction medium, untransduced and transduced hUCMSC were differentiated into adipocytes. Accumulation of lipid-rich vacuoles within the cytoplasm of the cells were observed and stained positively with Oil Red O (Figure 4.3 A & B). In contrast, hUCMSC maintained in regular MSC growth medium showed no morphological changes and stained negatively with Oil Red O (Figure 4.3C).



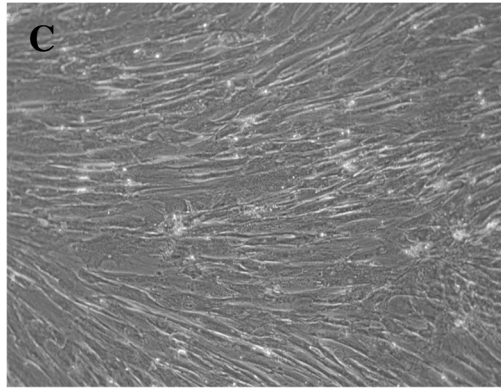


Figure 4.3 Adipogenesis of hUCMSC. Lipid droplets formed in the cells differentiated from (A) untransduced hUCMSC and (B) hUCMSC-IL12 and stained positively with Oil Red O. (C) hUCMSC maintained in regular growth medium (control). Nikon eclipse TS100 microscope, magnification: (A) and (B) 400X, (C) 100X.

4.1.2.2 Osteogenic differentiation

Both untransduced and transduced hUCMSC underwent osteogenic differentiation after 1 to 2 weeks of culture with osteogenic induction medium. Untransduced hUCMSC stained positively with Alizarin Red S (Figure 4.4 A). The transduced hUCMSC also stained positively with Alizarin Red S albeit in darker shade of brown (Figure 4.4 B). It is believed that the strong GFP expressed by the transduced hUCMSC interfered with the staining process and resulted in the difference seen in the transduced hUCMSC when compared to the untransduced hUCMSC. The red or brown precipitates in the cells represented the calcium deposits of matrix formation associated with osteoblasts formation. Undifferentiated hUCMSC cultured in regular MSC growth medium stained negatively with Alizarin Red S (Figure 4.4 C).

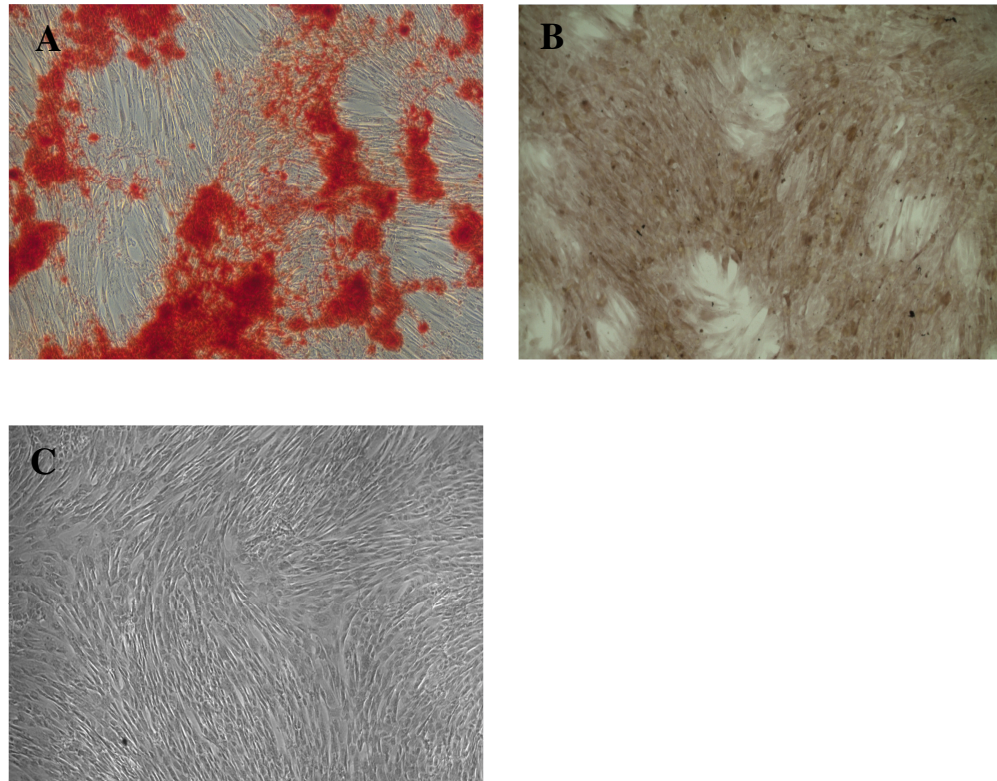


Figure 4.4 Osteogenic differentiation of hUCMSC. Alizarin Red S staining showed mineralisation of extracellular matrix produced by the osteogenic differentiated cells of (A) untransduced hUCMSC and (B) hUCMSC-IL12. (C) Uninduced cells maintained in regular growth medium (control) showed negative staining for Alizarin Red S. Nikon eclipse TS100 microscope, magnification: 40X.

4.1.2.3 Chondrogenic differentiation

Chondrogenic induction of the micromass cultures for 14 days resulted in formation of spheroid. At the end of the experiment, the spheroid in the well of a 24-well plate was clearly visible to the naked eye. The chondrogenic spheroids formed from untransduced or transduced hUCMSC were stained blue in colour with Alcian Blue (Figure 4.5 A to D). The hUCMSC in regular MSC growth medium showed no spheroid formation and stained negatively with Alcian Blue (Figure 4.5 E).

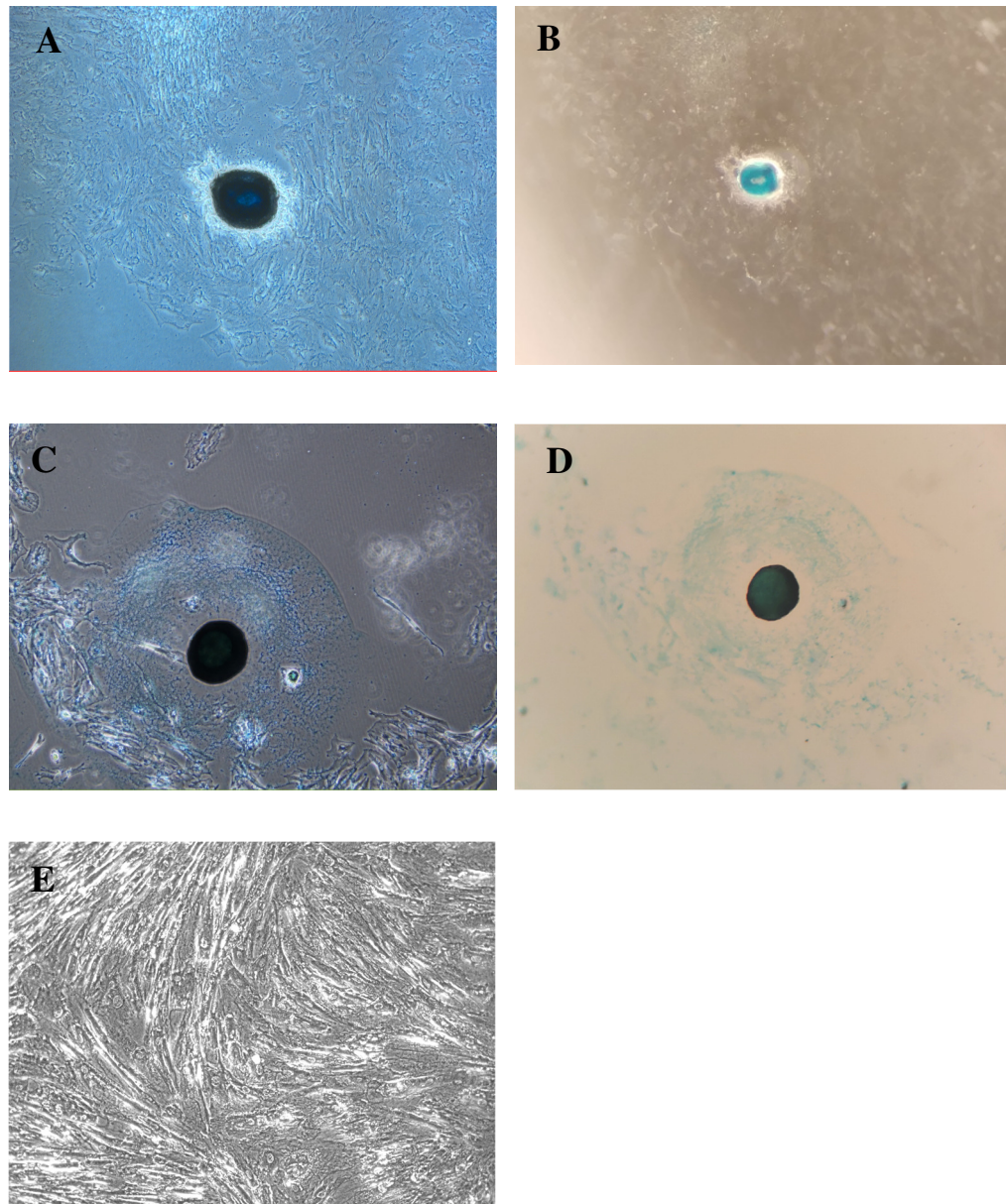


Figure 4.5 Chondrogenic differentiation of hUCMSC. Spheroid formed in micromass culture of untransduced hUCMSC (A and B) and hUCMSC-IL-12 (C and D) under induction for 2 weeks and stained positively with Alcian Blue. (E) Uninduced cells maintained in regular growth medium (control) showed negative staining for Alcian Blue. (A) and (E) Carl Zeiss Axio Observer A1, magnification: (A) 50X; (E) 100X. (B) and (D) Nikon stereomicroscope SMZ445, magnification: 40X. (C) Nikon eclipse TS100 microscope, magnification:40X.

4.2 Generation of Genetically Engineered Human Umbilical Cord-Derived Mesenchymal Stromal Cells Expressing Human Interleukin-12 (hUCMSC-IL12) Using Adenoviral Method

4.2.1 Amplification of hIL-12 gene

PCR primers used to amplify the hIL-12 gene were designed and synthesised in such a way that each end of the PCR product generated shared 15 bp of homology with the one end of the linearised pAdenoX-ZsGreen1 vector. Then, the hIL-12 gene was amplified using PCR and the PCR products were analysed using agarose gel electrophoresis and visualised under ultraviolet light. The expected band size was 1.6 kb as per the length of the hIL-12 gene (Figure 4.6). The DNA bands from lane 1 to 5 were excised and DNA purification was performed. Sample from lane 1 was used in the subsequent step to generate the adenovirus. The concentration and purity of the extracted DNA from lane 1 was shown in Table 4.1. The sample is shown to be of the required DNA purity with the A260/280 ratio between the range of 1.7 to 2.0.

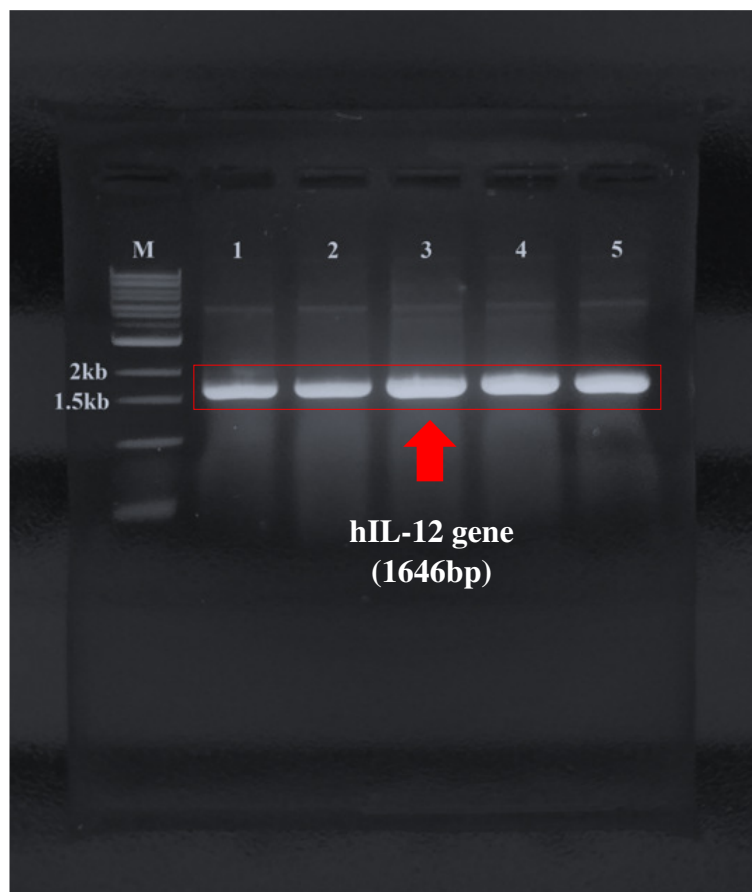


Figure 4.6 Agarose gel electrophoresis image of PCR product of hIL-12 gene amplification. Lane M: 1 kb Extend DNA Ladder (New England Biolabs, USA). Lane 1 to 5: Amplification of hIL-12 gene.

Table 4.1 Concentration and purity of the extracted DNA

Sample	Concentration (ng/ μ l)	Purity (A260/A280)	Purity (A260/A230)
1	102	1.845	1.990

4.2.2 Screening of clones using PCR

The presence of the recombinant plasmid encoding hIL-12 gene (pAdenoX-hIL-12) and recombinant plasmid encoding lacZ gene (pAdenoX-lacZ) transformed into Stellar competent cells were determined by conventional PCR. The results of agarose gel electrophoresis showed that the colonies amplified with Adeno-X

Screening Primer Mix 3 produced PCR products with expected sizes of 3.5kb and 4.9kb (Figure 4.7). These results verified that the transformed competent cells contained the plasmid of interest. Subsequently, the positive clones were amplified by inoculating them in liquid LB/Ampicillin medium and purified by NucleoBond Xtra Plasmid Midi Kit (Macherey-Nagel, Germany). The concentration and purity of the extracted DNA were shown in Table 4.2. The extracted plasmids showed good quality as the ratio of A260/280 obtained were in the range of 1.7 to 1.8.

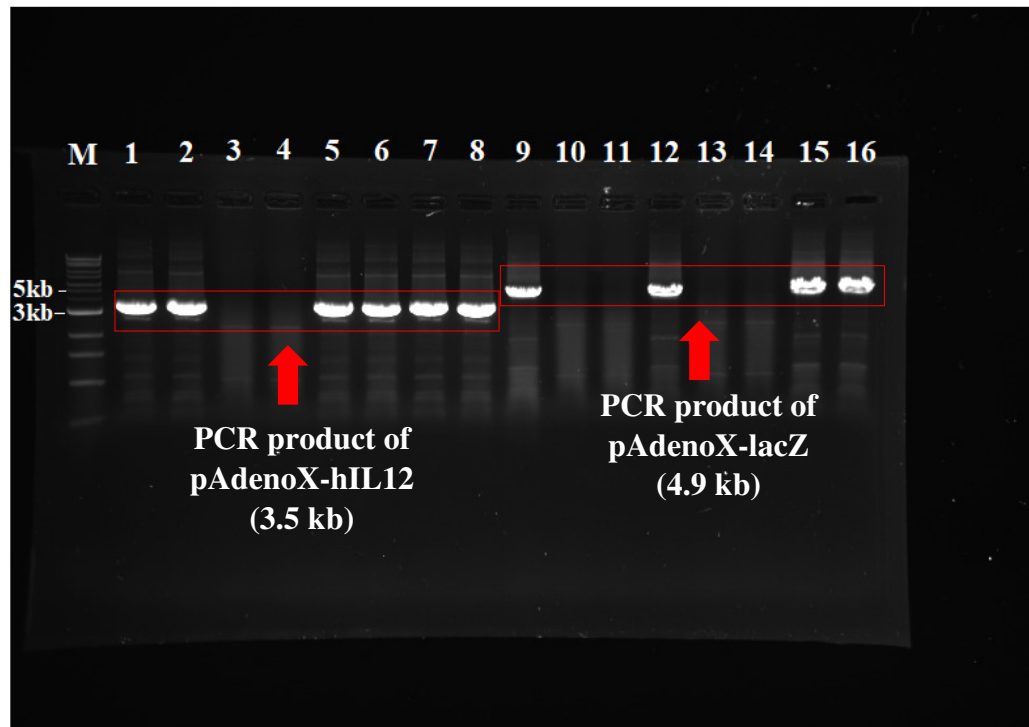


Figure 4.7 Agarose gel electrophoresis image of hIL-12 gene amplification. Lane M: 1 kb Extend DNA Ladder (New England Biolabs, USA). Lane 1 to 8: Colony screening for pAdenoX-hIL12; lane 9 to 16: Colony screening for pAdenoX-lacZ. Positive clones from lanes 2, 9, 10 and 16 were amplified and purified.

Table 4.2 Concentration and purity of the extracted recombinant plasmid DNA

Sample	Lane no.	Concentration (ng/ μ l)	Purity (A260/A280)	Purity (A260/A230)
pAdenoX-hIL12	2	754.5	1.81	2.05
pAdenoX-hIL12	9	603.7	1.77	1.96
pAdenoX-lacZ	10	217.9	1.84	2.25
pAdenoX-lacZ	16	490.3	1.77	1.95

4.2.3 Restriction Analysis of Recombinant Plasmids

Adenoviral recombinant plasmids were generated using In-Fusion Cloning method, namely recombinant plasmid expressing hIL-12 (pAdenoX-hIL12) and recombinant plasmid expressing lacZ (pAdenoX-lacZ). The recombinant plasmids were digested with NheI (New England Biolabs, USA) and XhoI (Promega, USA) restriction enzymes. The DNA fragments were separated on 1% agarose gel (Figure 4.8) and showed expected band sizes respectively (Table 4.3)

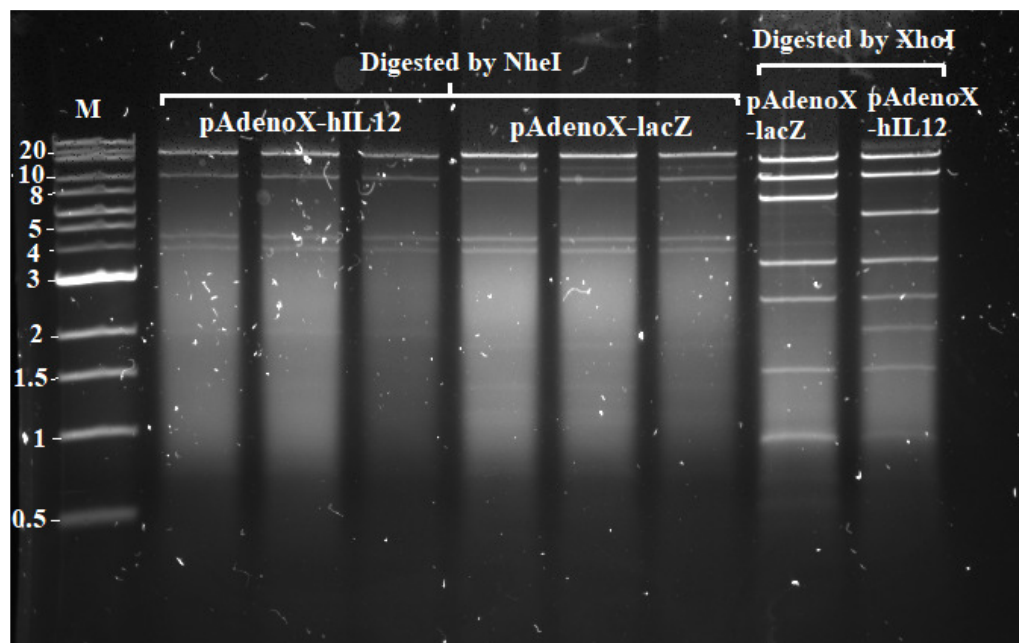


Figure 4.8 Agarose gel electrophoresis of the recombinant pAdenoX digested with NhoI or XhoI restriction enzymes. Lane M: 1 kb Extend DNA Ladder (New England Biolabs, USA). Expected band sizes were observed.

Table 4.3 Expected fragment sizes in recombinant pAdenoX vectors digested with NheI or XhoI

Vector	NheI	XhoI
pAdenoX-hIL12	687	595
	3848	1445
	4340	2466
	10342	3320
	18295	5483
		9703
		14500
pAdenoX-lacZ	687	595
	3848	1445
	4340	2466
	10342	3320
	19649	6837
		9703
		14500

Note: Fragment sizes highlighted in green are fragments containing the gene of interest.

4.2.4 Sequencing Analysis of Recombinant Plasmids

The identities of pAdenoX-hIL12 and pAdenoX-lacZ were further verified using Sanger sequencing. Primer walking was performed on the full gene of hIL-12 encoded by pAdenoX-hIL12. Results showed both the hIL-12 gene and lacZ gene were cloned successfully into the pAdenoX-ZsGreen1 adenoviral vector and no mutation was found in the full gene of hIL-12 (Appendix B). Sequence alignment was performed using SnapGene Viewer analysis software.

4.2.5 Digestion of Recombinant Plasmids with PacI Restriction Enzyme

In order to prepare the recombinant plasmids for transfection on HEK 293 cells, restriction digestion with PacI (New England Biolabs, USA) was performed and analysed on a 1% agarose gel. The plasmid portion of the recombinant pAdenoX vector migrated at approximately 3 kb while the adenoviral genome did not enter the gel but remained at the top of the lane (Figure 4.9). Then, the digestion reaction was subjected to DNA extraction. The concentration and purity of the extracted DNA is shown in Table 4.4. The extracted DNA showed good quality as the ratio of A260/280 obtained were in the range of 1.7 to 2.0.

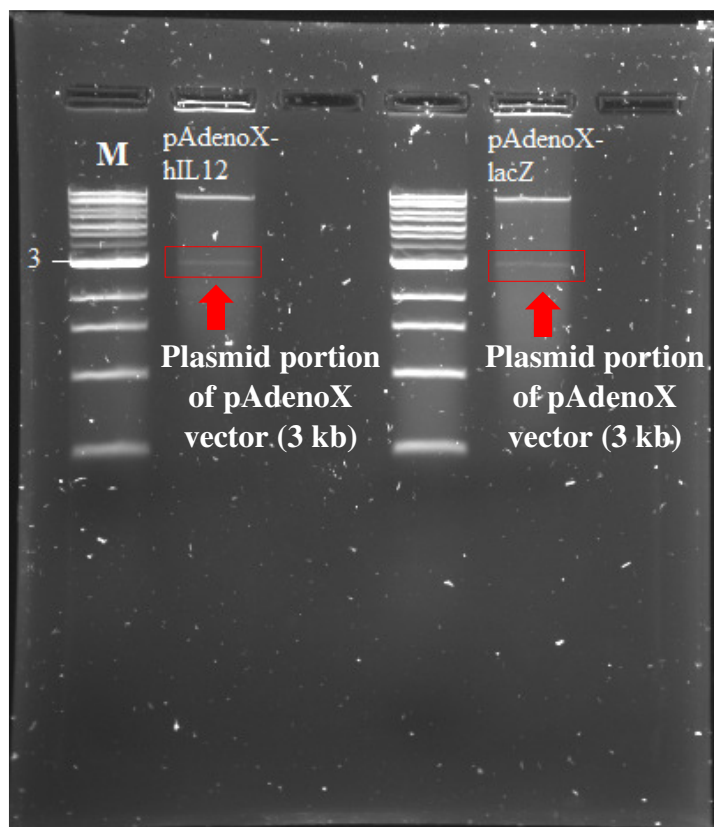


Figure 4.9 Agarose gel electrophoresis of the recombinant pAdenoX digested with Pacl restriction enzyme. Lane M: 1 kb Extend DNA Ladder (New England Biolabs, USA).

Table 4.4 Concentration and purity of the extracted plasmid DNA

Sample	Concentration (ng/μl)	Purity (A260/A280)
pAdenoX-hIL12	112.0	1.86
pAdenoX-lacZ	180.0	1.88

4.2.6 Packaging of AdenoX Recombinant Viruses

The linearised pAdenoX-hIL12 and pAdenoX-lacZ were transfected into HEK 293 cells in order to package the AdenoX adenovirus expressing hIL-12 (AdhIL12) and AdenoX adenovirus expressing lacZ (AdlacZ). Infected HEK

293 cells typically remain intact but they may round up and detach from the plate. These changes are collectively referred to as cytopathic effect (CPE). Late CPE was observed on day 9 post-transfection with AdhIL-12 (Figure 4.10) and AdlacZ (Figure 4.12). Cells were harvested by three freeze-thaw cycles and stored in -20°C. Transfected HEK 293 cells also showed GFP expression as AdhIL-12 (Figure 4.11) and AdlacZ were expressing GFP as well (Figure 4.13).

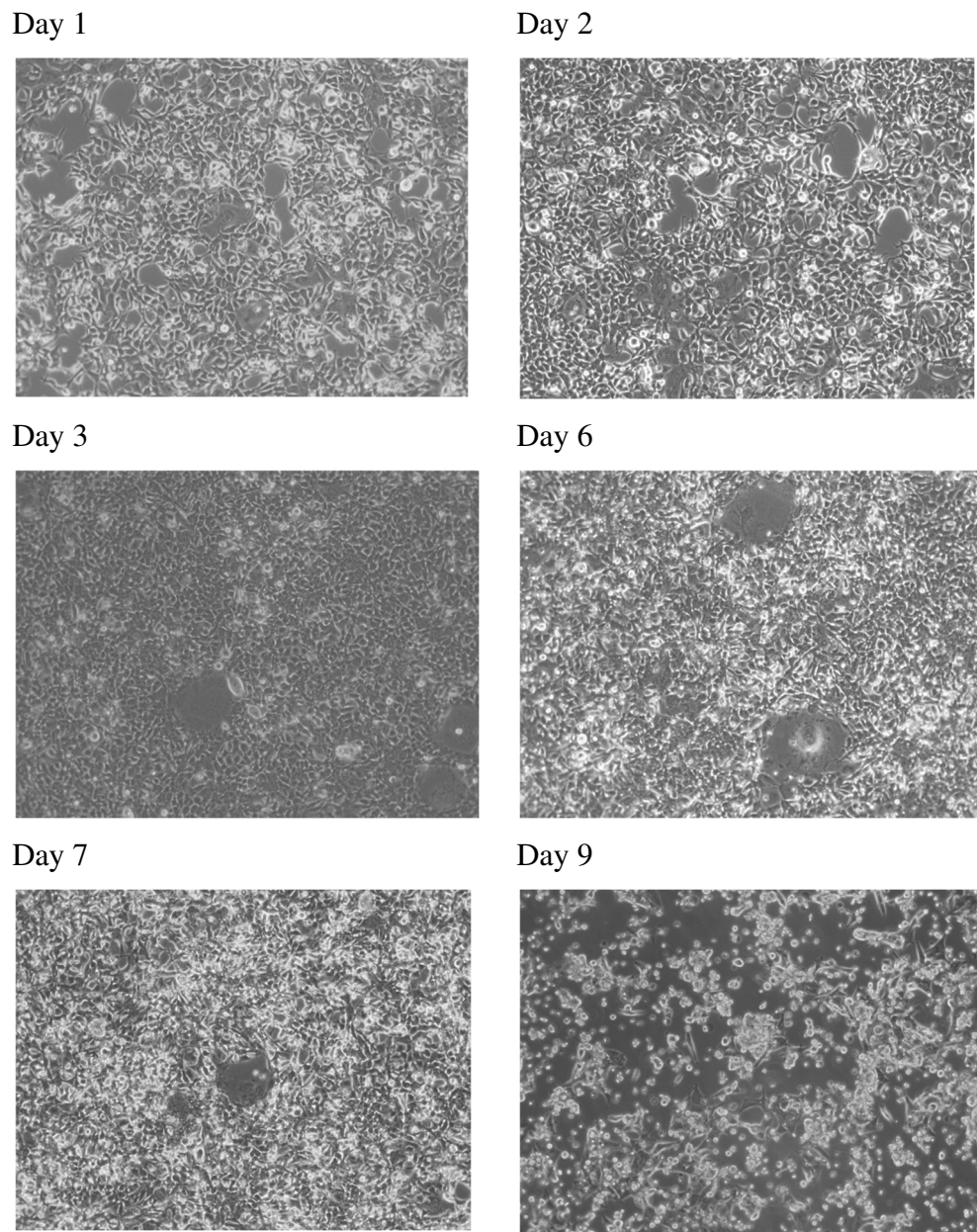


Figure 4.10 HEK 293 cells transfected with pAdenoX-hIL12 observed under inverted microscope. HEK 293 cells showed cytopathic effect after transfection with pAdenoX-hIL12. Carl Zeiss Axio Observer A1, magnification: 100X.

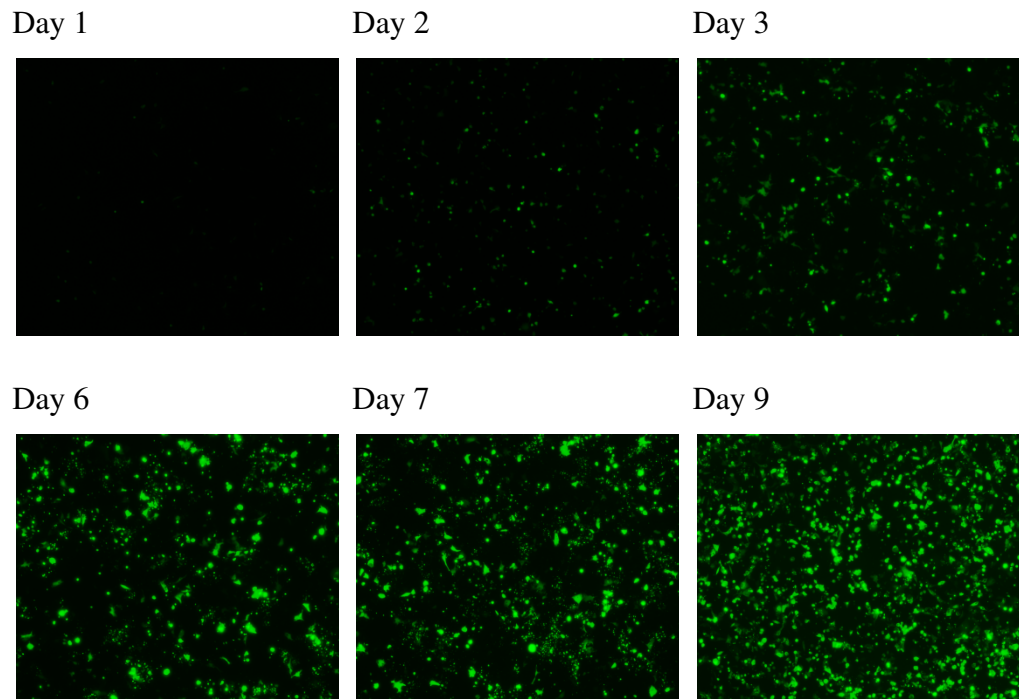
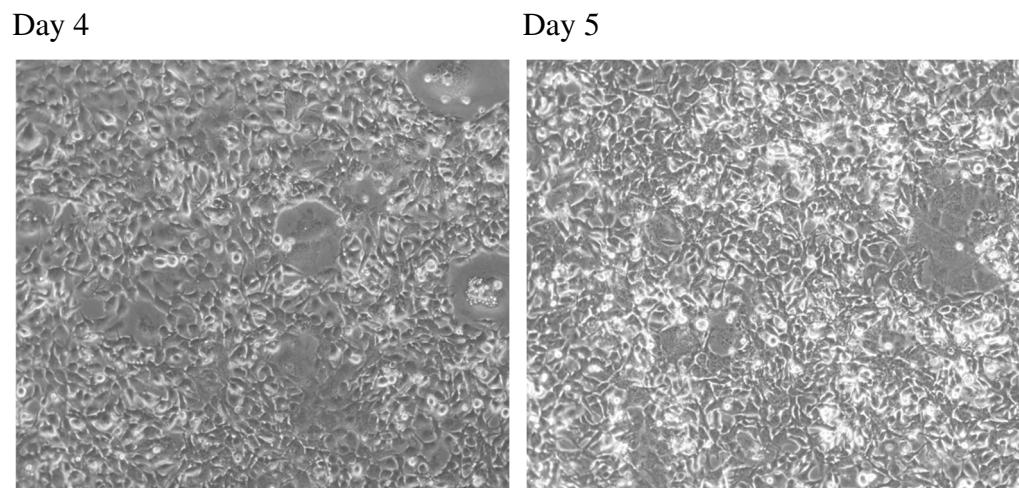
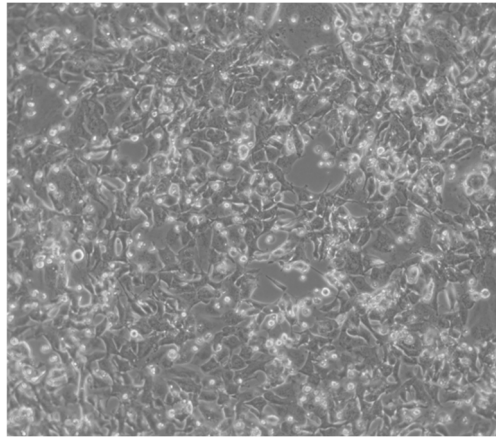


Figure 4.11 HEK 293 cells transfected with linearised pAdenoX-hIL12 observed under fluorescence microscope. HEK 293 cells showed green fluorescence after transfection with pAdenoX-hIL12. Carl Zeiss Axio Observer A1, magnification: 40X.



Day 7



Day 9

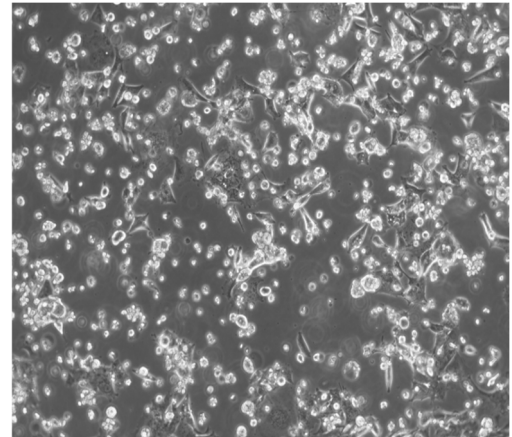
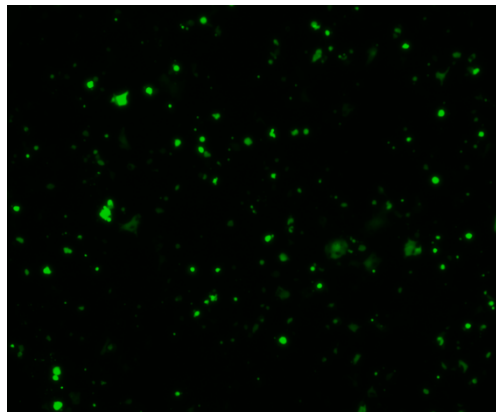
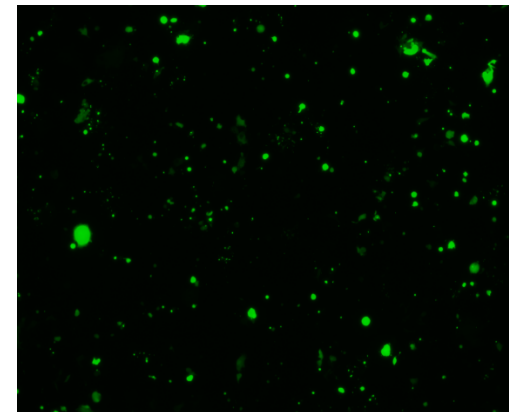


Figure 4.12 HEK 293 cells transfected with pAdenoX-hIL12 observed under inverted microscope. HEK 293 cells showed cytopathic effect after transfection with pAdenoX-lacZ (control). Carl Zeiss Axio Observer A1, magnification: 100X.

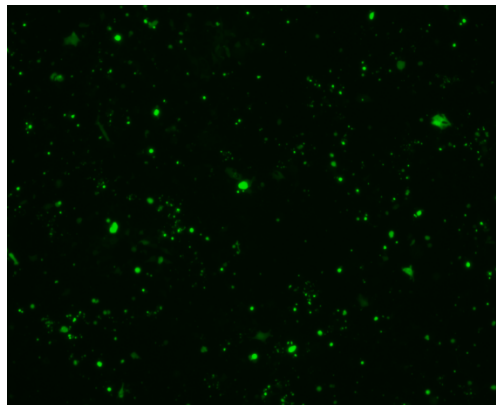
Day 4



Day 5



Day 7



Day 9

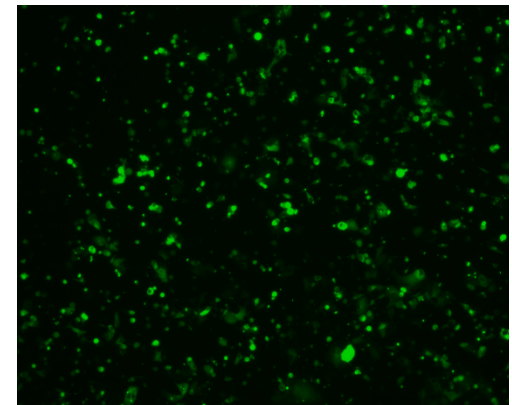


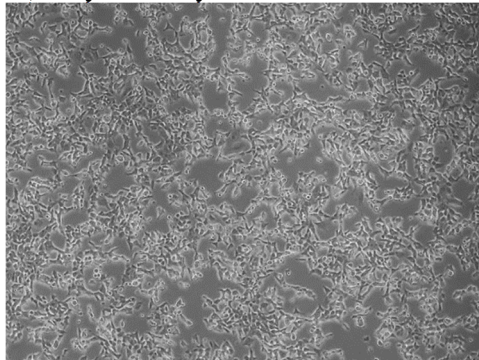
Figure 4.13 HEK 293 cells transfected with linearised pAdenoX-lacZ observed under fluorescence microscope. HEK293 cells showed green

fluorescence after transfection with pAdenoX-lacZ (control). Carl Zeiss Axio Observer A1, magnification: 40X.

4.2.7 Primary Amplification of AdenoX Recombinant Viruses

In order to amplify the AdenoX viral particles, 50% of the harvested lysate in Section 4.1.3.6 were used to infect fresh HEK 293 cells seeded on a 90mm culture plate. The primary amplification viral stock for AdhIL-12 and AdlacZ were collected on day 2 (Figure 4.14) and day 3 (Figure 4.16) post-transduction respectively, when the late CPE was observed. Transfected HEK 293 cells also showed GFP expression as AdhIL-12 (Figure 4.15) and AdlacZ were expressing GFP as well (Figure 4.17). The recombinant viruses were lysed with three consecutive freeze-thaw cycles and the lysate was collected and stored in -20°C.

A) Day 1: Early CPE observed.



B) Day 2: Late CPE observed.

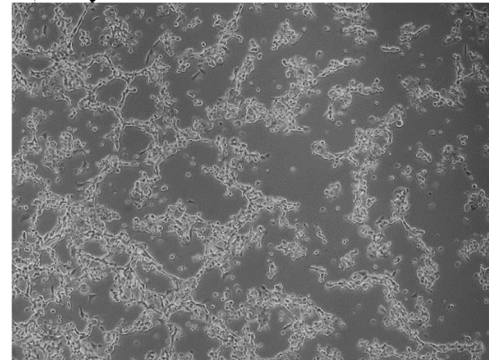
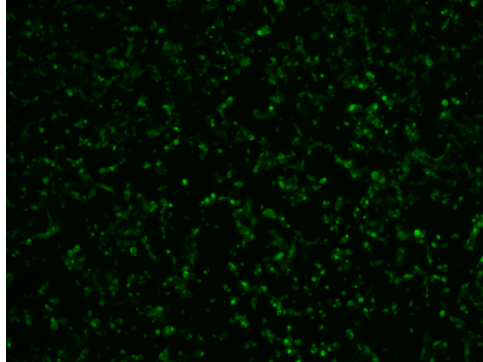


Figure 4.14 HEK 293 cells showed cytopathic effect after transduction with AdhIL-12. (A) Day 1 post-transduction showed early CPE; (B) Day 2 post-transduction showed late CPE. Carl Zeiss Axio Observer A1, magnification: 40X.

A) Day 1: 50% transduction efficiency.



B) Day 2: >90% transduction efficiency.

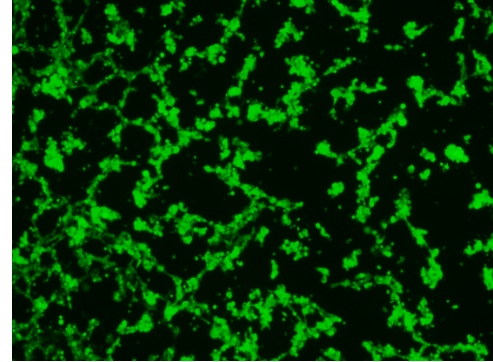
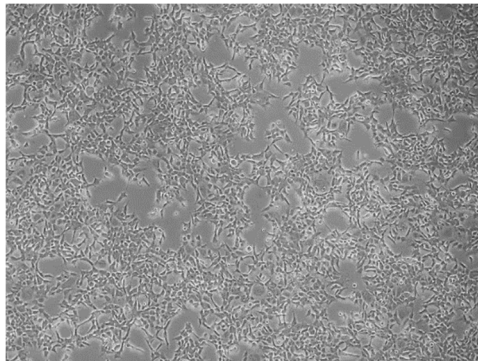
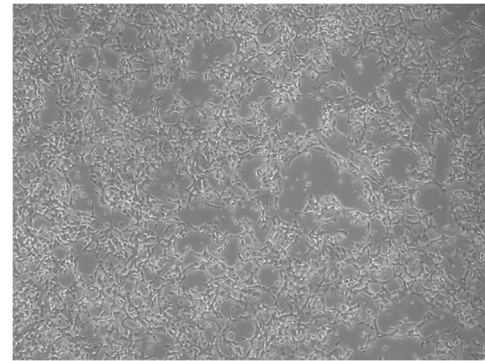


Figure 4.15 HEK 293 cells showed green fluorescence after transduction with AdhIL-12. (A) Day 1 post-transduction showed 50% transduction efficiency; (B) Day 2 post-transduction showed >90% transduction efficiency. Carl Zeiss Axio Observer A1, magnification: 40X.

Day 1



Day 2



Day 3

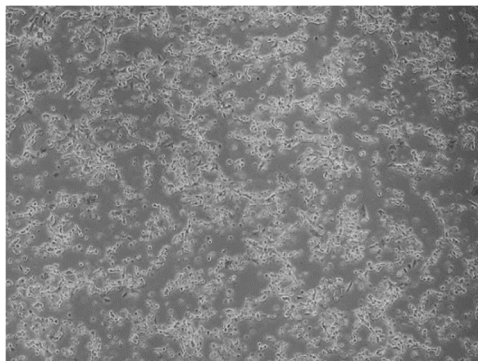
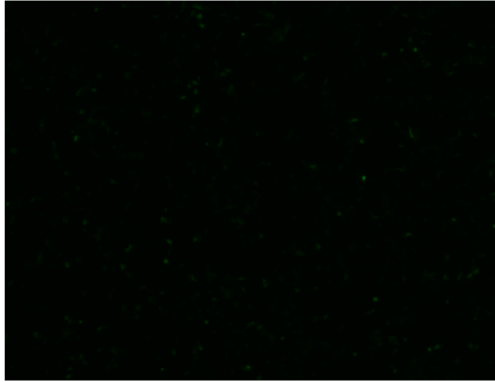
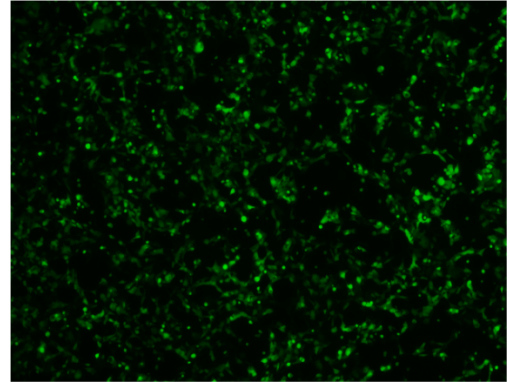


Figure 4.16 HEK 293 cells showed cytopathic effect after transduction with AdlacZ. Carl Zeiss Axio Observer A1, magnification: 40X.

Day 1



Day 2



Day 3

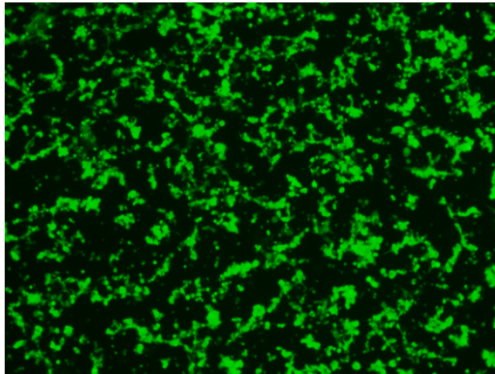


Figure 4.17 HEK 293 cells showed green fluorescence after transduction with AdlacZ. Carl Zeiss Axio Observer A1, magnification: 40X.

4.2.8 Titration of Recombinant Adenovirus

The titration of Ad-hIL12 and AdlacZ primary amplification stock were performed using the Adeno-X qPCR Titration kit (TakaraBio, USA) according to the manufacturer's protocol.

4.2.8.1 Titration for AdhIL-12

In order to titrate the concentration of AdhIL-12, a standard curve was constructed (Figure 4.18). The constructed standard curve was accepted as the correlation coefficient (R^2) was 0.973 and the value of slope (M) obtained was

between -3.0 and -3.6 (Figure 4.18). The Ct values of the serial dilution of control was shown in Table 4.5. Table 4.6 shows the Ct value and calculated copy number of hIL-12 samples with different dilutions. Only sample dilutions with Ct value falling within the range of Ct values of control (8.5 to 23.3) were selected to calculate the concentration of AdhIL-12.

Table 4.5 Ct value for control dilutions

Control concentration	Ct value (Mean)
5×10^7	8.55944252
5×10^6	10.99899101
5×10^5	14.45525646
5×10^4	17.74892235
5×10^3	23.30673218

hIL12 (0.0001x)	22.25206	5041.056514	5.04 x 10 ⁷
hIL12 (0.00001x)	26.50532	337.9751699	3.38 x 10 ⁷

Calculation for AdhIL-12 viral DNA copy number:

Mean of copy number = [(1.40+4.18+3.30+24.8+5.04) x10⁷]/5 = 7.74 x 10⁷

50 µl of sample was purified and eluted in 30 µl.

Copies/ml

= (7.74x10⁷ copies) (1000 µl/ml) (30 µl elution) / (50 µl sample) (2 µl per well)
= **2.32x10¹⁰ copies/ml**

4.2.8.2 Titration for AdlacZ

Similarly, a standard curve for AdlacZ was constructed (Figure 4.19). The constructed standard curve was accepted as the correlation coefficient (R²) was 0.986 and the value of slope (M) obtained was between -3.0 and -3.6. The Ct values of the serial dilution of control was shown in Table 4.7. Table 4.8 shows the Ct value and calculated copy number of lacZ samples with different dilutions. Sample dilutions with Ct value falling within the range of Ct values of control (8.5 to 20.6) were chosen to calculate the concentration of AdlacZ.

Table 4.7 Ct value for control dilutions

Control concentration	Ct value (Mean)
5 x 10 ⁷	8.46541214
5 x 10 ⁶	11.47512627
5 x 10 ⁵	14.07284069
5 x 10 ⁴	17.55538559

5×10^3	20.59268188
-----------------	-------------

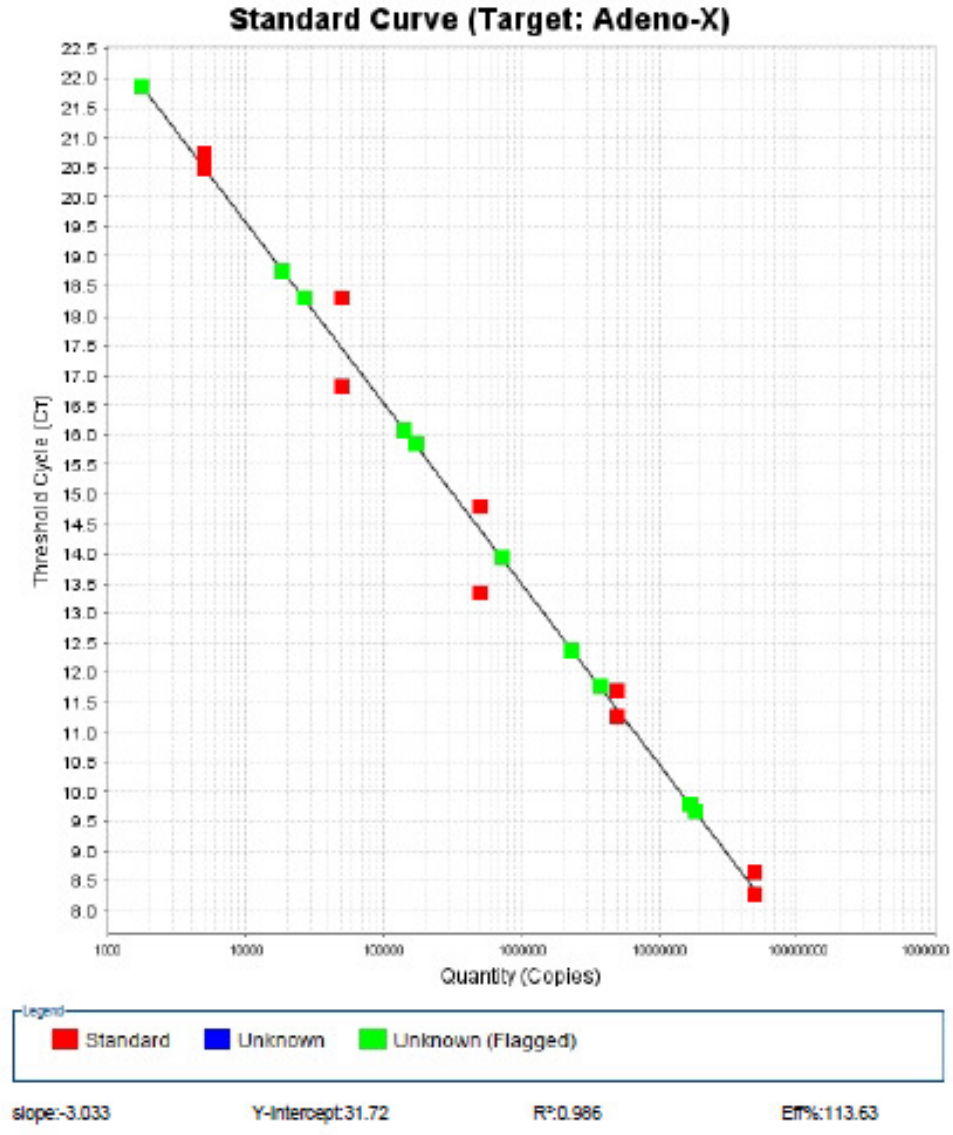


Figure 4.19 Standard curve of Adeno-X control titration. Standard curve generated from five serial dilution of Adeno-X control template against the respective threshold cycle (C_t value).

Table 4.8 Ct value and copy number of samples with different dilutions

Sample dilutions	Ct value (Mean)	Copy number	Final copy number
lacZ (1x)	9.739433	17665952.68	1.77×10^7
lacZ (0.1x)	12.08807	2970130.477	2.97×10^7
lacZ (0.01x)	15.00722	323827.2914	3.24×10^7
lacZ (0.001x)	17.30524	56577.18956	5.66×10^7
lacZ (0.0001x)	20.08123	6876.679423	6.88×10^7

Calculation for AdlacZ viral DNA copy number:

$$\begin{aligned} \text{Mean of copy number} &= [(1.77+2.97+3.24+5.66+6.88) \times 10^7]/5 \\ &= 4.10 \times 10^7 \end{aligned}$$

73 μ l of sample was purified and eluted in 30 μ l.

Copies/ml

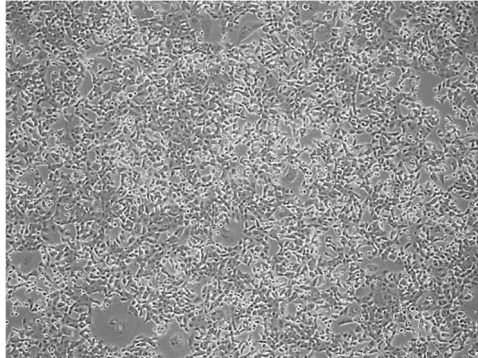
$$\begin{aligned} &= (4.10 \times 10^7 \text{ copies}) (1000 \mu\text{l/ml}) (30 \mu\text{l elution}) / (73 \mu\text{l sample}) (2 \mu\text{l per well}) \\ &= \mathbf{8.43 \times 10^9 \text{ copies/ml}} \end{aligned}$$

4.2.9 High Titer Amplification of AdenoX Recombinant Viruses

HEK 293 cells seeded in five 150mm culture plates were transduced with primary amplification stock of AdenoX recombinant viruses at MOI 5. High titer AdhIL-12 viral stock was collected when the late CPE was observed on day 2 post-transduction (Figure 4.20). AdlacZ was collected on day 3 post-transduction when late CPE observed (Figure 4.22). Transfected HEK 293 cells also showed GFP expression as AdhIL-12 (Figure 4.21) and AdlacZ were expressing GFP as well (Figure 4.23). Similarly, AdenoX recombinant viruses were collected by three consecutive freeze-thaw cycles and the lysate was resuspended in 5ml of culture media and proceeded for purification. Purified

AdenoX recombinant viruses were eluted with 3ml of elution buffer and aliquoted into small volume in multiple microcentrifuge tubes and stored in -80°C.

A) Day 1: Early CPE observed.



B) Day 2: Late CPE observed.

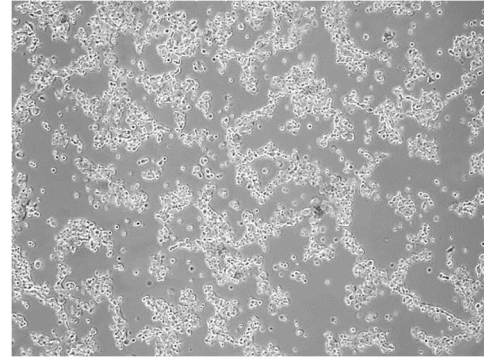
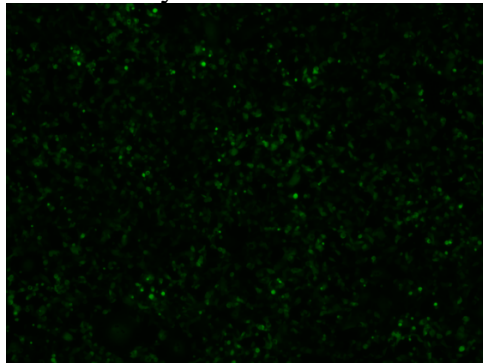


Figure 4.20 HEK 293 cells showed cytopathic effect after transduction with AdhIL-12. (A) Day 1 post-transduction showed early CPE; (B) Day 2 post-transduction showed late CPE. Carl Zeiss Axio Observer A1, magnification: 40X

A) Day 1: 20% transduction efficiency.



B) Day 2: >90% transduction efficiency.

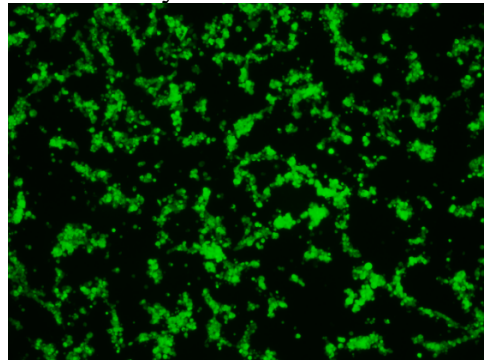
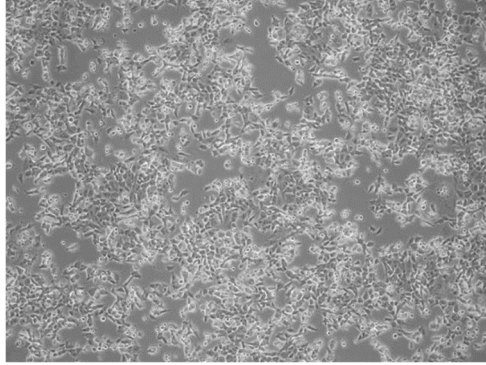
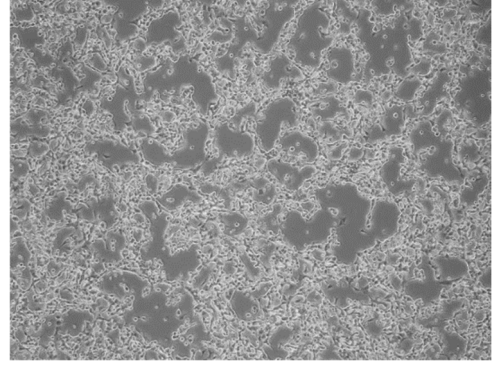


Figure 4.21 HEK 293 cells showed green fluorescence after transduction with AdhIL-12. (A) Day 1 post-transduction showed 20% transduction efficiency; (B) Day 2 post-transduction showed >90% transduction efficiency. Carl Zeiss Axio Observer A1, magnification: 40X.

Day 1



Day 2



Day 3

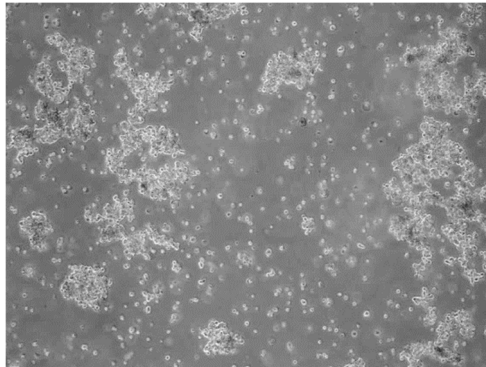
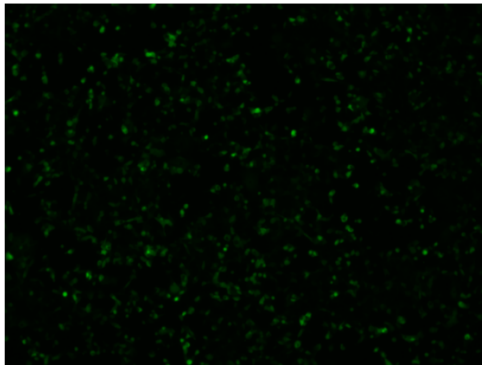
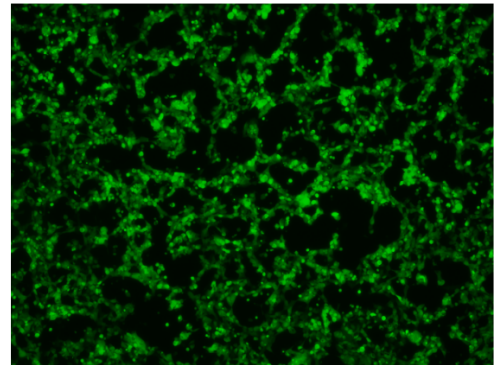


Figure 4.22 HEK 293 cells showed cytopathic effect after transduction with AdlacZ (control). Carl Zeiss Axio Observer A1, magnification: 40X.

Day 1



Day 2



Day 3

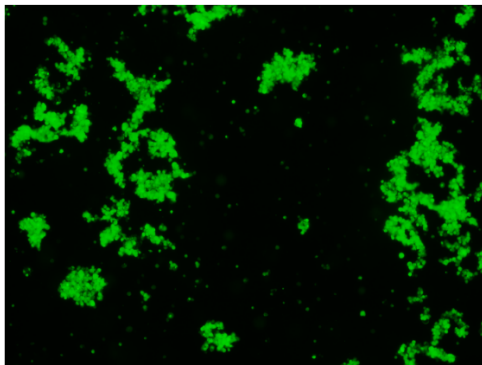


Figure 4.23 HEK 293 cells showed green fluorescence after transduction with AdlacZ (control). Carl Zeiss Axio Observer A1, magnification: 40X.

4.2.10 Verification of Recombinant Adenovirus Construct

The AdhIL-12 and AdlacZ constructs were verified using PCR method. The hIL12-specific primer and Adeno-X Screening Primer Mix 3 were used for the PCR. Agarose gel electrophoresis was conducted to analyse the PCR products and then gel was visualised under ultraviolet light. The gel electrophoresis of PCR products for both of the recombinant adenoviruses showed expected band sizes as shown in Table 4.9. There were other bands of different sizes observed for gel electrophoresis of AdlacZ because the primer used was a mixture instead of lacZ gene-specific primer.

Table 4.9 Size of gene of interest

Gene of interest	Size (bp)
hIL-12	1646
lacZ	3000
AdlacZ	4900

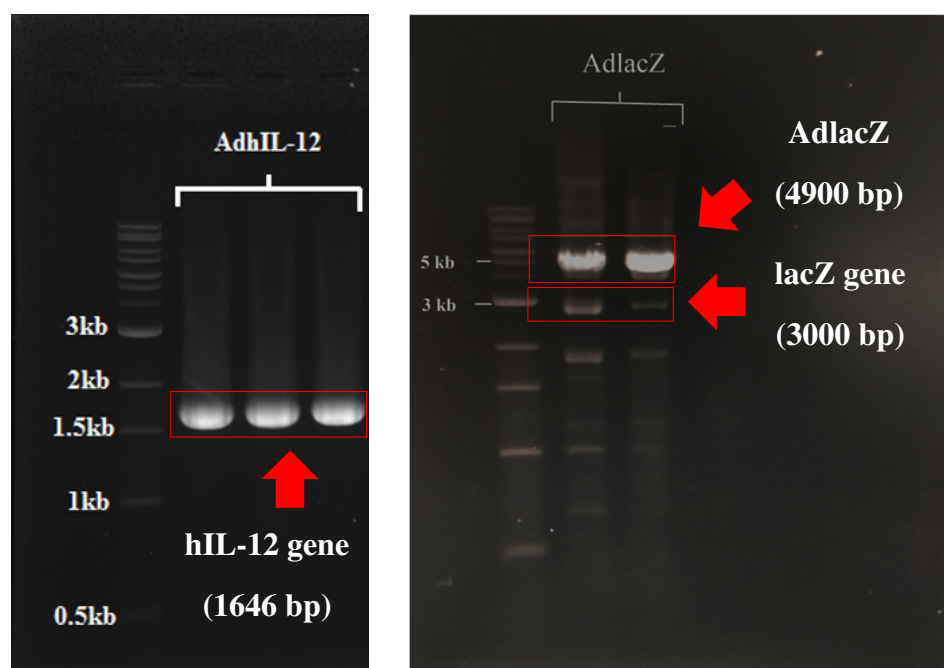


Figure 4.24 Agarose gel electrophoresis of PCR products of AdhIL-12 and AdlacZ.

4.2.11 Functional Titer of AdhIL-12 and AdlacZ

Functional titer of AdhIL-12 and AdlacZ was performed using plaque forming assay. The plaques were visible on day 7 post-infection. A total of 79 plaques were counted at the dilution factor of 10^{-5} (Figure 4.25) to give a titer count of 7.9×10^7 ifu/ml (Table 4.10) for AdhIL-12. For AdlacZ, 23 plaques

were counted at the dilution factor of 10^{-5} (Figure 4.26) to give a titer count of 2.3×10^7 ifu/ml (Table 4.10).

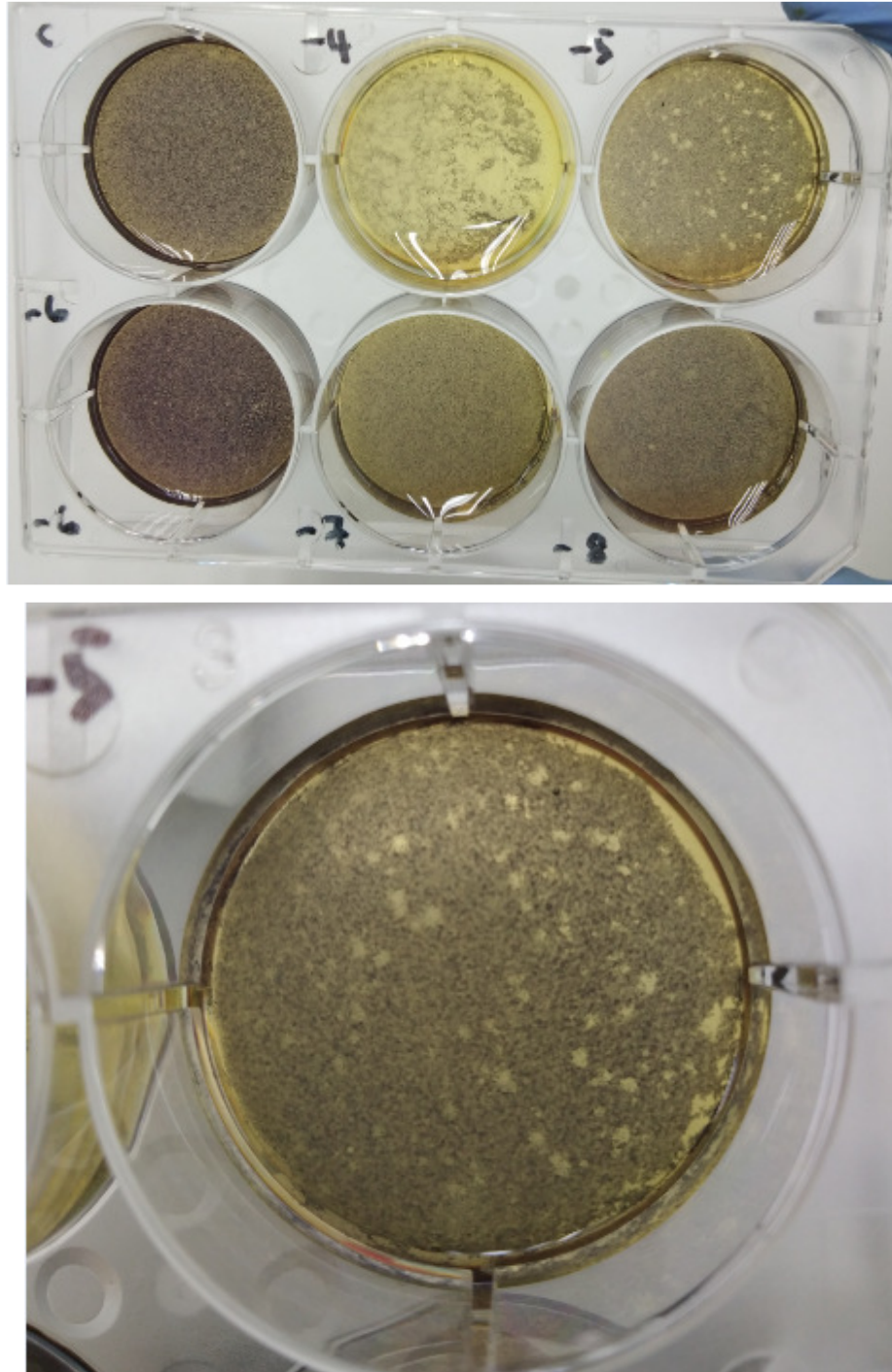


Figure 4.25 Functional titration of AdhIL-12. Plaques were obvious in the well which the cells were infected with AdhIL-12 dilution at 10^{-5} .

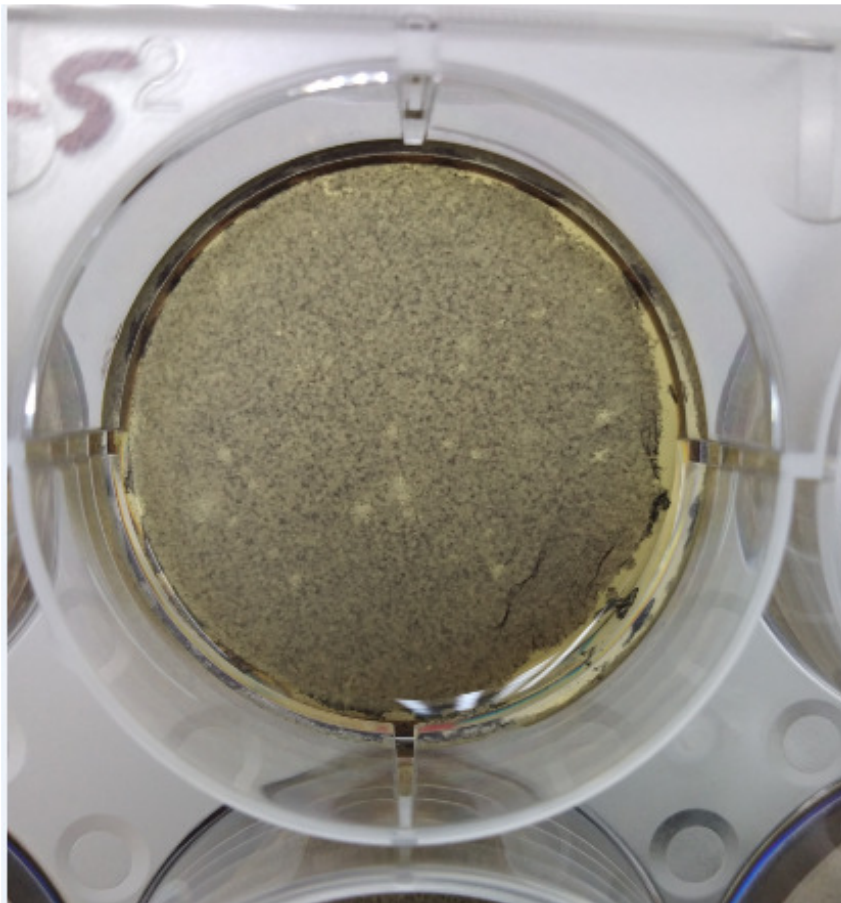
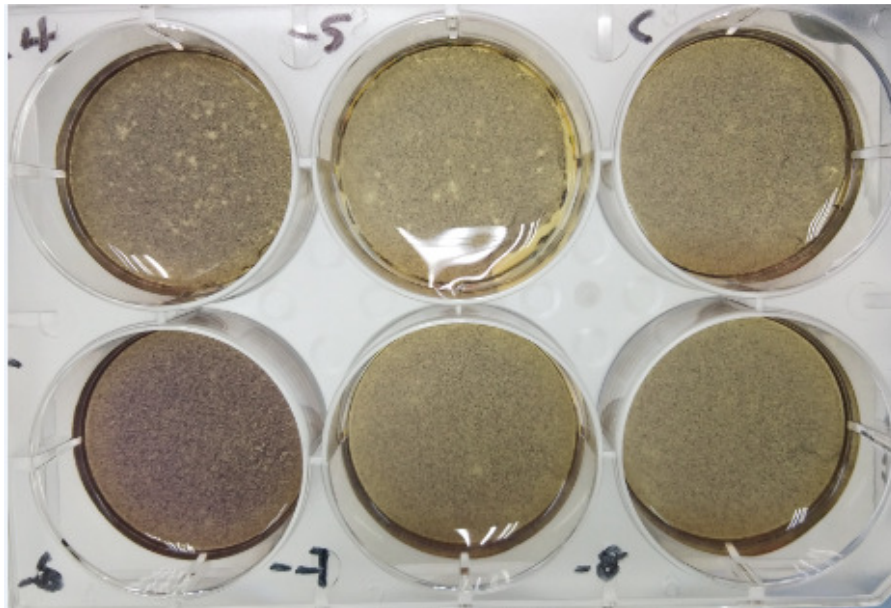


Figure 4.26 Functional titration of AdlacZ. Plaques were obvious in the well which the cells were infected with AdlacZ dilution at 10^{-5} .

Table 4.10 Functional titer of AdhIL-12 and AdlacZ

Recombinant adenovirus	Plaque count	Functional titer (ifu/ml)
AdhIL-12	79	7.9×10^7
AdlacZ	23	2.3×10^7

4.3 Comparison between Viral and Non-viral Method in Generation of hUCMSC Expressing hIL-12

The two methods which were used to generate hUCMSC expressing hIL-12 (hUCMSC-IL12) were compared in terms of transfection efficiency, hIL-12 protein expression level and post-transfection cell viability. Adenoviral method was selected for downstream co-culture assays as the results showed superior condition in all aspects of the comparison.

4.3.1 Transfection Efficiency

The transfection efficiency of hUCMSC-IL12 generated by both methods were compared. Adenoviral method showed higher of transfection efficiency ($63.6 \pm 10.6\%$) compared to only $26.9 \pm 16.7\%$ of transfection efficiency ($P = 0.001$) using the electroporation method (Figure 4.27).

Comparison of transfection efficiency

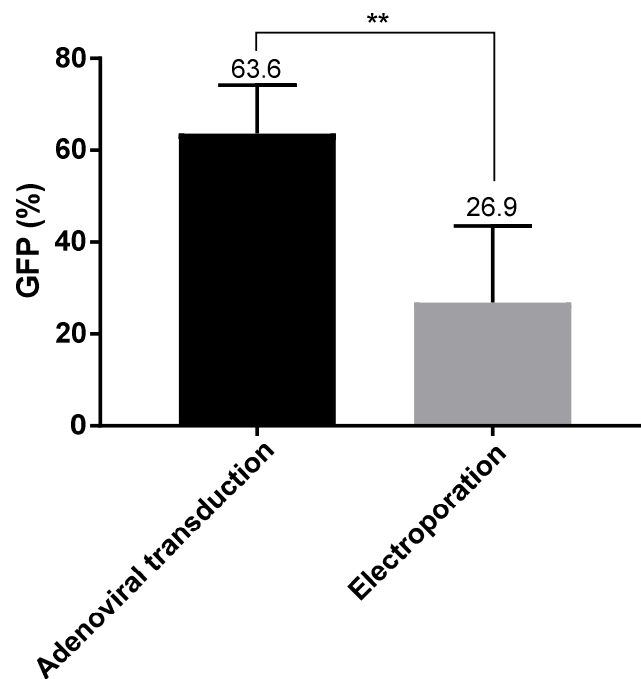


Figure 4.27 Comparison of transfection efficiency between hUCMSC-IL12 generated by adenoviral vector and electroporation (n=3). Data were expressed as mean \pm SD. (** = p<0.01)

4.3.2 Expression of hIL-12 Protein

The hIL-12 protein expressed by the transfected hUCMSC was analysed using ELISA. The ELISA kit measured only hIL-12 p70 heterodimer protein in the cell culture supernatant of the transfected hUCMSC. Adenoviral method showed significantly higher hIL-12 protein level compared to electroporation at 1.2×10^7 pg/ml and 41 pg/ml respectively (P = 0.011) (Figure 4.28).

Comparison of hIL-12 protein expression

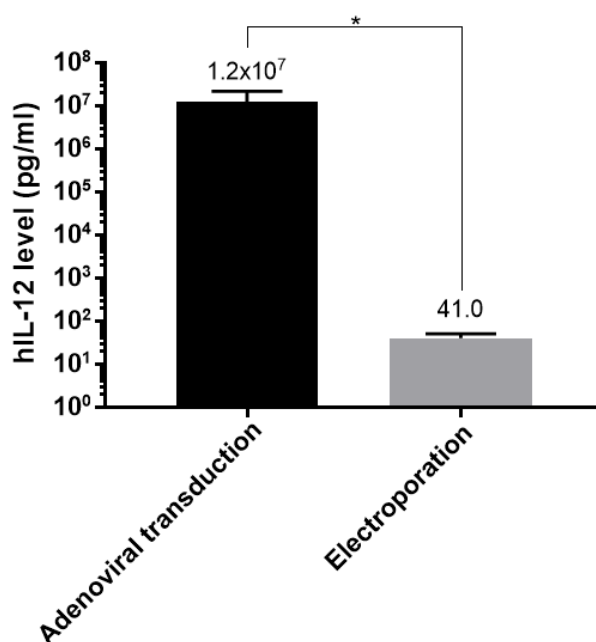


Figure 4.28 Comparison of hIL-12 protein expression between hUCMSC-IL12 generated by adenoviral vector and electroporation (n=3). Data were expressed as mean \pm SD. (* = $p < 0.05$)

4.3.3 Cell Viability of hUCMSC Post-transfection

In the context of hUCMSC viability post transfection, adenoviral method again showed better outcome compared to electroporation, with viability reported at $82.6 \pm 23.6\%$ compared to $55.1 \pm 28.6\%$ in electroporation. However, there is no significant difference ($P = 0.1$) between the two groups.

Comparison of post-transfection cell viability

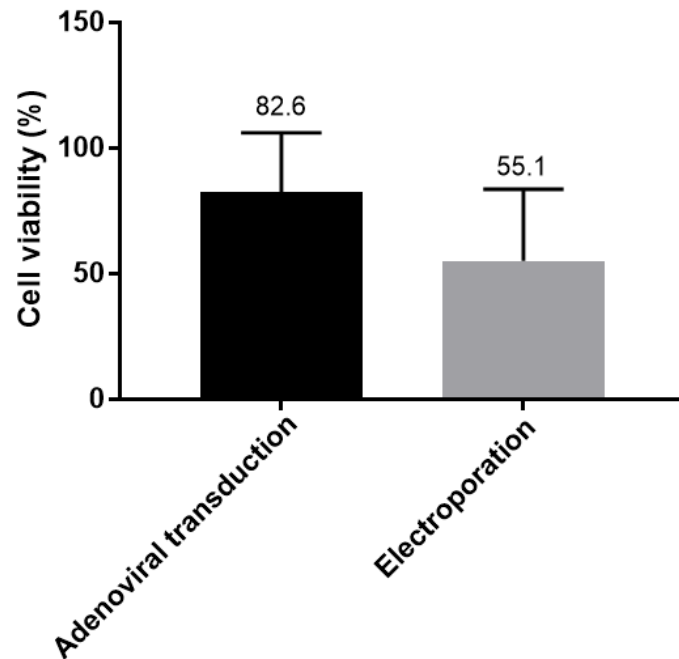


Figure 4.29 Comparison of hUCMSC viability post transfection between hUCMSC-IL12 generated by adenoviral vector and electroporation (n=3). Data were expressed as mean \pm SD.

4.4 Determination of Inhibition Effect of hUCMSC Expressing hIL-12 on Human Lung Cell Lines

The inhibition effect of hUCMSC-IL12 on H1975 human lung adenocarcinoma cells was determined in an *in vitro* co-culture system. Three days after hUCMSC-IL12 co-culture with H1975 cells, the viability of H1975 cells decreased by approximately 18% compared to H1975 cells cultured alone and further reduced to 66.8% ($P < 0.0001$) on day 5 after co-culture initiation (Figure 4.30). In contrast, there is no significant reduction in the cell viability of MRC-5 human lung fibroblast cells after co-culture with hUCMSC-IL12. These results demonstrated that hUCMSC-IL12 directly inhibited the growth of lung adenocarcinoma cells without the requirement of the host immune system. When

co-cultured with H1975 cells, no significant difference was observed in groups of untransduced hUCMSC and hUCMSC-lacZ. Interestingly, the cell viability of MRC-5 cells was significantly increased to 150.4% ($P = 0.0156$) after 5 days of co-culture with untransduced hUCMSC (Figure 4.31). No significant difference for the other groups was observed when co-cultured with the MRC-5 cells.

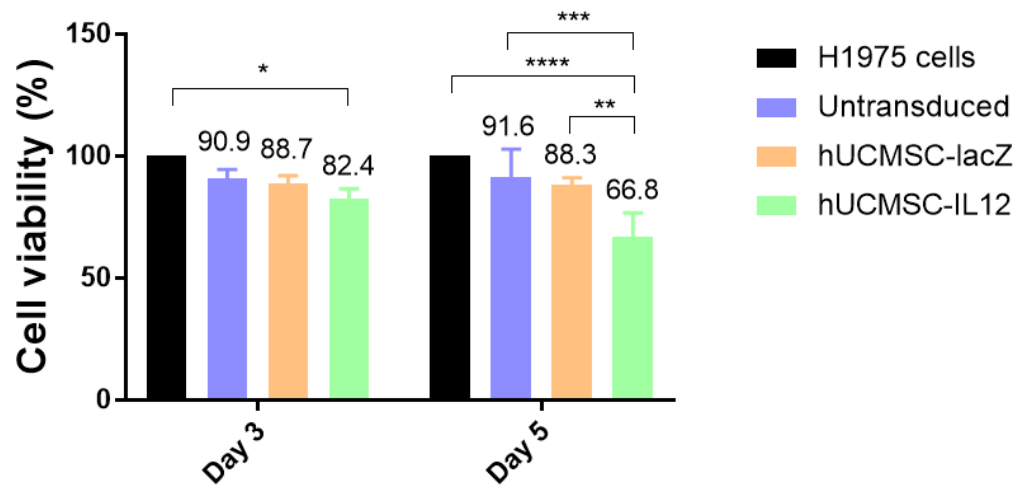


Figure 4.30 Inhibition effect of hUCMSC-IL12 on H1975 lung adenocarcinoma cells (n=6). Data were expressed as mean \pm SD. Statistical differences are indicated with * for $P < 0.05$, ** for $P < 0.01$, *** for $P < 0.001$ and **** for $P < 0.0001$ when compared to H1975 cells alone using two-way ANOVA.

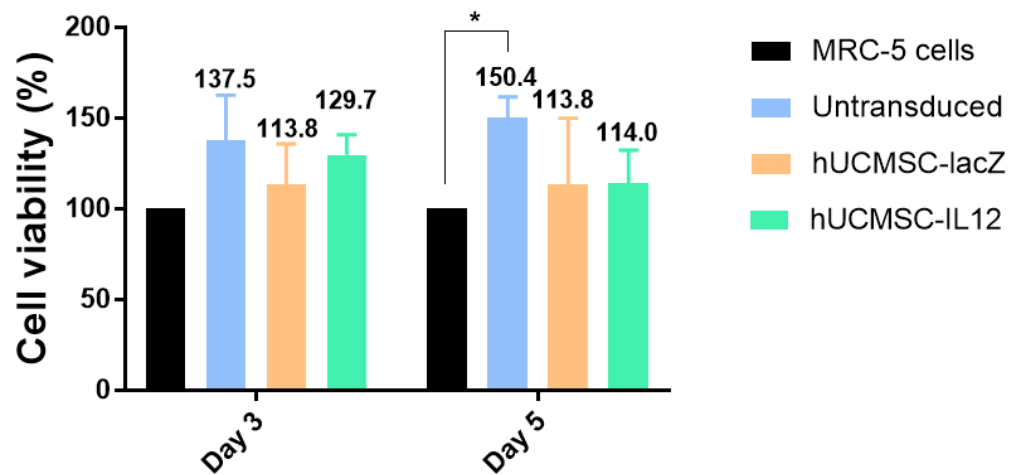


Figure 4.31 Inhibition effect of hUCMSC-IL12 on MRC-5 human normal lung fibroblast cells (n=6). Data were expressed as mean \pm SD. Statistical differences are indicated with * for $P < 0.05$ when compared to MRC-5 cells alone using two-way ANOVA.

4.5 Determination of hIL-12 Protein Expression Level in Co-culture Experiment

In order to determine the hIL-12 protein expression level in the co-culture experiments, the cell culture supernatant was collected and the protein expression was evaluated by ELISA, which showed that the hIL-12 level in both co-culture experiments were similar. The hIL-12 protein expressed by hUCMSC-IL12 was reported as $1.2 \pm 0.4 \mu\text{g/ml}$ on day 3 ($P = 0.0048$) and increased to $2.2 \pm 0.4 \mu\text{g/ml}$ on day 5 ($P = 0.0008$) after co-cultured with H1975 cells (Figure 4.32). Similarly, the hIL-12 protein concentration in the co-culture experiment with MRC-5 cells was $1.2 \pm 0.08 \mu\text{g/ml}$ on day 3 ($P < 0.0001$) and $2.2 \pm 0.1 \mu\text{g/ml}$ on day 5 ($P < 0.0001$) (Figure 4.33). No hIL-12 protein was detected in the supernatant of untransduced hUCMSC.

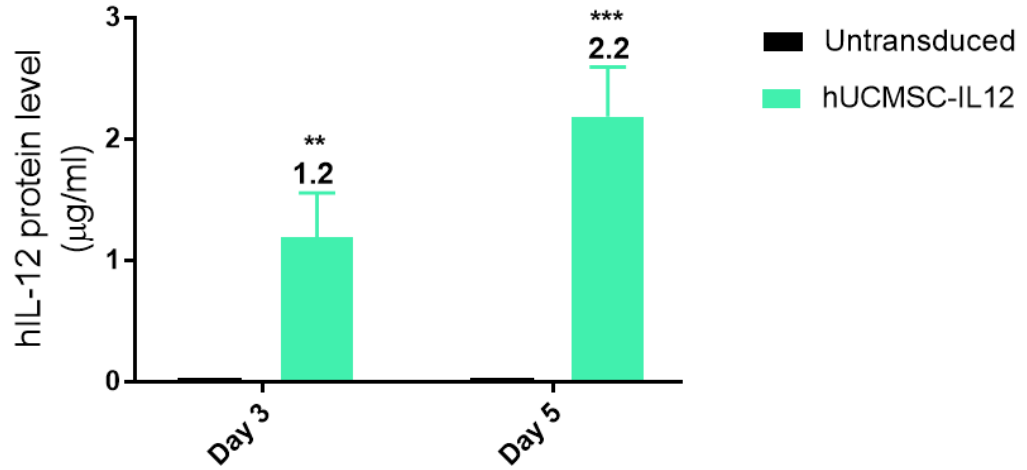


Figure 4.32 Protein expression of hIL-12 in untransduced and hUCMSC-IL12 when co-cultured with H1975 cells (n=6). Untransduced hUCMSC served as negative control. Data were expressed as mean \pm SD. Statistical differences are indicated with ** for $P < 0.01$ and * for $P < 0.001$ when compared to untransduced hUCMSC using unpaired t-test.**

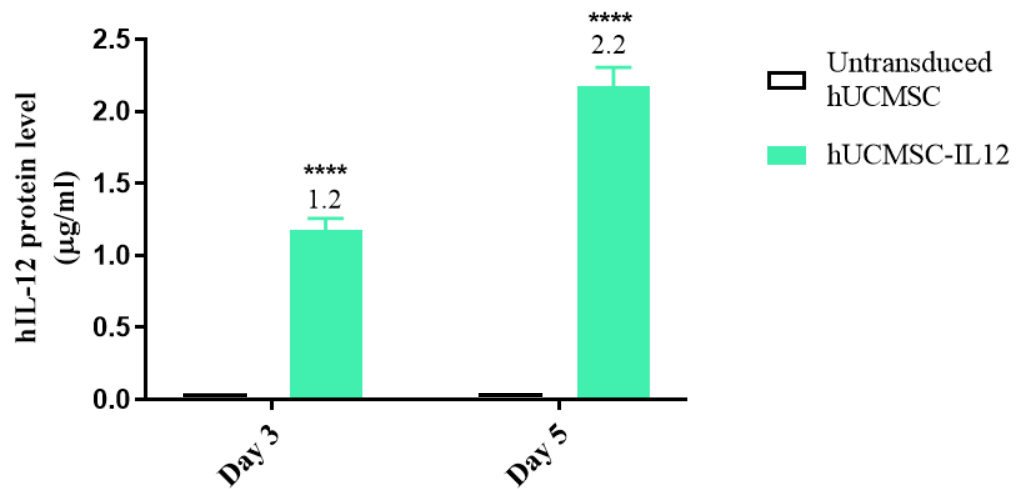


Figure 4.33 Protein expression of hIL-12 in untransduced and hUCMSC-IL12 when co-cultured with MRC-5 cells (n=6). Untransduced hUCMSC served as negative control. Data were expressed as mean \pm SD. Statistical differences are indicated with ** for $P < 0.0001$ when compared to untransduced hUCMSC using unpaired t-test.**

4.6 Determination of hIL-12 mRNA Expression Level of hUCMSC-IL12

In order to investigate the mRNA expression of hIL-12 in hUCMSC-IL12, qRT-PCR was performed. The fold changes of hIL-12 mRNA expression in hUCMSC-IL12 were calculated by the $\Delta\Delta C_t$ method with GAPDH as the endogenous control. Then, the relative quantification (RQ) values, which indicated the gene expression in the hUCMSC-IL12 samples relative to the untransduced hUCMSC samples, were calculated based on the formula below:

$$\begin{aligned} \Delta C_t (\text{hUCMSC-IL12 or hUCMSC}) & \\ &= C_t \text{ sample (hUCMSC-IL12 or hUCMSC)} - C_t \text{ GAPDH} \\ \Delta\Delta C_t &= \Delta C_t (\text{hUCMSC-IL12}) - \Delta C_t (\text{hUCMSC}) \\ \text{RQ} &= 2^{-\Delta\Delta C_t} \end{aligned}$$

The hIL-12 mRNA expression was detected at high level in hUCMSC-IL12, which was 6.0×10^6 ($P = 0.0313$) fold higher relative to control untransduced hUCMSC (Figure 4.34). The result was obtained from an average of 6 independent experiments.

The relative mRNA expression level of AdhIL-12 transduced hUCMSC

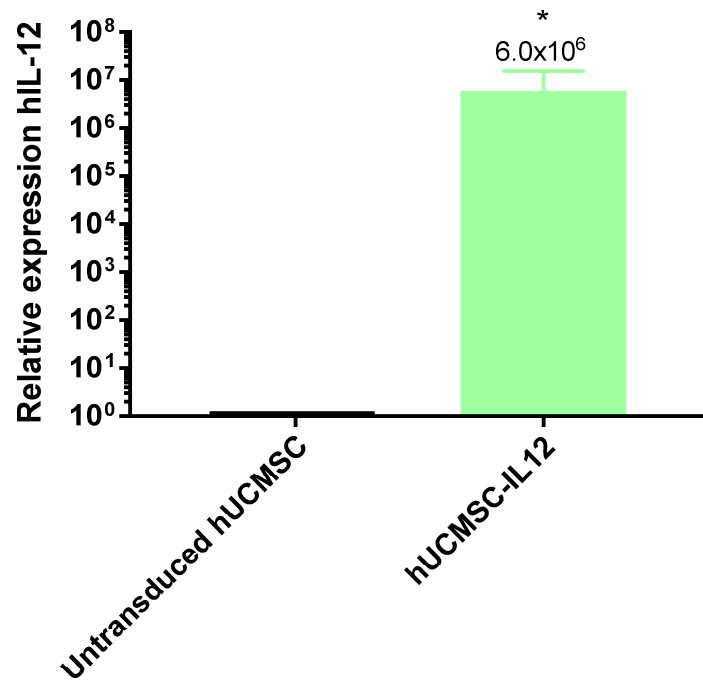


Figure 4.34 *In vitro* mRNA expression of hIL-12 in hUCMSC-IL12 relative to untransduced hUCMSC (n=6). Data were expressed as mean ± SD. Statistical difference is indicated with * for P < 0.05 when compared with control untransduced hUCMSC.

CHAPTER 5

DISCUSSION

5.1 Comparison of viral and non-viral method in generation of hUCMSC-IL12

In general, MSC can be genetically engineered using viral or non-viral methods. Typically, viral method showed much higher transduction efficiency compared to non-viral method. The most often utilised viral vector for gene therapy is recombinant adenovirus (Ad), which offers the following beneficial properties for gene therapy products: high gene-transfer efficiency, large gene carrying capacity, selective gene delivery, low cytotoxicity, potential therapeutic immunogenicity, ease of manufacturing and modification, and cost-effective commercial manufacture (Zhang et al., 2018). However, the utilisation of viral vector often triggered safety concerns when translated clinically. This was seen in the fatal case of a patient with partial ornithine transcarbamylase (OTC) deficiency who underwent adenoviral gene therapy (Raper et al., 2003). Consequently, other severe adverse events were reported whereby two patients with X-linked severe combined immune deficiency (XSCID) developed leukaemia more than 2 years after their retroviral gene therapy (Kohn, Sadelain and Glorioso, 2003). Since then, research is drastically reduced due to safety concerns regarding the use of viral vectors clinically. Despite these early setbacks, adenoviral vectors have recently gained prominence again in the field of gene therapy (Lee et al., 2017). In year 2004, Gendicine, a recombinant human

p53 adenovirus which was approved by China Food and Drug Administration (CFDA), was made available in the market. After more than ten years of use in the market, Gendicine (Ad-p53) has proven to have an excellent safety profile, shown to be effective against a variety of tumour types, and has been successfully used in conjunction with other types of conventional anticancer therapy (Li et al., 2021). Based on these results, adenoviral vector was selected as the viral vector used in this study. Adenoviral vector is a non-integrating viral vector with reported lower risk of genotoxicity (Athanasopoulos, Munye and Yáñez-Muñoz, 2017). The adenoviral vectors remain in the nucleus of the host cells as episomal DNA rather than integrating into the host genome (Singh, Kumar and Agrawal, 2019).

Among the variety of non-viral methods, electroporation was chosen in this study. The principle of electroporation is rather simple in which the permeability of target cell membrane is increased by applying electrical field and thus allows the introduction of plasmid DNA (gene of interest) into the cells. Park et al. demonstrated that the etanercept-synthesising MSC generated by electroporation showed anti-arthritic effect in a collagen-induced arthritis model (Park et al., 2017). In addition, electroporation has also been utilised in clinical trials. A phase II clinical trial of electroporated plasmid IL-12 in advanced melanoma patients completed in year 2019, showed the safety usage of the intratumoural electroporation approach (Algazi et al., 2020). However, there are some limitations on the electroporation usage in gene therapy. For instance, surgical procedure is required when transferring genetic material into internal organs via electroporation and usage on a large area of tissue is almost

impossible due to the small gap between the electrodes. The use of high voltage in electroporation will also lead to severe and unintended skin damage (Sokołowska and Błachnio-Zabielska, 2019). Therefore, it may be more challenging to translate the use of electroporation-based gene therapy in clinical settings.

In view of the advantages and limitations associated with both adenoviral vector and electroporation methods of gene delivery, the first part of this study was conducted to assess the best approach to use in generating hUCMSC-IL12. Parameters that were selected for comparison between these two methods include the transfection efficiency, level of hIL-12 protein expression and post-transfection hUCMSC cell viability. Results from this study showed that the adenoviral method is superior to electroporation method. There was a huge difference between the hIL-12 protein secreted by the hUCMSC-IL12 generated by the two methods, which were 1.2×10^7 pg/ml and 41 pg/ml for adenoviral vector and electroporation respectively. A study of oncolytic adenovirus (Ad5-yCD/mutTKSR39rep-mIL12) expressing two suicide genes and mouse interleukin-12 (IL-12) also reported IL-12 protein expression level as high as 10^7 pg/ml (Freytag, Barton and Zhang, 2013). It is noteworthy that the plasmid carrying the IL-12 gene in the study has the same backbone and same manufacturer as the pUNO1-hIL12 plasmid used in present study. This may suggest that the expression of the gene of interest, IL-12 can be powerful by these plasmids.

In addition, the results also showed that the post-transfection viability of hUCMSC was lower when using electroporation (55.1%) method compared to adenoviral (82.6%) method. It is vital to maintain the hUCMSC post-transfection viability because method with higher post-transfection viability can produce more viable cells carrying the hIL-12 gene in each transfection procedure. In other words, it will be more time and cost effective. Taken together, the adenoviral method was selected to be the better method to produce hUCMSC-IL-12 for the downstream assays.

5.2 Characterisation of hUCMSC and hUCMSC-IL12

Mesenchymal stromal cells can be isolated from Wharton's jelly in umbilical cord and expanded *in vitro*. In the year 1991, fibroblast-like cells were successfully isolated from Wharton's jelly and characterised by McElreavey et al. (McElreavey et al., 1991) and these cells were then identified as MSC. Wharton's jelly, named after the English anatomist and physician Thomas Wharton (1614–1673), is a gelatinous material found in the stroma of the umbilical cord (Arutyunyan et al., 2016). Two umbilical arteries and one umbilical vein are shielded from clumping by Wharton's jelly, which also helps to maintain the elasticity of the umbilical cord (Arutyunyan et al., 2016).

In the year 2019, the ISCT has published a guideline regarding the nomenclature of MSC. Following the recommendations of this guideline, the cells used in this study are termed as mesenchymal stromal cells. The MSC used

in this study were characterised by the immunophenotyping and trilineage differentiation assays.

MSC do not differentiate during *in vitro* cell expansion, in contrast to haematopoietic stem cells, as MSC differentiation needs certain signals (Yap et al., 2009). In addition, Scheers et al. have shown that UCMSC maintain their ability to proliferate and differentiate for a long enough time to enable for the necessary cell expansion to reach the numbers required for stem cell therapy (Scheers et al., 2013). The study also showed that UCMSC were able to retain the osteogenic and adipogenic differentiation properties up to passage 18. Usage of UCMSC has several advantages for example, not involving ethical issues like embryonic stem cells, being readily available and easy isolation method. More importantly, UCMSC are a good replacement for bone marrow-derived MSC (BMMSC) because the umbilical cord blood cells are immature cells which can yield a more primitive version of MSC compared with MSC derived from the bone marrow. Therefore, age-related reductions in MSC quantity, differentiation, and proliferative capability can be avoided (Ryu et al., 2010). With all these advantages, UCMSC were selected as the source of MSC in this study.

In this study, UCMSC is genetically engineered to express IL-12 using the adenoviral vector. Thus, it is of paramount importance to investigate the post transduction effects on UCMSC for any unanticipated phenotype changes and cellular toxicity to ensure the development of a clinically safe and effective approach. In addition, studies have shown that cultured MSC are prone to change their behaviour and activity in response to environmental changes since the environment in culture is different from the environment in the body (Zhou, Tsai

and Li, 2017). Wagner et al. showed that MSC encountered cellular senescence, slow proliferation rate and eventually cease to grow during cell culture (Wagner et al., 2008). These *in vitro* cell expansion-related problems will have a significant impact on the therapeutic quality of MSC which may potentially limit the clinical utility of MSC.

Dührsen et al. demonstrated that retrovirally transduced MSC to express herpes simplex virus thymidine kinase (HSV-TK) still maintained the MSC characteristics including surface marker expression, adipogenic and osteogenic differentiation properties (Dührsen et al., 2019). Another study using genetically engineered MSC by transduction with adeno-associated viruses (AAV) carrying anti-sense for miR-142 also showed the ability of transduced MSC in retaining the cell surface marker expression and trilineage differentiation properties of MSC (Yang et al., 2017). These findings are consistent with the results from this study which showed that hUCMSC-IL12 maintained their immunophenotypic characteristics and trilineage differentiation properties after adenoviral transduction indicating the potential of hUCMSC as the source for MSC in genetic engineering technology.

5.3 The Direct Inhibition Effect of hUCMSC-IL12 on H1975 Human Lung Adenocarcinoma Cells

The homing ability of MSC towards inflammatory sites, injured tissues and tumour sites led to the research and development of MSC as cellular vehicles in cell and gene therapy. Moreover, when administered to HLA-non-identical recipients, MSC do not trigger the host immune response and avoid

immunological rejection (Uchibori et al., 2014). Therefore, HLA-matching is not required prior to the administration of MSC into the recipients. Over the past decades, researchers were continuously putting efforts on using MSC to deliver anti-cancer agents to tumour sites. By enabling anti-cancer drugs to effectively concentrate at local tumour sites without increasing systemic concentrations, the systemic side effects of these agents can be lessened (Uchibori et al., 2014).

Although the anti-cancer effectiveness of IL-12 has been evidenced in many studies (Del Vecchio et al., 2007), however, clinical usage of recombinant human IL-12 has been constrained due to considerable toxicity from dosing identified in clinical trials on advanced malignancies (Leonard et al., 1997). Hence, one of the strategies to surmount this challenge is through cell and gene therapy in which adequate levels of IL-12 can be delivered and maintained at tumour sites to avoid the surge of IL-12 concentration systemically. Recently, Wu et al. demonstrated the antitumour effect of bone marrow-derived MSC expressing IL-12 in glioma-bearing xenograft mouse model (Wu et al., 2021). Moreover, in another study, MSC expressing IL-12 were able to inhibit the tumour growth and reduced the number of metastases in murine melanoma model (Kulach et al., 2021). The suppression of angiogenesis elicited by MSC expressing IL-12 cells and the rise in the proportion of M1 macrophages and CD8⁺ T lymphocytes within the tumour are the likely underlying mechanisms of tumour inhibition seen in this therapy.

Recently, Ahn et al. demonstrated an efficient method for treating orthotopic and metastatic lung cancer models with intravenous injection of

synthetic polymer/DNA nanoparticles that induced tumour-specific expression of the IL-12 gene under the control of the cancer-selective progression elevated gene 3 (PEG-3) promoter (Ahn et al., 2021). In this study, the survival of lung tumour-bearing mice was significantly improved after the treatment of the special constructed nanoparticles expressing murine single-chain IL-12 without any systemic toxicity. However, the use of nanoparticles in cancer therapy is commonly restricted by their poor targeting effectiveness and other technical issues such as scale-up production, equal optimisation, and performance forecasting (Gavas, Quazi and Karpiński, 2021).

Najmuddin et al. showed superior anti-tumoural and cytotoxic effects in the CT26 colon cancer model when using recombinant newcastle disease virus (NDV) strain expressing IL-12 (rAF-IL12), as compared to its parental wild-type, AF2240-i (Najmuddin et al., 2020). According to this study, rAF-IL12 effectively inhibited the growth of CT26 tumours in a murine *in vivo* model. Moreover, rAF-IL12 demonstrated the ability to induce apoptosis both *in vitro* and *in vivo*, leading to an increase in the expression of apoptosis-related genes and a decrease in the expression of oncogenes. Additionally, rAF-IL12 played a role in modulating the immune response specifically targeting the CT26 tumours.

Tumour-homing cells have been utilised as delivery vehicles for cancer treatment. Mesenchymal stem/stromal cells (MSCs), which exhibit tumour tropism, a capability for self-renewal and proliferation, and minimal immunogenicity, are the most desirable candidates for drug delivery vehicles for cancer therapy among the numerous types of tumour-homing cells (Takayama,

Kusamori and Nishikawa, 2021). In this study, the hUCMSC were genetically engineered to express hIL-12 and the *in vitro* growth inhibition effect on human lung adenocarcinoma cells was investigated.

Many studies have shown the antitumour effects of IL-12 on various tumour models. IL-12 can stimulate both the innate and adaptive immune responses as it functions to enhance the cytotoxicity of NK cells and T cells. In addition to this, IL-12 may have direct growth inhibition effect on the cancer cells as well through other signalling pathways. Direct growth inhibition will be useful in conditions where the treatment sites are hardly reachable by immune cells such as the central nervous system (CNS) or in patients who are immune-compromised such as those with HIV/AIDS or transplant patients who are taking certain immunosuppressive drugs. It is also useful in patients who has inborn errors of immunity (IEI) where the immune system is not functioning normally.

In order to investigate the direct inhibition effect of hUCMSC-IL12 on H1975 human lung adenocarcinoma cells, the co-culture assay with transwell system was conducted. The transwell inserts with 0.4 μm pore size were used which allowed the cytokines, in particularly hIL-12, secreted by hUCMSC-IL12 to pass through to the culture medium in the bottom chamber containing the H1975 cells. It is noteworthy that at this pore size, no cells can penetrate through the transwell inserts. In other words, only secretions from hUCMSC-IL12 will have direct contact with the H1975 cells in the co-culture system, but not hUCMSC-IL12. Based on the results from this study, hUCMSC-IL12 significantly inhibited the growth of H1975 cells *in vitro* after 3 days of co-

culture. There were no significant differences between hUCMSC or hUCMSC-lacZ that were co-cultured with the H1975 cells. Thus, these findings indicated that the inhibition effect seen was due to the hIL-12 released by the hUCMSC-IL12.

The direct effect of IL-12 on tumour cells has yet been thoroughly elucidated despite the fact that it has a variety of activities on immune cells. A study conducted by Su et al. suggested that the direct effects of IL-12 on tumour cells involved the activation of nuclear factor kappa-light-chain-enhancer of activated B cells (NF-kB) and enhanced IFN- γ -mediated signal transducer and activator of transcription 1 (STAT1) phosphorylation via IL-12 receptor β 1 (Su et al., 2001). This may also be the possible underlying mechanism of direct inhibition effect that is observed in this study. In addition, Su et al. also demonstrated that IL-12 receptor β 1 is selectively expressed on some tumour cells only. The role of NF-kB activation and STAT1 phosphorylation via IL-12 receptor β 1 in the growth inhibition of H1975 after treatment with hUCMSC-IL12 are still unknown at this point and will be vital to be elucidated in future study.

Thus far, the results have indicated significant growth inhibition of H1975 cells after treatment with hUCMSC-IL12 in the *in vitro* co-culture system. However, it did not translate to major inhibition observed on the H1975 cells. In the co-culture system of this study, only hUCMSC-IL12 were added into the wells. As the main function of IL-12 in tumour elimination is by stimulating NK cells and T cells to produce IFN- γ and improve their cytotoxicities, absence of

these cells may contribute to the lower growth inhibition rate seen. Addition of these immune cells in the co-culture system may improve the inhibitory effect of hUCMSC-IL12.

Since human models can only be engrafted in nude mice, the comprehensive evaluation of the *in vivo* antitumour effect of hUCMSC-IL12 may be hindered due to the lack of an immune system in these mice. Hence, the usage of immunocompetent mice is preferred. As such, patient-derived xenograft (PDX) models or genetically engineered mouse models (GEMMs) may be suitable animal models to be used for the *in vivo* study.

5.4 Co-culture of hUCMSC and Genetically Engineered hUCMSC with MRC-5 Human Lung Fibroblasts

For the co-culture assays of the MRC-5 human lung fibroblasts, results showed no significant effect of hUCMSC-IL12 or hUCMSC-lacZ on the MRC-5 cells. Interestingly, there is a significant increase in the cell viability of MRC-5 cells after 5 days co-culture with hUCMSC. Similar result was reported by Chen et al. (2021) where they observed significant increase in cell viability of MRC-5 cells when co-cultured with hUCMSC, after cigarette smoke (CS) extract exposure (Chen et al., 2021). Lung fibroblasts play a significant part in the healing of CS-damaged lung tissues (Togo et al., 2008). Hence, lung fibroblast dysfunction was the primary factor contributing to the loss of the ability to repair alveoli caused by CS (Miglino et al., 2012).

Therefore, it was suggested that the paracrine factors produced by hUCMSC to lung fibroblasts may play a role in the process of alveolar healing following cigarette smoke exposure that led to the increase in cell viability of MRC-5 cells (Chen et al., 2021). Prior to this, another study has shown that human MSC isolated from Wharton's Jelly, can secrete transforming growth factor (TGF)- β 1 (de Araújo Farias et al., 2018) which takes part in healthy lung growth and repair of lung damage by stimulating fibroblast proliferation, differentiation, migration, production and contraction of the extracellular matrix (Saleh, Fotook Kiaei and Kavianpour, 2022).

This may explain the observation of the co-culture assay with MRC-5 cells. The hUCMSC may have secreted paracrine factors that led to the increase of cell viability of MRC-5 cells. In fact, the lung function of various types of lung disease models has been shown to improve by MSC treatment (Cruz and Rocco, 2020). These lung diseases included asthma, chronic obstructive pulmonary disease (COPD), idiopathic pulmonary fibrosis (IPF), pulmonary arterial hypertension (PAH), and silicosis. Interestingly, the mechanism of MSC action varies between lung diseases, reflecting the capacity of MSC to perceive and react differentially to various inflammatory conditions. The data from clinical trials demonstrated that this method was safe for use across ages and disease types (Behnke et al., 2020). However, more research is still required to allow widespread clinical deployment of MSC-based treatments for all types of lung disease.

In this study, we selected MRC-5 human normal lung fibroblasts as the control cells. These cells originated from the lung tissue of a male foetus at 14-week-old gestation. They have been widely used as control cell lines in various research studies due to their normal nature and non-cancerous characteristics. As this is a proof-of-concept study, only one normal lung cell line was utilised. However, future studies would benefit from the inclusion of additional lung cell lines to obtain a more comprehensive data.

CHAPTER 6

CONCLUSIONS

6.1 CONCLUSION

Over the past decades, IL-12 has emerged as a promising antitumour agent. However, severe toxicities will be triggered when IL-12 is administered systemically due to the extremely high level of interferon- γ (IFN- γ) induced by this strategy. Thus, strategies that can achieve therapeutic effect of IL-12 while avoiding systemic toxicity simultaneously are required. MSC appear to be the suitable candidate as the cellular vehicle of IL-12 due to their homing ability to inflammatory/injured sites.

This study has successfully generated the hUCMSC expressing hIL-12 using both viral (adenoviral vector) and non-viral (electroporation) methods. The constructed hUCMSC-IL12 showed the ability to secrete recombinant hIL-12. The adenoviral method was shown to be superior to electroporation in the generation of hUCMSC-IL12 based on the transduction efficiency, post-transfection cell viability and hIL-12 protein expression level. Both the untransduced hUCMSC and hUCMSC-IL12 have the ability to differentiate into adipocytes, chondrocytes and osteoblasts when the respective induction medium was introduced to the cells. The hUCMSC-IL12 also maintained their cell surface markers similar to untransduced hUCMSC. These results confirmed that

hUCMSC-IL12 successfully maintained their integrity after adenoviral transduction to ensure the therapeutic quality of the genetically engineered hUCMSC if clinically translated.

In the co-culture experiments to determine the direct inhibition effect of hIL-12 secreted by hUCMSC-IL12 on H1975 human lung adenocarcinoma cells, the results demonstrated that hUCMSC-IL12 were able to suppress the growth of the cancer cells. In contrast, there is no inhibition effect of the hUCMSC-IL12 on MRC-5 human lung fibroblast cells. This indicates that hUCMSC-IL12 target only cancerous or inflammatory cells, but not normal cells. Apart from that, the co-culture experiment also demonstrated that untransduced hUCMSC promotes the growth of MRC-5 cells. It is believed that this finding was contributed by the paracrine factors secreted by hUCMSC, in particularly TGF- β 1 which helps in the growth of healthy lung cells.

In conclusion, this study provides the proof of concept that hUCMSC can be genetically engineered to express hIL-12 and exert growth inhibition effect on human lung adenocarcinoma cells, but not normal human lung fibroblast cells. The hUCMSC-based delivery of IL-12 is a feasible and promising approach to deliver IL-12 for antitumour therapy without triggering the systemic toxicities associated with IL-12. However, additional studies are required before this MSC-based therapy can be utilised clinically.

6.2 RECOMMENDATIONS OF FUTURE RESEARCH

The therapeutic potential of hUCMSC-IL12 to inhibit the growth of lung adenocarcinoma cells appears promising. However, there are specific issues that must be resolved in future study in order to improve the design and also the understanding of this MSC-based therapeutic approach.

The experiments in this study demonstrated the ability of hUCMSC-IL12 to inhibit the growth of lung adenocarcinoma cells in a transwell setting. This experimental set up may not precisely replicate the *in vivo* condition. However, as this is a proof-of-concept study, future investigations can be carried out to explore using 3D co-culture system or animal model to achieve a more comprehensive result. As IL-12 has immunoregulatory function by activating T cells and NK cells (Guo, Cao and Zhu, 2019), the *in vitro* co-culture experiment may be extended to include the immune cells so as to investigate if the presence of these cells can improve the growth inhibition potential of hUCMSC-IL12.

Besides, it is anticipated that the *in vivo* suppression effect of hUCMSC-IL12 will be better in the presence of the surrounding immune cells in the host system. Animal models also can be a tool to evaluate any adverse effects of the administered hUCMSC, particularly the hUCMSC that has been extensively manipulated *ex vivo*. It will be essential also to look into the *in vivo* properties of the genetically engineered hUCMSC in order to improve the delivery procedures. Furthermore, tracing the *in vivo* fate of hUCMSC would help in developing the optimal delivery method for this MSC-based therapy. Thus,

further investigation into the use of hUCMSC-IL12 as cellular vehicle of cancer therapy in an animal model is warranted.

As studies have shown the antitumour effects of IL-12 in a broad spectrum of tumours, the inhibition effects of hUCMSC-IL12 may be investigated in other cancer cells. This study has demonstrated the growth inhibition effect of hUCMSC-IL12 on H1975 cells. With this proof-of concept finding, other functional assays can be included in the future to further study the antitumour effect of hUCMSC-IL12 on H1975 cells.

In addition, the efficacy of IL-12 in combination with other cytokines may also be investigated. For instance, IL-18 has been proven to have synergistic effect with IL-12 (Baxevanis, Gritzapis and Papamichail, 2003). Last but not least, the mechanism of the growth inhibition effect of hUCMSC-IL12 may be investigated especially with regards to the NF-kB and STAT1 pathways. By understanding the underlying mechanisms, the efficacy of the hUCMSC-IL12 could be improved further.

REFERENCES

- Afanasyev, B. v, Elstner, E.E. and Zander, A.R., 2009. A . J . Friedenstein , founder of the mesenchymal stem cell concept. 1(3), pp.35–38. <https://doi.org/10.3205/ctt-2009-en-000029.01>.
- Agostini, F., Vicinanza, C., Biolo, G., Spessotto, P., da Ros, F., Lombardi, E., Durante, C. and Mazzucato, M., 2021. Nucleofection of adipose mesenchymal stem/stromal cells: Improved transfection efficiency for gmp grade applications. *Cells*, 10(12). <https://doi.org/10.3390/cells10123412>.
- Ahn, H.H., Carrington, C., Hu, Y., Liu, H. wen, Ng, C., Nam, H., Park, A., Stace, C., West, W., Mao, H.Q., Pomper, M.G., Ullman, C.G. and Minn, I., 2021. Nanoparticle-mediated tumor cell expression of mIL-12 via systemic gene delivery treats syngeneic models of murine lung cancers. *Scientific Reports*, 11(1). <https://doi.org/10.1038/s41598-021-89124-4>.
- Airoldi, I., Di Carlo, E., Cocco, C., Caci, E., Cilli, M., Sorrentino, C., Sozzi, G., Ferrini, S., Rosini, S., Bertolini, G., Truini, M., Grossi, F., Galiotta, L.J.V., Ribatti, D. and Pistoia, V., 2009. IL-12 can target human lung adenocarcinoma cells and normal bronchial epithelial cells surrounding tumor lesions. *PLoS ONE*, 4(7). <https://doi.org/10.1371/journal.pone.0006119>.
- Algazi, A., Bhatia, S., Agarwala, S., Molina, M., Lewis, K., Faries, M., Fong, L., Levine, L.P., Franco, M., Oglesby, A., Ballesteros-Merino, C., Bifulco, C.B., Fox, B.A., Bannavong, D., Talia, R., Browning, E., Le, M.H., Pierce, R.H., Gargosky, S., Tsai, K.K., Twitty, C. and Daud, A.I., 2020. Intratumoral delivery of tavokinogene telseplasmid yields systemic immune responses in metastatic melanoma patients. *Annals of Oncology*, 31(4), pp.532–540. <https://doi.org/10.1016/j.annonc.2019.12.008>.
- Aluigi, M., Fogli, M., Curti, A., Isidori, A., Gruppioni, E., Chiodoni, C., Colombo, M.P., Versura, P., D'Errico-Grigioni, A., Ferri, E., Baccarani, M. and Lemoli, R.M., 2006. Nucleofection Is an Efficient Nonviral Transfection Technique for Human Bone Marrow–Derived Mesenchymal Stem Cells. *Stem Cells*, 24(2), pp.454–461. <https://doi.org/10.1634/stemcells.2005-0198>.
- Ao, O., Ae, N., Aj, O., Bo, O., Adesina, O., Ss, E. and Aa, O., 2017. Cord blood banking : the prospects and challenges of implementation in Nigeria. 5(4), pp.273–278. <https://doi.org/10.15406/htij.2017.05.00126>.
- de Araújo Farias, V., Carrillo-Gálvez, A.B., Martín, F. and Anderson, P., 2018. *TGF-β and mesenchymal stromal cells in regenerative medicine, autoimmunity and cancer. Cytokine and Growth Factor Reviews*, <https://doi.org/10.1016/j.cytogfr.2018.06.002>.
- Arutyunyan, I., Elchaninov, A., Makarov, A. and Fatkhudinov, T., 2016. *Umbilical Cord as Prospective Source for Mesenchymal Stem Cell-Based Therapy. Stem Cells International*, <https://doi.org/10.1155/2016/6901286>.

- Athanasopoulos, T., Munye, M.M. and Yáñez-Muñoz, R.J., 2017. *Nonintegrating Gene Therapy Vectors. Hematology/Oncology Clinics of North America*, <https://doi.org/10.1016/j.hoc.2017.06.007>.
- Barrett, J.A., Cai, H., Miao, J., Khare, P.D., Gonzalez, P., Dalsing-Hernandez, J., Sharma, G., Chan, T., Cooper, L.J.N. and Lebel, F., 2018. Regulated intratumoral expression of IL-12 using a RheoSwitch Therapeutic System® (RTS®) gene switch as gene therapy for the treatment of glioma. *Cancer Gene Therapy*, 25(5–6), pp.106–116. <https://doi.org/10.1038/s41417-018-0019-0>.
- Barton, K.N., Siddiqui, F., Pompa, R., Freytag, S.O., Khan, G., Dobrosotskaya, I., Ajlouni, M., Zhang, Y., Cheng, J., Movsas, B. and Kwon, D., 2021. Phase I trial of oncolytic adenovirus-mediated cytotoxic and interleukin-12 gene therapy for the treatment of metastatic pancreatic cancer. *Molecular Therapy - Oncolytics*, 20, pp.94–104. <https://doi.org/10.1016/j.omto.2020.11.006>.
- Baxevanis, C.N., Gritzapis, A.D. and Papamichail, M., 2003. In Vivo Antitumor Activity of NKT Cells Activated by the Combination of IL-12 and IL-18. *The Journal of Immunology*, 171(6), pp.2953–2959. <https://doi.org/10.4049/jimmunol.171.6.2953>.
- Behnke, J., Kremer, S., Shahzad, T., Chao, C.M., Böttcher-Friebertshäuser, E., Morty, R.E., Bellusci, S. and Ehrhardt, H., 2020. *MSC based therapies—new perspectives for the injured lung. Journal of Clinical Medicine*, <https://doi.org/10.3390/jcm9030682>.
- Berraondo, P., Etxeberria, I., Ponz-Sarvisé, M. and Melero, I., 2018. Revisiting interleukin-12 as a cancer immunotherapy agent. *Clinical Cancer Research*, 24(12), pp.2716–2718. <https://doi.org/10.1158/1078-0432.CCR-18-0381>.
- Caplan, A.I., 1991. Mesenchymal Stem Cells *. *Journal of Orthopaedic Research*, 9(5), pp.641–650.
- Caplan, A.I., 2017. Mesenchymal Stem Cells : Time to Change the Name ! *Stem Cells Translational Medicine*, 6, pp.1445–1451. <https://doi.org/http://dx.doi.org/10.1002/sctm.17-0051>.
- Car, B.D., Eng, V.M., Lipman, J.M., Anderson, T.D. and Pharmaceu, D., 1999. The Toxicology of Interleukin-12: A Review. *Toxicologic Pathology*, 27(1), pp.58–63.
- Car, B.D., Eng, V.M., Schnyder, B., Lahir, M., Shakhov, A.N., Woerly, G., Huang, S., Aguet, M., Anderson, T.D. and Ryffel, B., 1995. Role of Interferon- γ in Interleukin 12-Induced Pathology in Mice. *American Journal of Pathology*, 147(6).
- Chen, X.Y., Chen, Y.Y., Lin, W., Chen, C.H., Wen, Y.C., Hsiao, T.C., Chou, H.C., Chung, K.F. and Chuang, H.C., 2021. Therapeutic Potential of Human Umbilical Cord-Derived Mesenchymal Stem Cells in Recovering From Murine Pulmonary Emphysema Under Cigarette Smoke Exposure. *Frontiers in Medicine*, 8. <https://doi.org/10.3389/fmed.2021.713824>.

Chiocca, E.A., Yu, J.S., Lukas, R. v., Solomon, I.H., Ligon, K.L., Nakashima, H., Triggs, D.A., Reardon, D.A., Wen, P., Stopa, B.M., Naik, A., Rudnick, J., Hu, J.L., Kumthekar, P., Yamini, B., Buck, J.Y., Demars, N., Barrett, J.A., Gelb, A.B., Zhou, J., Lebel, F. and Cooper, L.J.N., 2019. Regulatable interleukin-12 gene therapy in patients with recurrent high-grade glioma: Results of a phase 1 trial. *Science Translational Medicine*, 11(505). <https://doi.org/10.1126/scitranslmed.aaw5680>.

Choi, I.K., Lee, J.S., Zhang, S.N., Park, J., Lee, K.M., Sonn, C.H. and Yun, C.O., 2011. Oncolytic adenovirus co-expressing IL-12 and IL-18 improves tumor-specific immunity via differentiation of T cells expressing IL-12RB 2 or IL-18R α . *Gene Therapy*, [online] 18(9), pp.898–909. <https://doi.org/10.1017/CBO9781139055345>.

Chulpanova, D.S., Kitaeva, K. V., Tazetdinova, L.G., James, V., Rizvanov, A.A. and Solovyeva, V. V., 2018. Application of Mesenchymal stem cells for therapeutic agent delivery in anti-tumor treatment. *Frontiers in Pharmacology*, 9(MAR), pp.1–10. <https://doi.org/10.3389/fphar.2018.00259>.

Constantin, G., Majeed, M., Giagulli, C., Piccio, L., Kim, J.Y., Butcher, E.C. and Laudanna, C., 2000. Chemokines trigger immediate β 2 integrin affinity and mobility changes: Differential regulation and roles in lymphocyte arrest under flow. *Immunity*, 13(6), pp.759–769. [https://doi.org/10.1016/S1074-7613\(00\)00074-1](https://doi.org/10.1016/S1074-7613(00)00074-1).

Cruz, F.F. and Rocco, P.R.M., 2020. *The potential of mesenchymal stem cell therapy for chronic lung disease. Expert Review of Respiratory Medicine*, <https://doi.org/10.1080/17476348.2020.1679628>.

Dembinski, J.L., Wilson, S.M., Spaeth, E.L., Studeny, M., Zompetta, C., Samudio, I., Roby, K., Andreeff, M. and Marini, F.C., 2013. Tumor stroma engraftment of gene-modified mesenchymal stem cells as anti-tumor therapy against ovarian cancer. *Cytotherapy*, 15(1), pp.20–32. <https://doi.org/10.1016/j.jcyt.2012.10.003>.

DJ M. and JM W., 2022. *Lung Adenocarcinoma (2022)*. 2022nd ed. In: *StatPearls [Internet]. Treasure Island (FL)*. StatPearls Publishing , Treasure Island (FL).

DMcelreavey, K., Iirvine, A., v I N Tennis, K.E. and I R W I N McLEAN, W.H., 1991. *Isolation, culture and characterisation of fibroblast-like cells derived from the Wharton's jelly portion of human umbilical cord*.

Dominici, M., Blanc, K. Le, Mueller, I., Marini, F.C., Krause, D.S., Deans, R.J., Keating, A., Prockop, D.J. and Horwitz, E.M., 2006. Minimal criteria for defining multipotent mesenchymal stromal cells . The International Society for Cellular Therapy position statement. 8(4), pp.315–317. <https://doi.org/10.1080/14653240600855905>.

Đorđević, M., Paunović, V., Jovanović Tucović, M., Tolić, A., Rajić, J., Dinić, S., Uskoković, A., Grdović, N., Mihailović, M., Marković, I., Arambašić

Jovanović, J. and Vidaković, M., 2022. Nucleofection as an Efficient Method for Alpha TC1-6 Cell Line Transfection. *Applied Sciences (Switzerland)*, 12(15). <https://doi.org/10.3390/app12157938>.

Dührsen, L., Hartfuß, S., Hirsch, D., Geiger, S., Mair, C.L., Sedlacik, J., Guenther, C., Westphal, M., Lamszus, K., Hermann, F.G. and Schmidt, N.O., 2019. Preclinical analysis of human mesenchymal stem cells: Tumor tropism and therapeutic efficiency of local HSV-TK suicide gene therapy in glioblastoma. *Oncotarget*, 10(58), pp.6049–6061. <https://doi.org/10.18632/oncotarget.27071>.

Einem, J.C. Von, Peter, S., Günther, C., Volk, H., Salat, C., Stoetzer, O., Nelson, P.J., Michl, M., Modest, P., Holch, J.W., Angele, M., Bruns, C. and Niess, H., 2017. Treatment of advanced gastrointestinal cancer with genetically modified autologous mesenchymal stem cells - TREAT-ME-1 - a phase I, first in human, first in class trial. 8(46), pp.80156–80166.

Fakiruddin, K.S., Baharuddin, P., Lim, M.N., Fakharuzi, N.A., Yusof, N.A.N.M. and Zakaria, Z., 2014. Nucleofection optimization and in vitro antitumorigenic effect of TRAIL-expressing human adipose-derived mesenchymal stromal cells. *Cancer Cell International*, 14(1). <https://doi.org/10.1186/s12935-014-0122-8>.

Freytag, S.O., Barton, K.N. and Zhang, Y., 2013. Efficacy of oncolytic adenovirus expressing suicide genes and interleukin-12 in preclinical model of prostate cancer. *Gene Therapy*, 20(12), pp.1131–1139. <https://doi.org/10.1038/gt.2013.40>.

Friedenstein, A.J., Chailakhjan, R.K. and Lalykina, K.S., 1970. The development of fibroblast colonies in monolayer cultures of guinea pig bone marrow and spleen cells. *Cell Tissue Kinet.*, 3, pp.393–403.

Gabriel, N., Samuel, R. and Jayandharan, G.R., 2017. Targeted delivery of AAV-transduced mesenchymal stromal cells to hepatic tissue for ex vivo gene therapy. *Journal of Tissue Engineering and Regenerative Medicine*, 11(5), pp.1354–1364. <https://doi.org/10.1002/term.2034>.

Gaffen, S.L. and Liu, K.D., 2004. Overview of interleukin-2 function, production and clinical applications. *Cytokine*, 28(3), pp.109–123. <https://doi.org/10.1016/j.cyto.2004.06.010>.

Gambotto, A., Tüting, T., McVey, D.L., Kovesdi, I., Tahara, H., Lotze, M.T. and Robbins, P.D., 1999. Induction of antitumor immunity by direct intratumoral injection of a recombinant adenovirus vector expressing interleukin-12. *Cancer Gene Therapy*, 6(1), pp.45–53. <https://doi.org/10.1038/sj.cgt.7700013>.

Gately, M.K., Daisy Carvajal, fb M., Warriar, R.R., Kolinsky, K.D., Wilkinson, V.L., Dwyer, C.M., Higgins, G.F., Podlaski, F.J., Stern, A.S., PRESKYb, D.H., Roche Znc, H.-L., Con Naught On, S.E., Gillessen, S., Faherty, D.A. and Familletti, P., n.d. *Interleukin-12 Antagonist Activity of Mouse Interleukin-12 p40 Homodimer in Vitro and in Vivo*. [online] *Annals New York Academy of Sciences*. Available at: <www.pdfliib.com>.

Gavas, S., Quazi, S. and Karpiński, T.M., 2021. *Nanoparticles for Cancer Therapy: Current Progress and Challenges*. *Nanoscale Research Letters*, <https://doi.org/10.1186/s11671-021-03628-6>.

de Groot, P.M., Wu, C.C., Carter, B.W. and Munden, R.F., 2018. *The epidemiology of lung cancer*. *Translational Lung Cancer Research*, <https://doi.org/10.21037/tlcr.2018.05.06>.

Gubler U, Chua AO, Schoenhaut DS, Dwyer CM, McComas W, Motyka R, Nabavi N, Wolitzky AG, Quinn PM, Familletti PC and Gately MK, 1991. Coexpression of two distinct genes is required to generate secreted bioactive cytotoxic lymphocyte maturation factor (1991). *Immunology*, 88, pp.4143–4147.

Guo, Y., Cao, W. and Zhu, Y., 2019. *Immunoregulatory functions of the IL-12 family of cytokines in antiviral systems*. *Viruses*, <https://doi.org/10.3390/v11090772>.

Halim, N.S.S.A., Fakiruddin, K.S., Ali, S.A. and Yahaya, B.H., 2014. A comparative study of non-viral gene delivery techniques to human adipose-derived mesenchymal stem cell. *International Journal of Molecular Sciences*, 15(9), pp.15044–15060. <https://doi.org/10.3390/ijms150915044>.

Hamann, A., Nguyen, A. and Pannier, A.K., 2019a. *Nucleic acid delivery to mesenchymal stem cells: A review of nonviral methods and applications*. *Journal of Biological Engineering*, <https://doi.org/10.1186/s13036-019-0140-0>.

Hamann, A., Nguyen, A. and Pannier, A.K., 2019b. *Nucleic acid delivery to mesenchymal stem cells: A review of nonviral methods and applications*. *Journal of Biological Engineering*, <https://doi.org/10.1186/s13036-019-0140-0>.

Han, J., Zhao, J., Xu, J. and Wen, Y., 2014. Mesenchymal stem cells genetically modified by lentivirus-mediated interleukin-12 inhibit malignant ascites in mice. *Experimental and Therapeutic Medicine*, 8(4), pp.1330–1334. <https://doi.org/10.3892/etm.2014.1918>.

Han, S.W., Nakamura, C., Kotobuki, N., Obataya, I., Ohgushi, H., Nagamune, T. and Miyake, J., 2008. High-efficiency DNA injection into a single human mesenchymal stem cell using a nanoneedle and atomic force microscopy. *Nanomedicine: Nanotechnology, Biology, and Medicine*, 4(3), pp.215–225. <https://doi.org/10.1016/j.nano.2008.03.005>.

Henschler, R., Deak, E. and Seifried, E., 2008. Homing of mesenchymal stem cells. *Transfusion Medicine and Hemotherapy*, 35(4), pp.306–312. <https://doi.org/10.1159/000143110>.

Hirsch, M.L., Wolf, S.J. and Samulski, R.J., 2016. Delivering transgenic DNA exceeding the carrying capacity of AAV vectors. In: *Methods in Molecular Biology*. Humana Press Inc. pp.21–39. https://doi.org/10.1007/978-1-4939-3271-9_2.

Idriss, H.T. and Naismith, J.H., 2000. TNF α and the TNF receptor superfamily: Structure-function relationship(s). *Microscopy Research and Technique*, 50(3),

pp.184–195. [https://doi.org/10.1002/1097-0029\(20000801\)50:3<184::AID-JEMT2>3.0.CO;2-H](https://doi.org/10.1002/1097-0029(20000801)50:3<184::AID-JEMT2>3.0.CO;2-H).

Kabat, M., Bobkov, I., Kumar, S. and Grumet, M., 2020. Trends in mesenchymal stem cell clinical trials 2004-2018: Is efficacy optimal in a narrow dose range? *Stem Cells Translational Medicine*, 9(1), pp.17–27. <https://doi.org/10.1002/sctm.19-0202>.

Karp, J.M. and Teo, G.S.L., 2009. Mesenchymal Stem Cell Homing: The Devil Is in the Details. *Cell Stem Cell*, 4(3), pp.206–216. <https://doi.org/10.1016/j.stem.2009.02.001>.

Kern, S., Eichler, H., Stoeve, J., Kluter, H. and Bieback, K., 2006a. Comparative Analysis of Mesenchymal Stem Cells from Bone Marrow , Umbilical Cord Blood , or Adipose Tissue. *Stem Cells*, 24, pp.1294–1301. <https://doi.org/10.1634/stemcells.2005-0342>.

Kern, S., Eichler, H., Stoeve, J., Klüter, H. and Bieback, K., 2006b. Comparative Analysis of Mesenchymal Stem Cells from Bone Marrow, Umbilical Cord Blood, or Adipose Tissue. *STEM CELLS*, 24(5), pp.1294–1301. <https://doi.org/10.1634/stemcells.2005-0342>.

Kilpinen, L., Tigistu-Sahle, F., Oja, S., Greco, D., Parmar, A., Saavalainen, P., Nikkilä, J., Korhonen, M., Lehenkari, P., Käkälä, R. and Laitinen, S., 2013. Aging bone marrow mesenchymal stromal cells have altered membrane glycerophospholipid composition and functionality. *Journal of Lipid Research*, 54(3), pp.622–635. <https://doi.org/10.1194/jlr.M030650>.

Kim, J.A., Cho, K., Shin, M.S., Lee, W.G., Jung, N., Chung, C. and Chang, J.K., 2008. A novel electroporation method using a capillary and wire-type electrode. *Biosensors and Bioelectronics*, 23(9), pp.1353–1360. <https://doi.org/10.1016/j.bios.2007.12.009>.

Kobayashi, B.Y.M., Fitz, L., Ryan, M., Hewick, R.M., Clark, S.C., Chan, S., Loudon, R., Sherman, F., Cd, C.D. and Nk, N.-C.D., 1989. Identification And Purification Of Natural Killer Cell Stimulatory Factor (NKSF), A Cytokine With Multiple Biologic Effects On Human Lymphocytes. 170(September).

Kohn, D.B., Sadelain, M. and Glorioso, J.C., 2003. *Occurrence of leukaemia following gene therapy of X-linked SCID*. *Nature Reviews Cancer*, <https://doi.org/10.1038/nrc1122>.

Kolluri, K.K., Laurent, G.J. and Janes, S.M., 2013. Mesenchymal stem cells as vectors for lung cancer therapy. *Respiration*, 85(6), pp.443–451. <https://doi.org/10.1159/000351284>.

Komel, T., Bosnjak, M., Kranjc Brezar, S., de Robertis, M., Mastrodonato, M., Scillitani, G., Pesole, G., Signori, E., Sersa, G. and Cemazar, M., 2021. Gene electrotransfer of IL-2 and IL-12 plasmids effectively eradicated murine B16.F10 melanoma. *Bioelectrochemistry*, 141. <https://doi.org/10.1016/j.bioelechem.2021.107843>.

Kułach, N., Pilny, E., Cichoń, T., Czapla, J., Jarosz-Biej, M., Rusin, M., Drzyzga, A., Matuszczak, S., Szala, S. and Smolarczyk, R., 2021. Mesenchymal stromal cells as carriers of IL-12 reduce primary and metastatic tumors of murine melanoma. *Scientific Reports*, 11(1). <https://doi.org/10.1038/s41598-021-97435-9>.

Kumar, A., Taghi Khani, A., Sanchez Ortiz, A. and Swaminathan, S., 2022. *GM-CSF: A Double-Edged Sword in Cancer Immunotherapy*. *Frontiers in Immunology*, <https://doi.org/10.3389/fimmu.2022.901277>.

Lasek, W., Zagożdżon, R. and Jakobisiak, M., 2014. *Interleukin 12: Still a promising candidate for tumor immunotherapy?* *Cancer Immunology, Immunotherapy*, <https://doi.org/10.1007/s00262-014-1523-1>.

Lee, C.S., Bishop, E.S., Zhang, R., Yu, X., Farina, E.M., Yan, S., Zhao, C., Zeng, Z., Shu, Y., Wu, X., Lei, J., Li, Y., Zhang, W., Yang, C., Wu, K., Wu, Y., Ho, S., Athiviraham, A., Lee, M.J., Wolf, J.M., Reid, R.R. and He, T.C., 2017a. Adenovirus-mediated gene delivery: Potential applications for gene and cell-based therapies in the new era of personalized medicine. *Genes and Diseases*, 4(2), pp.43–63. <https://doi.org/10.1016/j.gendis.2017.04.001>.

Lee, C.S., Bishop, E.S., Zhang, R., Yu, X., Farina, E.M., Yan, S., Zhao, C., Zeng, Z., Shu, Y., Wu, X., Lei, J., Li, Y., Zhang, W., Yang, C., Wu, K., Wu, Y., Ho, S., Athiviraham, A., Lee, M.J., Wolf, J.M., Reid, R.R. and He, T.C., 2017b. *Adenovirus-mediated gene delivery: Potential applications for gene and cell-based therapies in the new era of personalized medicine*. *Genes and Diseases*, <https://doi.org/10.1016/j.gendis.2017.04.001>.

Leonard et al., 1997. Effects of single-dose interleukin-12 exposure on interleukin-12-associated toxicity and interferon-gamma production. *Blood*, 90(7), pp.2541–2548.

Leonard, J.P., Sherman, M.L., Fisher, G.L., Buchanan, L.J., Larsen, G., Atkins, M.B., Sosman, J.A., Dutcher, J.P., Vogelzang, N.J. and Ryan, J.L., n.d. *Effects of Single-Dose Interleukin-12 Exposure on Interleukin-12-Associated Toxicity and Interferon-gamma Production*. [online] Available at: <<https://ashpublications.org/blood/article-pdf/90/7/2541/1415768/2541.pdf>>.

Li, X., Zhang, P., Liu, X. and Lv, P., 2015a. Expression of interleukin-12 by adipose-derived mesenchymal stem cells for treatment of lung adenocarcinoma. *Thoracic Cancer*, 6(1), pp.80–84. <https://doi.org/10.1111/1759-7714.12151>.

Li, Y., Guo, W., Li, X., Zhang, J., Sun, M., Tang, Z., Ran, W., Yang, K., Huang, G. and Li, L., 2021. Expert consensus on the clinical application of recombinant adenovirus human p53 for head and neck cancers. *International Journal of Oral Science*, 13(1). <https://doi.org/10.1038/s41368-021-00145-1>.

Li, Y., Li, B., Li, C.J. and Li, L.J., 2015b. *Key points of basic theories and clinical practice in rAd-p53 (Gendicine™) gene therapy for solid malignant tumors*. *Expert Opinion on Biological Therapy*, <https://doi.org/10.1517/14712598.2015.990882>.

- Liu, X., Hu, J., Li, Y., Cao, W., Wang, Y., Ma, Z. and Li, F., 2018. Mesenchymal stem cells expressing interleukin-18 inhibit breast cancer in a mouse model. *Oncology Letters*, 15(5), pp.6265–6274. <https://doi.org/10.3892/ol.2018.8166>.
- Liu, X., Hu, J., Sun, S., Li, F., Cao, W., Wang, Y.U., Ma, Z. and Yu, Z., 2015. Mesenchymal stem cells expressing interleukin-18 suppress breast cancer cells in vitro. (20), pp.1192–1200. <https://doi.org/10.3892/etm.2015.2286>.
- Liu, Z., Lee, F.-T., Hanai, N., Smyth, F.E., Burgess, A.W., Old, L.J. and Scott, A.M., 2002. Cytokine enhancement of in vitro antibody-dependent cellular cytotoxicity mediated by chimeric anti-GD3 monoclonal antibody KM871. *Cancer Immunity*, [online] 2, p.13. Available at: <<http://www.cancerimmunity.org/v2p13/020813.htm>>.
- Lundstrom, K., 2018. Viral vectors in gene therapy. *Diseases*, 6(42), pp.139–143. <https://doi.org/10.3390/diseases6020042>.
- Madeira, C., Mendes, R.D., Ribeiro, S.C., Boura, J.S., Aires-Barros, M.R. and Cabral, J.M.S., 2010. Nonviral gene delivery to mesenchymal stem cells using cationic liposomes for gene and cell therapy. *Journal of Biomedicine and Biotechnology*, 2010, pp.1–12. <https://doi.org/10.1155/2010/735349>.
- Mangraviti et al., 2016. Non-virally engineered human adipose mesenchymal stem cells produce BMP4, target brain tumours, and extend survival. *Biomaterials*, 100, pp.53–66. <https://doi.org/10.1016/j.physbeh.2017.03.040>.
- Meyerrose, T.E., Roberts, M., Ohlemiller, K.K., Vogler, C.A., Wirthlin, L., Nolte, J.A. and Sands, M.S., 2008. Lentiviral-Transduced Human Mesenchymal Stem Cells Persistently Express Therapeutic Levels of Enzyme in a Xenotransplantation Model of Human Disease. *Stem Cells*, 26(7), pp.1713–1722. <https://doi.org/10.1634/stemcells.2008-0008>.
- Migliano, N., Roth, M., Lardinois, D., Sadowski, C., Tamm, M. and Borger, P., 2012. Cigarette smoke inhibits lung fibroblast proliferation by translational mechanisms. *European Respiratory Journal*, 39(3), pp.705–711. <https://doi.org/10.1183/09031936.00174310>.
- Milone, M.C. and O’Doherty, U., 2018. *Clinical use of lentiviral vectors. Leukemia*, <https://doi.org/10.1038/s41375-018-0106-0>.
- Mizukami, A. and Swiech, K., 2018. Mesenchymal stromal cells: From discovery to manufacturing and commercialization. *Stem Cells International*, 2018. <https://doi.org/10.1155/2018/4083921>.
- Mohme, M., Maire, C.L., Geumann, U., Schliffke, S., Dührsen, L., Fita, K., Akyüz, N., Binder, M., Westphal, M., Guenther, C., Lamszus, K., Hermann, F.G. and Schmidt, N.O., 2020. Local Intracerebral Immunomodulation Using Interleukin-Expressing Mesenchymal Stem Cells in Glioblastoma. *Clinical cancer research : an official journal of the American Association for Cancer Research*, 26(11), pp.2626–2639. <https://doi.org/10.1158/1078-0432.CCR-19-0803>.

- Muhammad, T., Sakhawat, A., Khan, A.A., Ma, L., Gjerset, R.A. and Huang, Y., 2019. Mesenchymal stem cell-mediated delivery of therapeutic adenoviral vectors to prostate cancer. *Stem Cell Research and Therapy*, 10(1), pp.1–12. <https://doi.org/10.1186/s13287-019-1268-z>.
- Musiał-Wysocka, A., Kot, M. and Majka, M., 2019. *The Pros and Cons of Mesenchymal Stem Cell-Based Therapies. Cell Transplantation*, <https://doi.org/10.1177/0963689719837897>.
- Najmuddin, S.U.F.S., Amin, Z.M., Tan, S.W., Yeap, S.K., Kalyanasundram, J., Ani, M.A.C., Veerakumarasivam, A., Chan, S.C., Chia, S.L., Yusoff, K. and Alitheen, N.B., 2020. Cytotoxicity study of the interleukin-12-expressing recombinant Newcastle disease virus strain, rAF-IL12, towards CT26 colon cancer cells in vitro and in vivo. *Cancer Cell International*, 20(1). <https://doi.org/10.1186/s12935-020-01372-y>.
- Nakajima, M., Nito, C., Sowa, K., Suda, S., Nishiyama, Y., Nakamura-Takahashi, A., Nitahara-Kasahara, Y., Imagawa, K., Hirato, T., Ueda, M., Kimura, K. and Okada, T., 2017. Mesenchymal Stem Cells Overexpressing Interleukin-10 Promote Neuroprotection in Experimental Acute Ischemic Stroke. *Molecular Therapy - Methods and Clinical Development*, 6(September), pp.102–111. <https://doi.org/10.1016/j.omtm.2017.06.005>.
- Naso, M.F., Tomkowicz, B., Perry, W.L. and Strohl, W.R., 2017. *Adeno-Associated Virus (AAV) as a Vector for Gene Therapy. BioDrugs*, <https://doi.org/10.1007/s40259-017-0234-5>.
- Nayerossadat, N., Ali, P. and Maedeh, T., 2012. Viral and nonviral delivery systems for gene delivery. *Advanced Biomedical Research*, 1(1), p.27. <https://doi.org/10.4103/2277-9175.98152>.
- Ni, J., Miller, M., Stojanovic, A., Garbi, N. and Cerwenka, A., 2012. Sustained effector function NK cells against established tumors. *The Journal of Experimental Medicine*, 209(13), pp.2351–2365. <https://doi.org/10.1084/jem.20120944>.
- Niess, H., Thomas, M.N., Schiergens, T.S., Kleespies, A., Jauch, K.W., Bruns, C., Werner, J., Nelson, P.J. and Angele, M.K., 2016. Genetic engineering of mesenchymal stromal cells for cancer therapy: Turning partners in crime into Trojan horses. *Innovative Surgical Sciences*, 1(1), pp.19–32. <https://doi.org/10.1515/iss-2016-0005>.
- Nitzsche, F., Müller, C., Lukomska, B., Jolkkonen, J., Deten, A. and Boltze, J., 2017. Concise Review: MSC Adhesion Cascade—Insights into Homing and Transendothelial Migration. *Stem Cells*, 35(6), pp.1446–1460. <https://doi.org/10.1002/stem.2614>.
- Park, N., Rim, Y.A., Jung, H., Kim, J., Yi, H., Kim, Y., Jang, Y., Jung, S.M., Lee, J., Kwok, S.K., Park, S.H. and Ju, J.H., 2017. Etanercept-synthesising mesenchymal stem cells efficiently ameliorate collagen-induced arthritis. *Scientific Reports*, [online] 7, pp.1–12. <https://doi.org/10.1038/srep39593>.

Parkin, D.M., Bray, F.I. and Devesa, S.S., 2001. Cancer burden in the year 2000. The global picture. *European Journal of Cancer*, [online] 37, pp.4–66. Available at: <www.ejconline.com>.

Peta, K.T., Ambele, M.A. and Pepper, M.S., 2021. *Similarities between tumour immune response and chronic wound microenvironment: Influence of mesenchymal stromal/stem cells*. *Journal of Immunology Research*, <https://doi.org/10.1155/2021/6649314>.

Raper, S.E., Chirmule, N., Lee, F.S., Wivel, N.A., Bagg, A., Gao, G.P., Wilson, J.M. and Batshaw, M.L., 2003. Fatal systemic inflammatory response syndrome in a ornithine transcarbamylase deficient patient following adenoviral gene transfer. *Molecular Genetics and Metabolism*, 80(1–2), pp.148–158. <https://doi.org/10.1016/j.ymgme.2003.08.016>.

Ries, C., Egea, V., Karow, M., Kolb, H., Jochum, M. and Neth, P., 2007. MMP-2, MT1-MMP, and TIMP-2 are essential for the invasive capacity of human mesenchymal stem cells: differential regulation by inflammatory cytokines. *Blood*, 109(9), pp.4055–4063. <https://doi.org/10.1182/blood-2006-10-051060>.The.

Rombouts, W.J.C. and Ploemacher, R.E., 2003. Primary murine MSC show highly efficient homing to the bone marrow but lose homing ability following culture. *Leukemia*, 17(1), pp.160–170. <https://doi.org/10.1038/sj.leu.2402763>.

Ruano, D., López-Martín, J.A., Moreno, L., Lassaletta, Á., Bautista, F., Andión, M., Hernández, C., González-Murillo, Á., Melen, G., Alemany, R., Madero, L., García-Castro, J. and Ramírez, M., 2020. First-in-Human, First-in-Child Trial of Autologous MSCs Carrying the Oncolytic Virus Icovir-5 in Patients with Advanced Tumors. *Molecular Therapy*, 28(4), pp.1033–1042. <https://doi.org/10.1016/j.ymthe.2020.01.019>.

Ryu, C.H., Park, S.A., Kim, S.M., Lim, J.Y., Jeong, C.H., Jun, J.A., Oh, J.H., Park, S.H., Oh, W. II and Jeun, S.S., 2010. Migration of human umbilical cord blood mesenchymal stem cells mediated by stromal cell-derived factor-1/CXCR4 axis via Akt, ERK, and p38 signal transduction pathways. *Biochemical and Biophysical Research Communications*, 398(1), pp.105–110. <https://doi.org/10.1016/j.bbrc.2010.06.043>.

Sackstein, R., Merzaban, J.S., Cain, D.W., Dagia, N.M., Spencer, J.A., Lin, C.P. and Wohlgemuth, R., 2008. Ex vivo glycan engineering of CD44 programs human multipotent mesenchymal stromal cell trafficking to bone. *Nature Medicine*, 14(2), pp.181–187. <https://doi.org/10.1038/nm1703>.

Sage, E.K., Thakrar, R.M. and Janes, S.M., 2016. Genetically engineered mesenchymal stromal cells in cancer therapy. *Cytotherapy*, 18(11), pp.1435–1445. <https://doi.org/10.1016/j.jcyt.2016.09.003>: 10.1016/j.jcyt.2016.09.003.

Saleh, M., Fotook Kiaei, S.Z. and Kavianpour, M., 2022. *Application of Wharton jelly-derived mesenchymal stem cells in patients with pulmonary fibrosis*. *Stem Cell Research and Therapy*, <https://doi.org/10.1186/s13287-022-02746-x>.

Sangro, B., Mazzolini, G., Ruiz, J., Herraiz, M., Quiroga, J., Herrero, I., Benito, A., Larrache, J., Pueyo, J., Subtil, J.C., Olagüe, C., Sola, J., Sádaba, B., Lacasa, C., Melero, I., Qian, C. and Prieto, J., 2004. Phase I trial of intratumoral injection of an adenovirus encoding interleukin-12 for advanced digestive tumors. *Journal of Clinical Oncology*, 22(8), pp.1389–1397. <https://doi.org/10.1200/JCO.2004.04.059>.

Sato, M., Shames, D.S., Gazdar, A.F. and Minna, J.D., 2007. A translational view of the molecular pathogenesis of lung cancer. *Journal of Thoracic Oncology*, 2(4), pp.327–343. <https://doi.org/10.1097/01.JTO.0000263718.69320.4c>.

Sato-Dahlman, M., Larocca, C.J., Yanagiba, C. and Yamamoto, M., 2020. Adenovirus and immunotherapy: Advancing cancer treatment by combination. *Cancers*, 12(5). <https://doi.org/10.3390/cancers12051295>.

Schabath, M.B. and Cote, M.L., 2019. Cancer progress and priorities: Lung cancer. *Cancer Epidemiology Biomarkers and Prevention*, 28(10), pp.1563–1579. <https://doi.org/10.1158/1055-9965.EPI-19-0221>.

Schaffert, D. and Wagner, E., 2008. Gene therapy progress and prospects: Synthetic polymer-based systems. *Gene Therapy*, 15(16), pp.1131–1138. <https://doi.org/10.1038/gt.2008.105>.

Scheers, I., Lombard, C., Paganelli, M., Campard, D., Najimi, M., Gala, J.L., Decottignies, A. and Sokal, E., 2013. Human Umbilical Cord Matrix Stem Cells Maintain Multilineage Differentiation Abilities and Do Not Transform during Long-Term Culture. *PLoS ONE*, 8(8). <https://doi.org/10.1371/journal.pone.0071374>.

Schioppa, T., Uranchimeg, B., Saccani, A., Biswas, S.K., Doni, A., Rapisarda, A., Bernasconi, S., Saccani, S., Nebuloni, M., Vago, L., Mantovani, A., Melillo, G. and Sica, A., 2003. Regulation of the Chemokine Receptor CXCR4 by Hypoxia. *Journal of Experimental Medicine*, 198(9), pp.1391–1402. <https://doi.org/10.1084/jem.20030267>.

Schrepfer, S., Deuse, T., Reichenspurner, H., Fischbein, M.P., Robbins, R.C. and Pelletier, M.P., 2007. Stem Cell Transplantation: The Lung Barrier. *Transplantation Proceedings*, 39(2), pp.573–576. <https://doi.org/10.1016/j.transproceed.2006.12.019>.

Shen, C., Chan, T., Chen, C. and Hsu, Y., 2016. Human umbilical cord matrix-derived stem cells expressing interferon- β gene inhibit breast cancer cells via apoptosis. *Oncotarget*, 7(23), pp.34172–34179. <https://doi.org/https://doi.org/10.18632/oncotarget.8997>.

Shi, M., Li, J., Liao, L., Chen, B., Li, B., Chen, L., Jia, H. and Zhao, R.C., 2007. Regulation of CXCR4 expression in human mesenchymal stem cells by cytokine treatment: Role in homing efficiency in NOD/SCID mice. *Haematologica*, 92(7), pp.897–904. <https://doi.org/10.3324/haematol.10669>.

Shiokawa, M., Takahashi, T., Murakami, A., Kita, S., Ito, M., Sugamura, K. and Ishii, N., 2010. In vivo assay of human NK-dependent ADCC using NOD/SCID/ γ cnnull (NOG) mice. *Biochemical and Biophysical Research Communications*, 399(4), pp.733–737. <https://doi.org/10.1016/j.bbrc.2010.07.145>.

Siegel, R.L., Miller, K.D., Fuchs, H.E. and Jemal, A., 2022. Cancer statistics, 2022. *CA: A Cancer Journal for Clinicians*, 72(1), pp.7–33. <https://doi.org/10.3322/caac.21708>.

Silva-Pilipich, N., Lasarte-Cía, A., Lozano, T., Martín-Otal, C., Lasarte, J.J. and Smerdou, C., 2022. Intratumoral electroporation of a self-amplifying RNA expressing IL-12 induces antitumor effects in mouse models of cancer. *Molecular Therapy - Nucleic Acids*, 29, pp.387–399. <https://doi.org/10.1016/j.omtn.2022.07.020>.

Singh, S., Kumar, R. and Agrawal, B., 2019. Adenoviral Vector-Based Vaccines and Gene Therapies: Current Status and Future Prospects. In: *Adenoviruses*. IntechOpen. <https://doi.org/10.5772/intechopen.79697>.

Sokołowska, E. and Błachnio-Zabielska, A.U., 2019. A critical review of electroporation as a plasmid delivery system in mouse skeletal muscle. *International Journal of Molecular Sciences*, <https://doi.org/10.3390/ijms20112776>.

Steingen, C., Brenig, F., Baumgartner, L., Schmidt, J., Schmidt, A. and Bloch, W., 2008. Characterization of key mechanisms in transmigration and invasion of mesenchymal stem cells. *Journal of Molecular and Cellular Cardiology*, 44(6), pp.1072–1084. <https://doi.org/10.1016/j.yjmcc.2008.03.010>.

Stern, A.S., Podlaski, F.J., Hulmes, J.D., Pan, Y.-C.E., Quintt, P.M., Wolitzkyf, A.G., Familletti, P.C., Stremlo, D.L., Truitt\$, T., Chizzonite ¶, R. and Gatelyt, M.K., 1990. Purification to homogeneity and partial characterization of cytotoxic lymphocyte maturation factor from human B-lymphoblastoid cells (lymphokine-activated killer cells/interleukin 2/T-cell growth factor/natural killer cell/tumor necrosis factor). *Immunology Communicated by John J. Burns*, 87, pp.6808–6812.

Strauss, J., Heery, C.R., Kim, J.W., Jochems, C., Donahue, R.N., Montgomery, A.S., McMahon, S., Lamping, E., Marte, J.L., Madan, R.A., Bilusic, M., Silver, M.R., Bertotti, E., Schlom, J. and Gulley, J.L., 2019. First-in-human phase I trial of a tumor-targeted cytokine (NHS-IL12) in subjects with metastatic solid tumors. *Clinical Cancer Research*, 25(1), pp.99–109. <https://doi.org/10.1158/1078-0432.CCR-18-1512>.

Studený, M., Marini, F.C., Champlin, R.E., Zompetta, C., Fidler, I.J. and Andreeff, M., 2002. Bone marrow-derived mesenchymal stem cells as vehicles for interferon- β delivery into tumors. *Cancer Research*, 62(13), pp.3603–3608. <https://doi.org/10.1158/0008-5472.can-08-4698>.

Su, W., Ito, T., Oyama, T., Kitagawa, T., Yamori, T., Fujiwara, H. and Matsuda, H., 2001. The direct effect of IL-12 on tumor cells: IL-12 acts directly on tumor cells to activate NF- κ B and enhance IFN- γ -mediated STAT1 phosphorylation. *Biochemical and Biophysical Research Communications*, 280(2), pp.503–512. <https://doi.org/10.1006/bbrc.2000.4150>.

Sung, H., Ferlay, J., Siegel, R.L., Laversanne, M., Soerjomataram, I., Jemal, A. and Bray, F., 2021. Global Cancer Statistics 2020: GLOBOCAN Estimates of Incidence and Mortality Worldwide for 36 Cancers in 185 Countries. *CA: A Cancer Journal for Clinicians*, 71(3), pp.209–249. <https://doi.org/10.3322/caac.21660>.

Takayama, Y., Kusamori, K. and Nishikawa, M., 2021. Mesenchymal stem/stromal cells as next-generation drug delivery vehicles for cancer therapeutics. *Expert Opinion on Drug Delivery*, 18(11), pp.1627–1642. <https://doi.org/10.1080/17425247.2021.1960309>.

Tang, E.R., Schreiner, A.M. and Pua, B.B., 2014. *Advances in lung adenocarcinoma classification: A summary of the new international multidisciplinary classification system (IASLC/ATS/ERS)*. *Journal of Thoracic Disease*, <https://doi.org/10.3978/j.issn.2072-1439.2014.09.12>.

Thun, M., Peto, R., Boreham, J. and Lopez, A.D., 2012. Stages of the cigarette epidemic on entering its second century. *Tobacco Control*, 21(2), pp.96–101. <https://doi.org/10.1136/tobaccocontrol-2011-050294>.

Togo, S., Holz, O., Liu, X., Sugiura, H., Kamio, K., Wang, X., Kawasaki, S., Ann, Y., Fredriksson, K., Skold, C.M., Mueller, K.C., Branscheid, D., Welker, L., Watz, H., Magnussen, H. and Rennard, S.I., 2008. Lung fibroblast repair functions in patients with chronic obstructive pulmonary disease are altered by multiple mechanisms. *American Journal of Respiratory and Critical Care Medicine*, 178(3), pp.248–260. <https://doi.org/10.1164/rccm.200706-929OC>.

Trinchieri, G., 2003. *Interleukin-12 and the regulation of innate resistance and adaptive immunity*. *Nature Reviews Immunology*, <https://doi.org/10.1038/nri1001>.

Tugues, S., Burkhard, S.H., Ohs, I., Vrohligs, M., Nussbaum, K., vom Berg, J., Kulig, P. and Becher, B., 2015. *New insights into IL-12-mediated tumor suppression*. *Cell Death and Differentiation*, <https://doi.org/10.1038/cdd.2014.134>.

Uchibori, R., Tsukahara, T., Ohmine, K. and Ozawa, K., 2014. Cancer gene therapy using mesenchymal stem cells. *International Journal of Hematology*, 99(4), pp.377–382. <https://doi.org/10.1007/s12185-014-1537-7>.

Ullah, I., Subbarao, R.B. and Rho, G.J., 2015. Human mesenchymal stem cells - current trends and future prospective. *Bioscience Reports*, [online] 35(2), pp.1–18. <https://doi.org/10.1042/BSR20150025>.

Ullah, M., Liu, D.D. and Thakor, A.S., 2019. Mesenchymal Stromal Cell Homing : Mechanisms and Strategies for Improvement. *ISCIENCE*, 15, pp.421–438. <https://doi.org/10.1016/j.isci.2019.05.004>.

United States. Public Health Service. Office of the Surgeon General., 2010. *How tobacco smoke causes disease : the biology and behavioral basis for smoking-attributable disease : a report of the Surgeon General*. U.S. Dept. of Health and Human Services, Public Health Service, Office of the Surgeon General.

Vannucci, L., Lai, M., Chiuppesi, F., Ceccherini-Nelli, L. and Pistello, M., 2013. Viral vectors: a look back and ahead on gene transfer technology. *New Microbiologica*, [online] 36, pp.1–22. Available at: <www.wiley.co.uk/genmed/clinical>.

Del Vecchio, M., Bajetta, E., Canova, S., Lotze, M.T., Wesa, A., Parmiani, G. and Anichini, A., 2007. *Interleukin-12: Biological properties and clinical application*. *Clinical Cancer Research*, <https://doi.org/10.1158/1078-0432.CCR-07-0776>.

Viswanathan, S., Shi, Y., Galipeau, J., Krampera, M., Leblanc, K., Martin, I., Nolte, J., Phinney, D.G. and Sensebe, L., 2019. Mesenchymal stem versus stromal cells: International Society for Cell & Gene Therapy (ISCT®) Mesenchymal Stromal Cell committee position statement on nomenclature. *Cytotherapy*, 21(10), pp.1019–1024. <https://doi.org/10.1016/j.jcyt.2019.08.002>.

Wagner, W., Horn, P., Castoldi, M., Diehlmann, A., Bork, S., Saffrich, R., Benes, V., Blake, J., Pfister, S., Eckstein, V. and Ho, A.D., 2008. Replicative senescence of mesenchymal stem cells: A continuous and organized process. *PLoS ONE*, 3(5). <https://doi.org/10.1371/journal.pone.0002213>.

Wang, W., Xu, X., Li, Z., Lendlein, A. and Ma, N., 2014. Genetic engineering of mesenchymal stem cells by non-viral gene delivery. *Clinical Hemorheology and Microcirculation*, 58(1), pp.19–48. <https://doi.org/10.3233/CH-141883>.

Watford, W.T., Moriguchi, M., Morinobu, A. and O’Shea, J.J., 2003. *The biology of IL-12: Coordinating innate and adaptive immune responses*. *Cytokine and Growth Factor Reviews*, [https://doi.org/10.1016/S1359-6101\(03\)00043-1](https://doi.org/10.1016/S1359-6101(03)00043-1).

Weiss, J.M., Subleski, J.J., Wigginton, J.M. and Wiltrout, R.H., 2007. Immunotherapy of Cancer by IL-12-based Cytokine Combinations. *Expert Opinion on Biological Therapy*, 7(11), pp.1705–1721. <https://doi.org/https://doi.org/10.1517/14712598.7.11.1705>.

Wu, J., Xie, S., Li, H., Zhang, Y., Yue, J., Yan, C., Liu, K., Liu, Y., Xu, R. and Zheng, G., 2021. Antitumor effect of IL-12 gene-modified bone marrow mesenchymal stem cells combined with Fuzheng Yiliu decoction in an in vivo glioma nude mouse model. *Journal of Translational Medicine*, 19(1). <https://doi.org/10.1186/s12967-021-02809-2>.

Wynn, R.F., Hart, C.A., Corradi-Perini, C., O’Neill, L., Evans, C.A., Wraith, J.E., Fairbairn, L.J. and Bellantuono, I., 2004. A small proportion of mesenchymal stem cells strongly expresses functionally active CXCR4 receptor

capable of promoting migration to bone marrow. *Blood*, 104(9), pp.2643–2645. <https://doi.org/10.1182/blood-2004-02-0526>.

Xiang, S., Tong, H., Shi, Q., Fernandes, J.C., Jin, T., Dai, K. and Zhang, X., 2012. Uptake mechanisms of non-viral gene delivery. *Journal of Controlled Release*, <https://doi.org/10.1016/j.jconrel.2011.09.093>.

Yabroff, K.R., Wu, X.C., Negoita, S., Stevens, J., Coyle, L., Zhao, J., Mumphrey, B.J., Jemal, A. and Ward, K.C., 2022. Association of the COVID-19 Pandemic With Patterns of Statewide Cancer Services. *Journal of the National Cancer Institute*, 114(6), pp.907–909. <https://doi.org/10.1093/jnci/djab122>.

Yan, Y., Zhao, N., He, X., Guo, H., Zhang, Z. and Liu, T., 2018. Mesenchymal stem cell expression of interleukin-35 protects against ulcerative colitis by suppressing mucosal immune responses. *Cytotherapy*, 20(7), pp.911–918. <https://doi.org/10.1016/j.jcyt.2018.05.004>.

Yang, L.-X., Wei, C.-L., Guo, M.-L., Zhang, Y., Bai, F. and Ma, S.-G., 2017. Improvement of therapeutic effects of mesenchymal stem cells in myocardial infarction through genetic suppression of microRNA-142. *Oncotarget*, [online] pp.1–10. Available at: <www.impactjournals.com/oncotarget/>.

Yap, F., Cheong, S., Ammu, R. and Leong, C.-F., 2009. Transfected human mesenchymal stem cells do not lose their surface. 31(126), pp.113–120.

Yin, X., Hu, L., Zhang, Y., Zhu, C., Cheng, H., Xie, X., Shi, M., Zhu, P., Zhao, X., Chen, W., Zhang, L., Arakaki, C., Hao, S., Wang, M., Cao, W., Ma, S., Zhang, X.B. and Cheng, T., 2020. PDGFB-expressing mesenchymal stem cells improve human hematopoietic stem cell engraftment in immunodeficient mice. *Bone Marrow Transplantation*, 55(6), pp.1029–1040. <https://doi.org/10.1038/s41409-019-0766-z>.

Yu, Q., Chen, L., You, Y., Zou, C., Zhang, Y., Liu, Q. and Cheng, F., 2011. Erythropoietin combined with granulocyte colony-stimulating factor enhances MMP-2 expression in mesenchymal stem cells and promotes cell migration. *Molecular Medicine Reports*, 4(1), pp.31–36. <https://doi.org/10.3892/mmr.2010.387>.

Yuan, Z.Q., Kolluri, K.K., Sage, E.K., Gowers, K.H.C. and Janes, S.M., 2015. Mesenchymal stromal cell delivery of full-length tumor necrosis factor-related apoptosis-inducing ligand is superior to soluble type for cancer therapy. *Cytotherapy*, [online] 17(7), pp.885–896. <https://doi.org/10.1016/j.jcyt.2015.03.603>.

Zappa, C. and Mousa, S.A., 2016. Non-small cell lung cancer: current treatment and future advances. *Translational Lung Cancer Research*, [online] 5(3), pp.288–300. <https://doi.org/10.21037/tlcr.2016.06.07>.

Zhang, W.W., Li, L., Li, D., Liu, J., Li, X., Li, W., Xu, X., Zhang, M.J., Chandler, L.A., Lin, H., Hu, A., Xu, W. and Lam, D.M.K., 2018. The First Approved Gene Therapy Product for Cancer Ad-p53 (Gendicine): 12 Years in the Clinic. *Human Gene Therapy*, 29(2), pp.160–179. <https://doi.org/10.1089/hum.2017.218>.

Zhou, Y., Tsai, T.L. and Li, W.J., 2017. *Strategies to retain properties of bone marrow-derived mesenchymal stem cells ex vivo*. *Annals of the New York Academy of Sciences*, <https://doi.org/10.1111/nyas.13451>.

APPENDIX A

1) pUNO1-hIL12

pUNO1-<Gene>

Expression vector containing a fully sequenced open reading frame.

Catalog # puno1-<gene>

For research use only

Version # 14A23-JC

PRODUCT INFORMATION

Contents:

- 20 µg of lyophilized plasmid DNA
- 4 pouches of *E. coli* Fast-Media® Blas (2 TB and 2 Agar)
- 1 ml blasticidin at 10 mg/ml

Storage and Stability:

- Product is shipped at room temperature.
- Lyophilized DNA should be stored at -20°C.
- Resuspended DNA should be stored at -20°C and is stable up to 1 year.
- Store *E. coli* Fast-Media® at room temperature in a dry and cool place. Fast-Media® pouches are stable 2 years when stored properly.
- Store blasticidin at 4°C or -20°C for up to two years. Product is stable 2 weeks at 37°C. Avoid repeated freeze-thaw cycles.

Quality control:

- Plasmid construct has been confirmed by restriction analysis and full-length ORF sequencing.
- Plasmid DNA was purified by ion exchange chromatography.

GENERAL PRODUCT USE

• **Obtaining a gene to subclone into another vector.** The gene of interest is flanked by two unique restriction sites allowing its convenient excision. These restriction sites are compatible with other restriction sites contained in multiple cloning sites, thus facilitating subcloning.

• **Stable gene expression in mammalian cells.** pUNO1 plasmids can be used directly in transfection experiments both *in vitro* and *in vivo*. pUNO1 plasmids contain the blasticidin-resistance gene (*bsr*) driven by the CMV promoter/enhancer in tandem with the bacterial EM7 promoter. This allows the amplification of the plasmid in *E. coli*, as well as the selection of stable clones in mammalian cells using the same selective antibiotic. pUNO1 allows high levels of expression and secretion (where applicable) of the gene product.

METHODS

Plasmid resuspension:

Quickly spin the tube containing the lyophilized plasmid to pellet the DNA. To obtain a plasmid solution at 1 µg/µl, resuspend the DNA in 20 µl of sterile water. Store resuspended plasmid at -20°C.

Plasmid amplification and cloning:

Plasmid amplification and cloning can be performed in *E. coli* GT116 or other commonly used laboratory *E. coli* strains, such as DH5α.

Selection of bacteria with *E. coli* Fast-Media® Blas:

E. coli Fast-Media® Blas is a fast and convenient way to prepare liquid and solid media for bacterial culture by using only a microwave. See detailed protocol overleaf.

Blasticidin usage:

Blasticidin should be used at 25-100 µg/ml in bacteria and 1-30 µg/ml in mammalian cells. Blasticidin is supplied as a 10 mg/ml colorless solution in HEPES buffer.

TECHNICAL SUPPORT

Toll free (US): 888-457-5873
Outside US: (+1) 858-457-5873
Europe: +33 562-71-69-39
E-mail: info@invivogen.com
Website: www.invivogen.com

PLASMID FEATURES

• **EF-1α / HTLV hybrid promoter** is a composite promoter comprised of the Elongation Factor-1α (EF-1α) core promoter¹ and the 5' untranslated region of the Human T-Cell Leukemia Virus (HTLV). EF-1α utilizes a type 2 promoter that encodes for a "house keeping" gene. It is expressed at high levels in all cell cycles and lower levels during G0 phase. The promoter is also non-tissue specific; it is highly expressed in all cell types. The R segment and part of the U5 sequence (R-U5') of the HTLV Type 1 Long Terminal Repeat² has been coupled to the EF-1α promoter to enhance stability of DNA and RNA. This modification not only increases steady state transcription, but also significantly increases translation efficiency possibly through mRNA stabilization.

• **ORF:** pUNO1 provides an intronless ORF from the ATG to the stop codon, fully-sequenced, and typically flanked by convenient cloning sites for easy subcloning.

Typically, the 5' end of the ORF contains a unique NcoI, BspHI, BspLU111, or SphI site encompassing the ATG Start codon. When this 5' cloning site is not unique, another restriction (e.g. AgeI) is added a few bases upstream of the ATG.

The 3' end of the ORF contains a unique NheI site (or compatible site) after the Stop codon.

- AgeI is compatible with XmaI, BspEI, NgoMIV and SgrAI.
- NcoI is compatible with BspHI and BspLU111.
- NheI is compatible with XbaI, SpeI, and AvrII.

• **SV40 pAn:** The Simian Virus 40 late polyadenylation signal enables efficient cleavage and polyadenylation reactions, resulting in high levels of steady-state mRNA³.

• **pMB1 ori** is a minimal *E. coli* origin of replication to limit vector size, but with the same activity as the longer Ori.

• **CMV promoter & enhancer** drives the expression of the blasticidin resistance in mammalian cells.

• **Bsr (blasticidin resistance gene):** The *bsr* gene from *Bacillus cereus* encodes a deaminase that confers resistance to the antibiotic blasticidin. The *bsr* gene is driven by the CMV promoter/enhancer in tandem with the bacterial EM7 promoter. Therefore, blasticidin can be used to select stable mammalian cells transfectants and *E. coli* transformants.

• **Human beta-Globin polyA** is a strong polyadenylation (pAn) signal placed downstream of *bsr*. The use of beta-globin pAn minimizes interference⁴ and possible recombination events with the SV40 polyadenylation signal.

1. Kim DW, et al., 1990. Use of the human elongation factor 1α promoter as a versatile and efficient expression system. *Gene* 91(2):217-23. 2. Takebe Y, et al., 1988. SR alpha promoter: an efficient and versatile mammalian cDNA expression system composed of the simian virus 40 early promoter and the R-U5 segment of human T-cell leukemia virus type 1 long terminal repeat. *Mol Cell Biol.* 8(1):466-72. 3. Carswell S, & Alwine JC., 1989. Efficiency of utilization of the simian virus 40 late polyadenylation site: effects of upstream sequences. *Mol Cell Biol.* 9(10):4248-58. 4. Yu J, & Russell JE., 2001. Structural and functional analysis of an mRNP complex that mediates the high stability of human β-globin mRNA. *Mol Cell Biol.* 21(17):5879-88.



3950 Sorrento Valley Blvd. Suite 100
San Diego, CA 92121 - USA

Blasticidin

Selective antibiotic for the *bsr* or *BSD* genes

For research use only

PRODUCT INFORMATION

Contents:

Blasticidin hydrochloride is supplied as 1 ml tubes of a 10 mg/ml colorless solution in HEPES buffer (100% active compound), pH 7.5, filtered to sterility for customer convenience and cell culture tested.

Quality control:

Purity controlled by HPLC: >95%. Activity controlled by bioassays on bacteria and mammalian cell lines.

SPECIAL HANDLING

Blasticidin is a hazardous compound. Avoid contact with eyes, skin and clothes.

BACKGROUND

Blasticidin is a peptidyl nucleoside antibiotic isolated from the culture broth of *Streptomyces griseochromogenes*. It specifically inhibits protein synthesis in both prokaryotes and eukaryotes through inhibition of peptide bound formation in the ribosomal machinery. Blasticidin is used to select transfected cells carrying *bsr* or *BSD* resistance genes.

CAS number: 3513-03-9

Formula: C₁₇H₂₆N₈O₅, HCl

Molecular weight: 458.9

pKa values: 2.8, 4.2, 8.2 and 12.5

RESISTANCE TO BLASTICIDIN

Three blasticidin resistance genes have been cloned and sequenced: an acetyl transferase gene, *bsl* from a blasticidin producer strain¹, and two deaminase genes, *bsr* gene from *Bacillus cereus*^{2,3}, and *BSD* gene from *Aspergillus terreus*^{4,5}. Both *bsr* and *BSD* genes are used as dominant selectable markers for gene transfer experiments in mammalian and plant cells. Although blasticidin was developed as a selection agent for mammalian cells, the *bsr* and *BSD* resistance genes can also be used in *E. coli*.

CONDITIONS OF SELECTION

- *Escherichia coli* is poorly sensitive to blasticidin, but transformants resistant to blasticidin can be selected on low salt LB agar medium, pH 8, supplemented with 100 µg/ml blasticidin. High pH enhances activity of blasticidin. For optimum results, the use of InvivoGen's Fast-Media® Blas is recommended.

- **Mammalian cells:** The working concentration of blasticidin for mammalian cell lines varies from 1 to 10 µg/ml (ex. HeLa, HEK293, B16), in a few cases up to 30 µg/ml (ex. PC1.0). In a starting experiment we recommend to determine optimal concentrations of antibiotic required to kill your host cell line. After treatment, cell death occurs rapidly, as fast as G418 selection, allowing the selection of transfected cells with plasmids carrying the *bsr* or *BSD* genes in as little as 7 days post-transfection.

Note: Antibiotics work best when cells are actively dividing. If the cells become too dense, the antibiotic efficiency will decrease. It is best to split cells such that they are no more than 25% confluent.

TECHNICAL SUPPORT

Toll free (US): 888-457-5873
Outside US: (+1) 858-457-5873
Europe: +33 562-71-69-39
E-mail: info@invivogen.com
Website: www.invivogen.com

Fast-Media® Blas

Microwaveable media for selection and propagation of blasticidin-resistant *E. coli*

For research use only

PRODUCT INFORMATION

Contents:

Each Fast-Media® Blas pouch contains the necessary amount of powder for the preparation of 200 ml of medium supplemented with **blasticidin**. Agar media is LB-based (Lysogeny Broth also known as Luria Broth), liquid media is TB-based (Terrific Broth).

Effective concentration: Blasticidin 100 µg/ml

METHOD

For customer convenience, the following procedure is directly printed on each pouch.

1. Pour the pouch contents into a clean borosilicate glass bottle or flask.
2. Add 200 ml of distilled or deionized water.
3. Mix thoroughly by swirling the glass bottle or flask.
4. Heat in a microwave oven on MEDIUM power setting (about 450W) until bubbles start to appear (about 3 minutes).

Do not heat in a closed container.

5. Swirl gently to mix the preparation and re-heat for 30 seconds. Swirl gently again.
6. Repeat step 4 if necessary until the medium is completely dissolved. Do not overboil.
7. Allow the medium to cool to 50-55°C before use.

Caution: Any solution heated in a microwave oven may become superheated and suddenly boil when moved or touched. Handle with extreme care. Wear heat-proof gloves.

Note: Do not repeat this above procedure once the medium is prepared because the antibiotic will be adversely affected.

SPECIAL HANDLING

Caution should be exercised during handling of Fast-Media® due to potential allergenic properties of antibiotics. Wear protective gloves, do not breathe the dust.

FAST-MEDIA® FEATURES

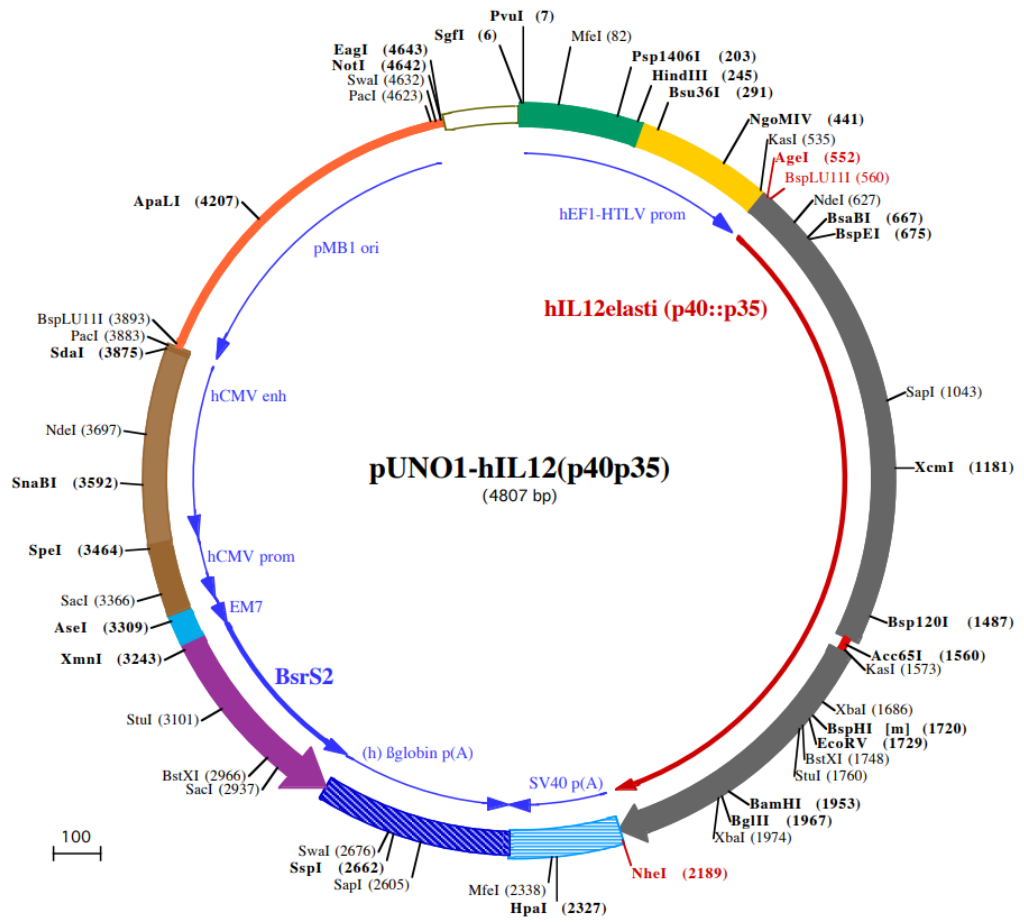
Fast-Media® offer researchers a quick and convenient way to prepare 200 ml of sterile *E. coli* growth medium in about five minutes using a **microwave** instead of an autoclave.

Fast-Media® is available with a large choice of antibiotics for selection, and chromogenic substrates, for the growth or selection of *E. coli* transformant colonies, as well as detection of blue/white colonies. Fast-Media® Base is supplied without selective antibiotics. See the variety of available Fast-Media® products at <http://www.invivogen.com/fast-media>.

1. Perez-Gonzalez JA, et al., 1990. Cloning and characterization of the gene encoding a blasticidin S acetyltransferase from *Streptomyces griseochromogenes* sp. Gene 86:129-34. 2. Irumi M, et al., 1991. Blasticidin S-resistance gene (*bsr*): A novel selectable marker for mammalian cells. Exp. Cell Res. 197:229-33. 3. Itaya M, et al., 1990. The blasticidin S resistance gene (*bsr*) selectable in a single copy state in the *Bacillus subtilis* chromosome. J. Biochem. 107: 799-801. 4. Kimura M, et al., 1994. Cloning of the blasticidin S deaminase gene (BSD) from *Aspergillus terreus* and its use as a selectable marker for *Schizosaccharomyces pombe* and *Pyricularia oryzae*. Mol. Gen. Genet. 242:121-9. 5. Kimura M, et al., 1994. Blasticidin S deaminase gene from *Aspergillus terreus* (BSD): a new drug resistance gene for transfection of mammalian cells. Biochim. Biophys. Acta. 1219:653-9.



3950 Sorrento Valley Blvd. Suite 100
San Diego, CA 92121 - USA



PvuI (7) **SglI (6)** **MfeI (82)**
1 GGATCTGCATCGCTCCGGTGCCCTCAGTGGGCGAGCGCACATCGCCACAGTCCCCGAGAAGTTGGGGGAGGGTGGGCAATTGAACGGTGCCTA
101 GAGAAGTGGCGGGGTAACGGAAAGTGATGCTGTACTGGCTCCGCCCTTTTCCCGAGGGTGGGGGAGAACCGTATATAAGTGCAGTAGTCCGC
Psp1406I (203) **HindIII (245)** **Bsu36I (291)**
201 GTGAACGTTCTTTTCCCAACGGGTTTCCGCCAACAACACAGCTGAAGCTTCAGGGCTCGCATCTCTCTTCCACGCGCCCGCCCTACCTGAGGCC
301 GCCATCCACGCCGGTTGAGTCGCTTCTGCGCCTCCCGCTGTGGTGGCTCTGAAGTCCGTCGCGCTAGGTAAGTTAAAGCTCAGGTCGAGACC
NgoMIV (441)
401 GGGCCTTTGTCCGGCGCTCCCTGGAGCTACCTAGACTCAGCCGGCTCTCCACGCTTTGCTGACCTGCTTGTCTCAACTCAGCTTTTGTTCGTTT
KasI (535) **AgeI (552)** **Bsp1406I (560)**
501 TCTGTTCTGCCGTTACAGATCAAGCTGTGACCGCGCCTACCTGAGATCACGGTCAACATGTGTCCACGACAGTGTGCTATCTTTGGTTTTCCCT
1 M C H Q L V I S W F S L
BspEI (675)
NdeI (627) **BsuBI (667)**
601 GGTTTTTCTGGCATCTCCCTCGTGGCCATATGGGAAGTATTTATGTCTGATGATGGATGGTATCCGGATGCCCTGGAGAAATGGTG
13 V F L A S P L V A I W E L K K D V Y V V E L D W Y P D A P G E M V
701 GTCCTCACCTGTGACACCCCTGAAGAAGTGGTATCACCTGGACCTGGACAGAGCAGTGGGCTTAGGCTTGGCAAAACCTGACCATCAAGTCA
47 V L T C D T P E E D G I T W T L D Q S S E V L G S G K T L T I Q V
801 AAGATTTGGAGATGCTGGCCAGTACACCTGTCAAAAGGAGCGGAGTTCTAAGCCATTCGCTCTGCTCTTCAAAAAGGAAAGTGAATTTGGTC
80 K E F G D A G Q Y T C H K G G E V L S H S L L L L H K K E D G I W S
901 CACTGATATTTAAAGACCAAGAAACCCAAAATAAGACTTTCTAAGATGCGAGCCAAAGAAATTTCTGGACGTTTCACTGCTGGTGGCTGAGC
113 T D I L K D Q K E P K N K T F L R C E A K N Y S G R F T C W W L T
SapI (1043)
1001 ACAATCAGTACTGATTTGACATTCAGTGTCAAAAGCAGCAGAGGCTCTTCTGACCCCAAGGGGTGACGTGCGGAGCTGTACACTCTCTGCAGAGAGAG
147 T I S T D L T F S V K S S R G S S D P Q G V T C G A A T L S A E R
XcmI (1181)
1101 TCAGAGGGGACAACAGGAGTATGAGTACTCAGTGGAGTCCAGGAGGACAGTGCCTGCCAGTCTGCTGAGGAGAGTCTGCCATTGAGGTCAATGGTGGGA
180 V R G D N K E Y E Y S V E C Q E D S A C P A A E E S L P I E V M V D
1201 TGCCGTTCAACAGCTCAAGTATGAAACTACACCAGCAGCTTCTTCATCAGGACATCATCAAACTGACCCACCAAGAAGTTCAGCTGAAGCCATTA
213 A V H K L K Y E N Y T S S F F I R D I I K P D P K N L Q L K P L
1301 AAGAATTTCTGGCAGGTGGAGGTGAGTACCTGACACCTGGAGTACTCAGATTCCTACTTCTCCCTGACATTCGCTTTCAGGTCAGGGGCA
247 K N S R Q V E V S W E Y P D T W S T P H S Y F S L T F C V Q V Q G
Bsp120I (1487)
1401 AGAGCAAGAGAGAAAAGAAAGATAGAGTCTTACGACAAAGACCTCAGCCACGGTCACTGCGCCAAAATGCCAGCATTAGCGTGGGGCCAGGACCG
280 K S K R E K K D R V F T D K T S A T V I C R K N A S I S V R A Q D R
Ace65I (1560) **KasI (1573)**
1501 CTACTAGTCTCATCTTGGAGCGAATGGGCATCTGTCCTGCGCTGAGTGTCTCTGGAGTAGGGGTACTGGGGTGGGCGCCAGAAACCTCCCGTGGCCACT
313 Y Y S S S W S E W A S V P C S V P G V G V P G V G A R N L P V A T
XbaI (1686)
1601 CCAGACCCAGGAATGTTCCCATGCCTTCCACTCCAAAACCTGCTGAGGGCCCTCAGCAACATGCTCCAGAAAGCCAGACAACTCTAGAATTTTACC
347 P D P G M F P C L H S Q N L L R A V S N M L Q K A R Q T L E F Y
EcoRV (1729)
BspHI (m) (1720) **BstXI (1748)** **StuI (1760)**
1701 CTTGCACTCTGAAGAGATTGATCATGAAGATATCAAAAAGATAAAAACAGCAGTGGAGGCTGTATCCATTGGAATTAACCAAGAATGAGAGTTG
380 P C T S E E I D H E D I T K D K T S T V E A C L P L E L T K N E S C
1801 CCTAAATCCAGAGAGACTCTTTCATAAATAATGGAGTTGCCTGGCTCCAGAAAGACCTCTTTATGATGGCCCTGTGCCTTAGTAGTATTTATGAA
413 L N S R E T S F I T N G S C L A S R K T S F M M A L C L S S I Y E
XbaI (1974)
BamHI (1953) **BglII (1967)**
1901 GACTTGAAGATGTACCAGGTGGAGTTCAAGACCATGAATGCAAAGCTGCTGATGGATCCTAAGAGGCAGATCTTTCTAGATCAAAACATGCTGGCAGTTA
447 D L K M Y Q V E F K T M N A K L L M D P K R Q I F L D Q N M L A V
2001 TTGATGAGCTGATGAGCCCTGAATTTCAACAGTGAAGTGTGCCAAAAATCCTCCTTGAAGAACCAGGATTTTATAAACTAAAACCAAGCTCTG
480 I D E L M Q A L N F N S E T V P Q K S S L E E P D F Y K T K I K L C
NheI (2189)
2101 CATACTTCTCATGCTTTCAGAAATTCGGGCGAGTACTATTGATAGAGTATGAGCTATCTGAATGCTTCTAAAAGCGAGGTCCTCCCTGCTAGCTGGCC
513 I L L H A F R I R A V T I D R V M S Y L N A S
2201 AGACATGATAAGATACATTGATGAGTTTGGACAAACCAACTAGAAGTCAAGTGAATAAATGCTTTATTTGTAATTTGTGATGCTATTGCTTTATTT
HpaI (2327) **MfeI (2338)**
2301 GTAACCATTAAGCTGCAATAAACAGTTAAACAACAATTCATTCATTTATGTTTCAGGTTCCAGGGGAGGTGTGGGAGGTTTTTAAAGCAAGT
2401 AAAACCTCTACAAATGGTATGGAATCTAAAATACAGCATAGCAAACTTAACTCCAAATCAAGCCTCTACTGAATCTTTTCTGAGGGATGAAT
2501 AAGGCATAGGCATCAGGGGCTGTGCCAATGTGATTAGCTGTTTGCAGCCTCACCTTTCTCATGGAGTTAAGATATAGTGTATTTTCCCAAGGTTTG
SapI (2605) **SspI (2662)** **SwaI (2676)**
2601 AACTAGCTCTTCATTTCTTTATGTTTTAAATGCACCTGCCACATCCCTTTTGTAGTAAAATATTCAGAAATAATTTAAATACATCATTGCAATGAA

2701 AATAAAATGTTTTTATTAGGCAGAATCCAGATGCTCAAGGCCCTCATAATATCCCCAGTTTAGTAGTTGGACTTAGGGAACAAAGGAACCTTAATAG

2801 AAATGGACAGCAAGAAAGCGAGCTTCTAGCTTTAGTTCCTGGTGTACTTGAGGGGATGAGTTCCTCAATGGTGGTTTTGACCAGCTTGCCATTCATCT
 144 • N R T Y K L P I L E E I T T K V L K G N M E

2901 CAATGAGCACAAAGCAGTCAGGAGCATAGTCAGAGATGAGCTCTCGCACATGCCACAGGGGCTGACCACCTGATGGATCTGTCCACCTCATCAGAGTA
 118 I L V F C D P A Y D S I L E R C M G C P S V V R I S R D V E D S Y

3001 GGGGTGCTGACAGCCACAATGGTGTCAAAGTCTTCTGCCGTTGCTCACAGCAGACCAATGGCAATGGCTTCAGCACAGACAGTACCCTGCCAATG
 85 P H R V A V I T D F D K Q G N S V A S G I A I A E A C V T V R G I

3101 TAGGCCTCAATGGACAGCAGAGATGATCTCCAGTCTTGGTCTGTATGGCCGCCGACATGGTCTTGTGTCTCATAGAGCATGGTATCTTCT
 51 Y A E I H V A S I I E G T K T R I A A G V H H K N D E Y L M T I K E

3201 CAGTGGCGACCTCCACCAGCTCCAGATCTGTCTGAGAGATGTTAAGGTCTTCATGGTGGCCCTCATAGTGAGTCGATTATACATATGCCGATATACT
 18 T A V E V L E L D Q Q S I N F T K M

3301 ATGCCGATGATTAATTGCAAAACAGCGTGGATGGCGTCTCCAGCTTATCTGACGGTTCACATAACGAGCTCTGCTTATATAGACCTCCACCCTACACG
 AseI (3309) SacI (3366)

3401 CCTACCGCCATTGTGCTCAATGGGCGGAGTTGTACGACATTTTGAAAAGTCCCGTTGATTTCTAGTCAAACAACTCCCATTGACGTCAATGGGG
 SpeI (3464)

3501 TGGAGACTTGGAAATCCCCTGAGTCAAACCGCTATCCACGCCATTGATGTACTGCCAAAACCGCATCATCATGGTAATAGCGATGACTAATACGTAGA
 SnaBI (3592)

3601 TGTACTGCCAAGTAGGAAAGTCCATAAAGTCATGTACTGGGCATAATGCCAGGCGGGCCATTACCCTGATTGACGTCAATAGGGGGCTACTGGCAT
 NdeI (3697)

3701 ATGATACACTTGTACTGCCAAGTGGCAGTTTACCCTAAATACTCCACCATTGACGTCAATGGAAAGTCCCTATTGGCGTTACTATGGGAACATAC

3801 GTCATTATTGACGTCAATGGGCGGGGTCGTTGGCGGTGAGCAGGCGGGCCATTTACCGTAAGTTATGTAACGCCGTCAGGTTAAITAAAGAACATGTG
 Pacl (3883) SdaI (3875) BspLU111 (3893)

3901 AGCAAAAGGCCAGCAAAAGCCAGGAACCGTAAAAAGCCGCTTGTGGCTTTTCCATAGGCTCCGCCCCCTGACGAGCATCACAAAATCGACGC

4001 TCAAGTCAGAGGTGGCAAACCCGACAGGACTATAAAGATACACAGGCTTTCCCTTGAAGTCCCTCGTCCGCTCTCTGTTCCGACCTGCCCTTA

4101 CCGGATACCTGTCGCCCTTCTCCCTTCGGGAAGCGTGGCGCTTCTCATAGCTCACGCTGTAGGTATCTCAGTTCGGTGTAGGTGTTGCTCCCAAGCT

4201 GGGCTGTGTGCAGAACCCCGCTCAGCCGACCGTGGCGCTTATCCGGTAACATCGTCTTGTAGTCCAACCCGGTAAGACACGACTTATCGCCACTG
 ApaLI (4207)

4301 GCAGCAGCCACTGGTAACAGGATTAGCAGAGCGAGGTATGTAGCGGTGCTACAGAGTCTTGAAGTGGTGCCTAACTACGGCTACACTAGAAGAACAG

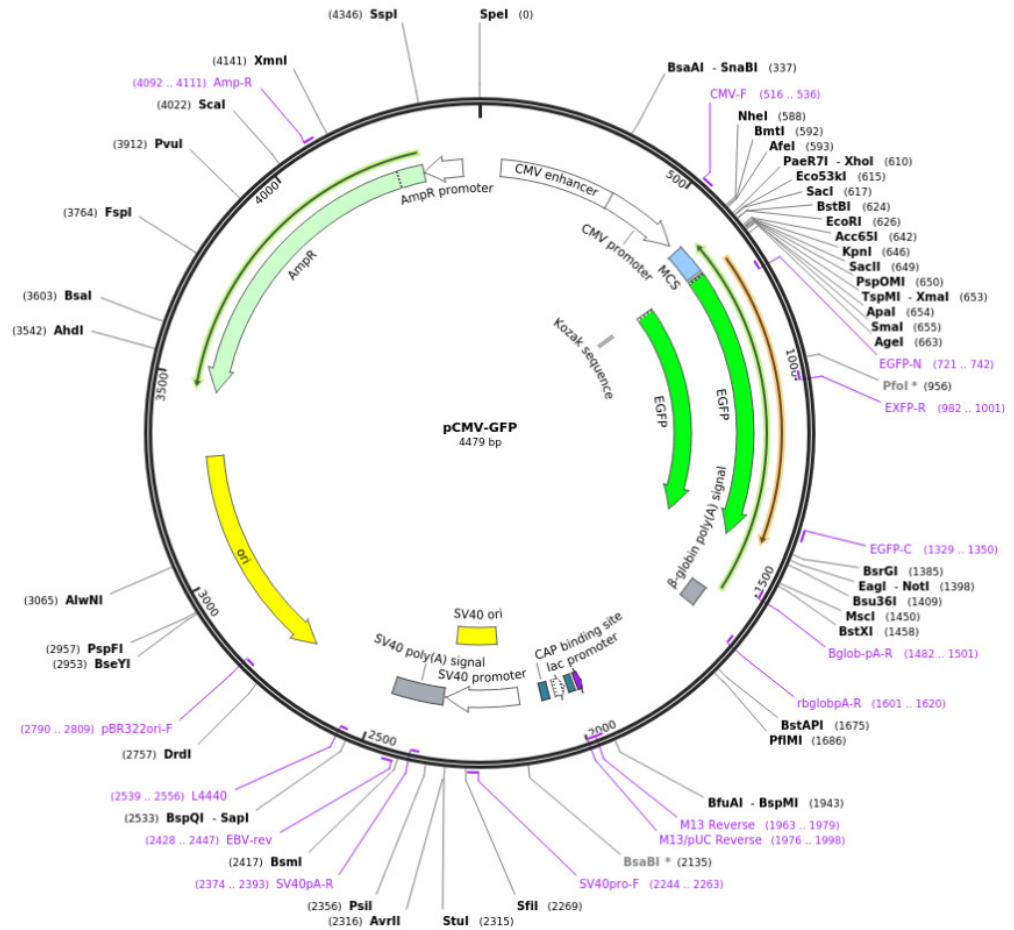
4401 TATTTGGTATCTGCGCTCTGCTGAAGCAGTTACCTTCGGAAAAAGTGGTAGCTCTTGATCGGCAAAACAAACCACGCTGGTAGCGGTGTTTTT

4501 TGTTTGCAAGCAGCAGATTACCGCAGAAAAAAGGATCTCAAGAAGATCCTTGGATCTTTCTACGGGTCTGACGCTCAGTGGAAACGAAACTCACGT

4601 TAAGGGATTTGGTCAATGGCTAGTTAATTAACATTTAAATCAGCGGCCCAATAAAATATCTTTATTTTACATCTGTGTGTTTTTTGGTGTGA
 Pacl (4623) SnaI (4632) EagI (4643) NotI (4642)

4701 ATCGTAACATACGCTCTCCATCAAAACAAAACGAAACAAAACAACTAGCAAAATAGGCTGTCCCGAGTGAAGTGCAGGTGCCAAGCAATTTCTC
 4801 TATCGAA

2) pCMV-GFP

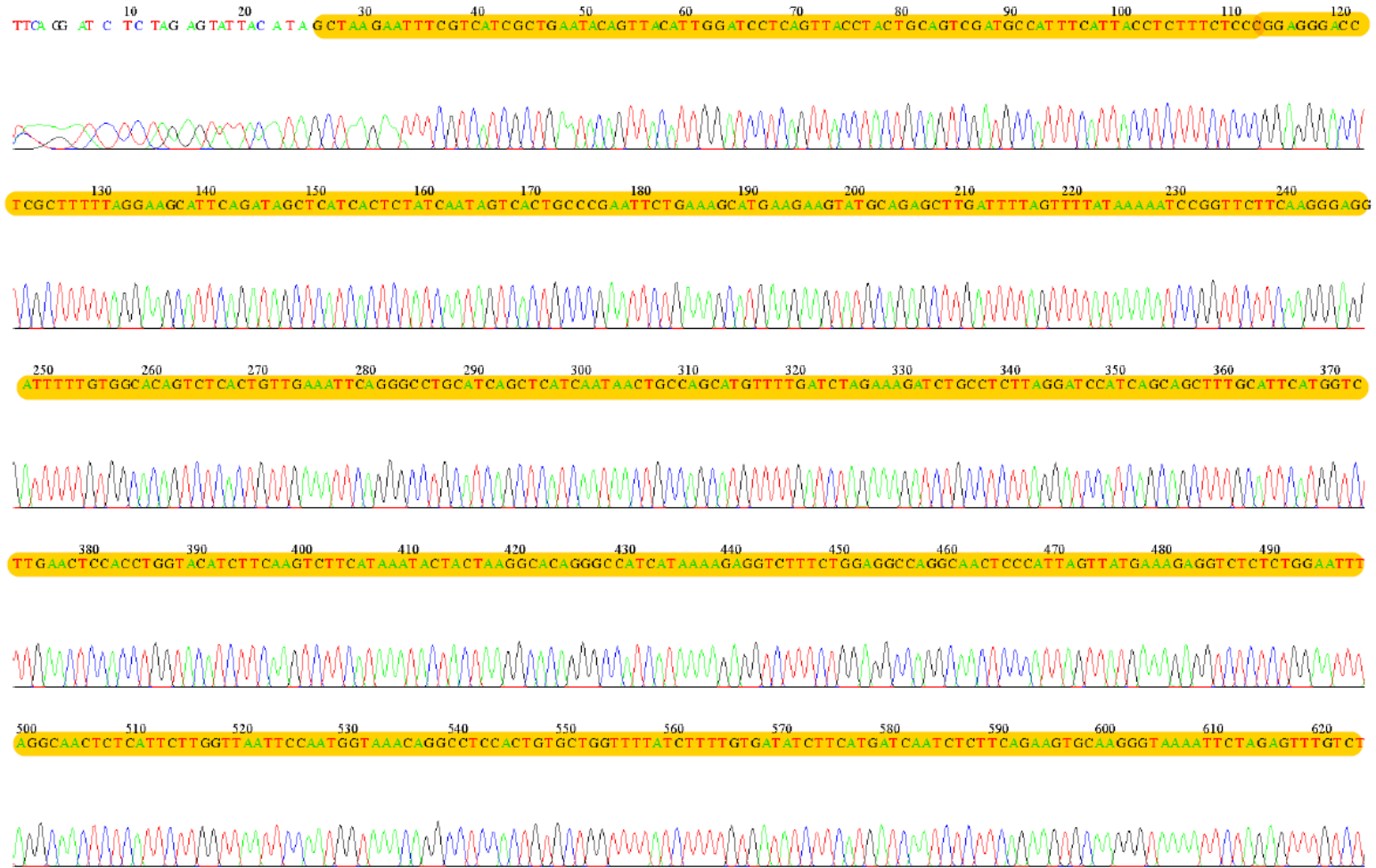


APPENDIX B: 1) Results of Sanger Sequencing of pAdenoX-hIL12 recombinant plasmid

Note: Location of hIL-12 gene is highlighted in orange.



File: pIL12_12-6-20_Pcmv_3_cloning_site.ab1 Run Ended: 2020/7/18 4:51:30 Signal G:1167 A:1522 C:1969 T:1837
Sample: pIL12_12-6-20_Pcmv_3_cloning_site Lane: 87 Base spacing: 15.662064 1285 bases in 15432 scans Page 1 of 2



File: pIL12_12-6-20_Pcmv_3_cloning_site.ab1

Run Ended: 2020/7/18 4:51:30

Signal G:1167 A:1522 C:1969 T:1837

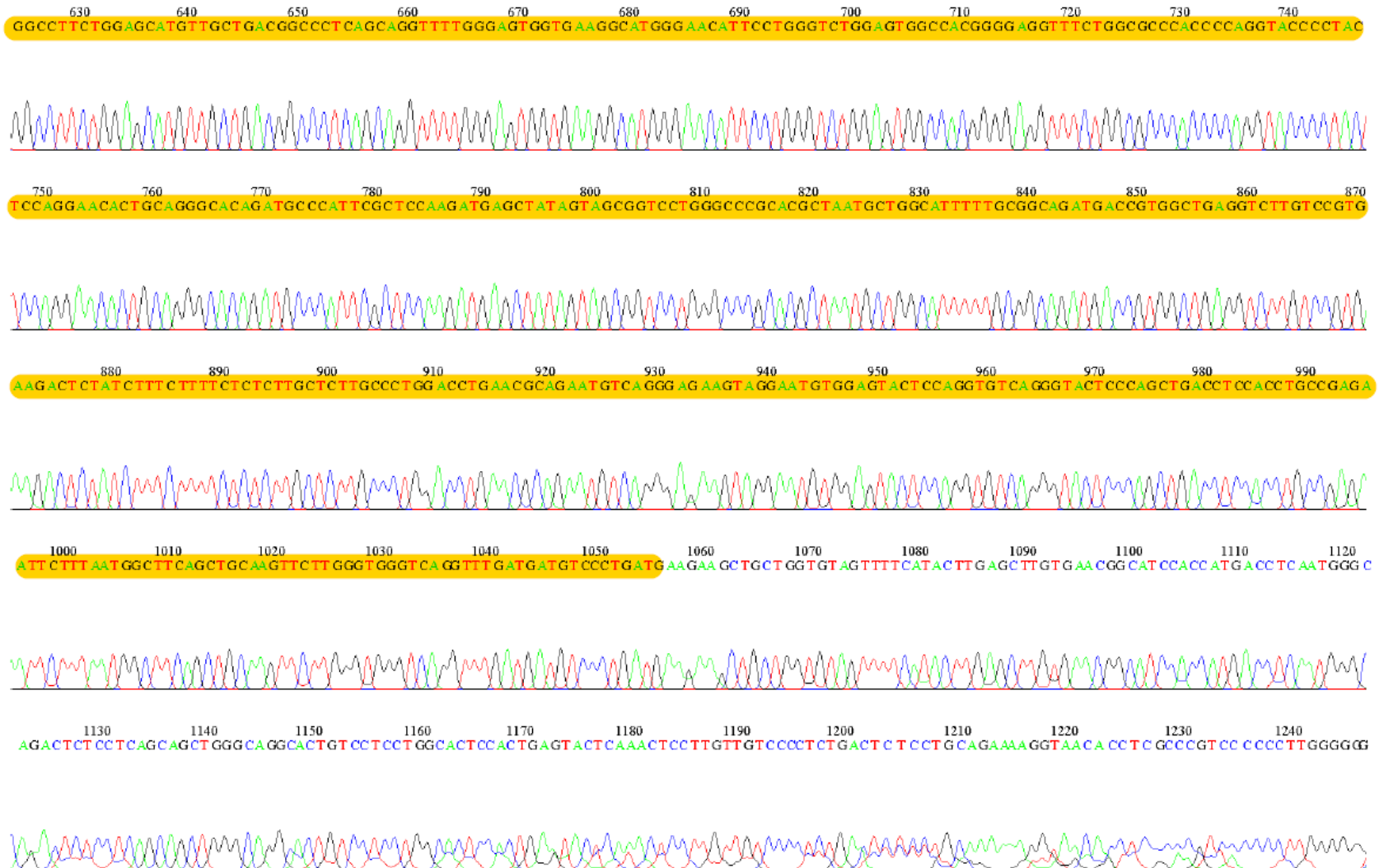
Sample: pIL12_12-6-20_Pcmv_3_cloning_site

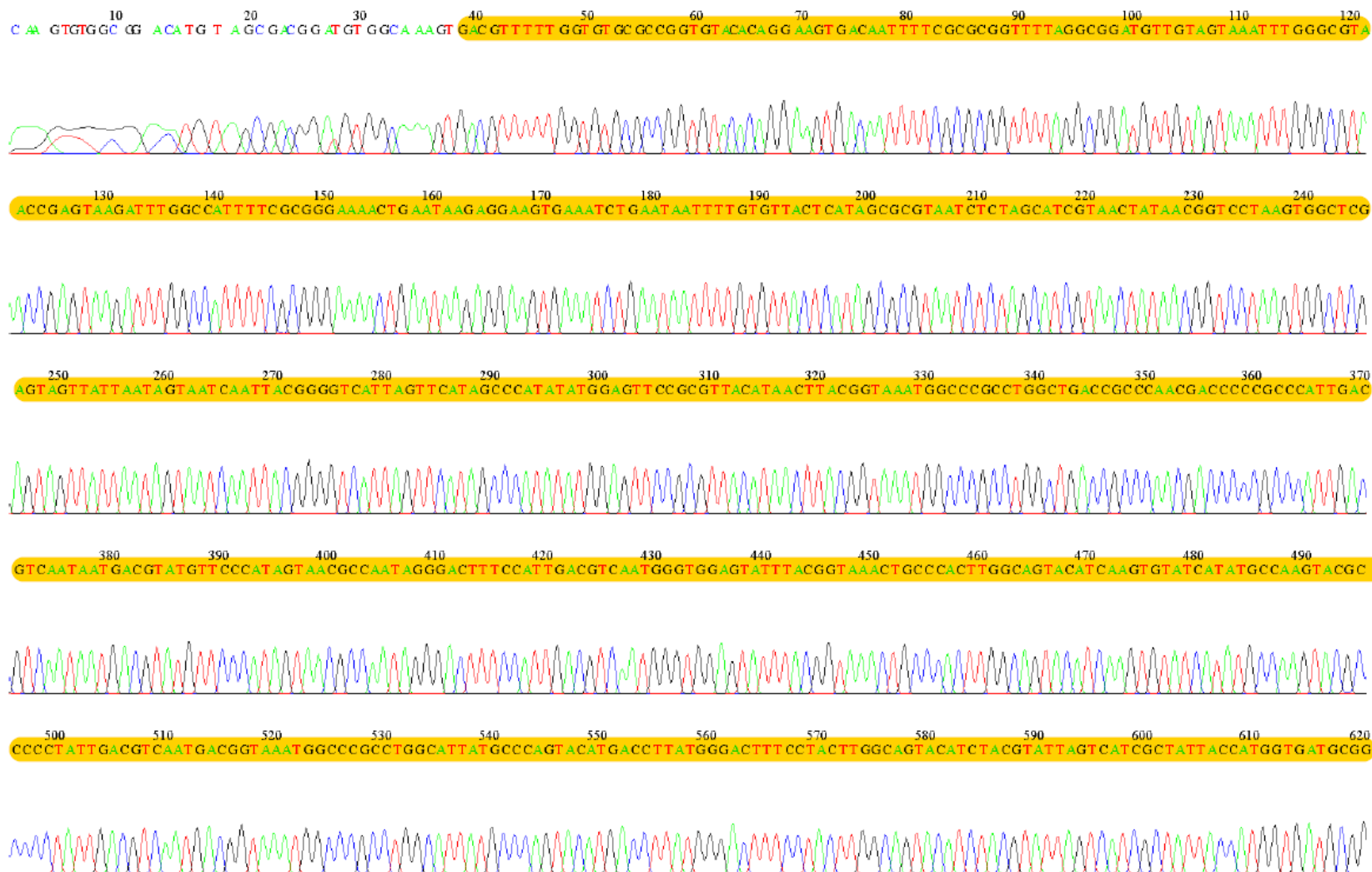
Lane: 87

Base spacing: 15.662064

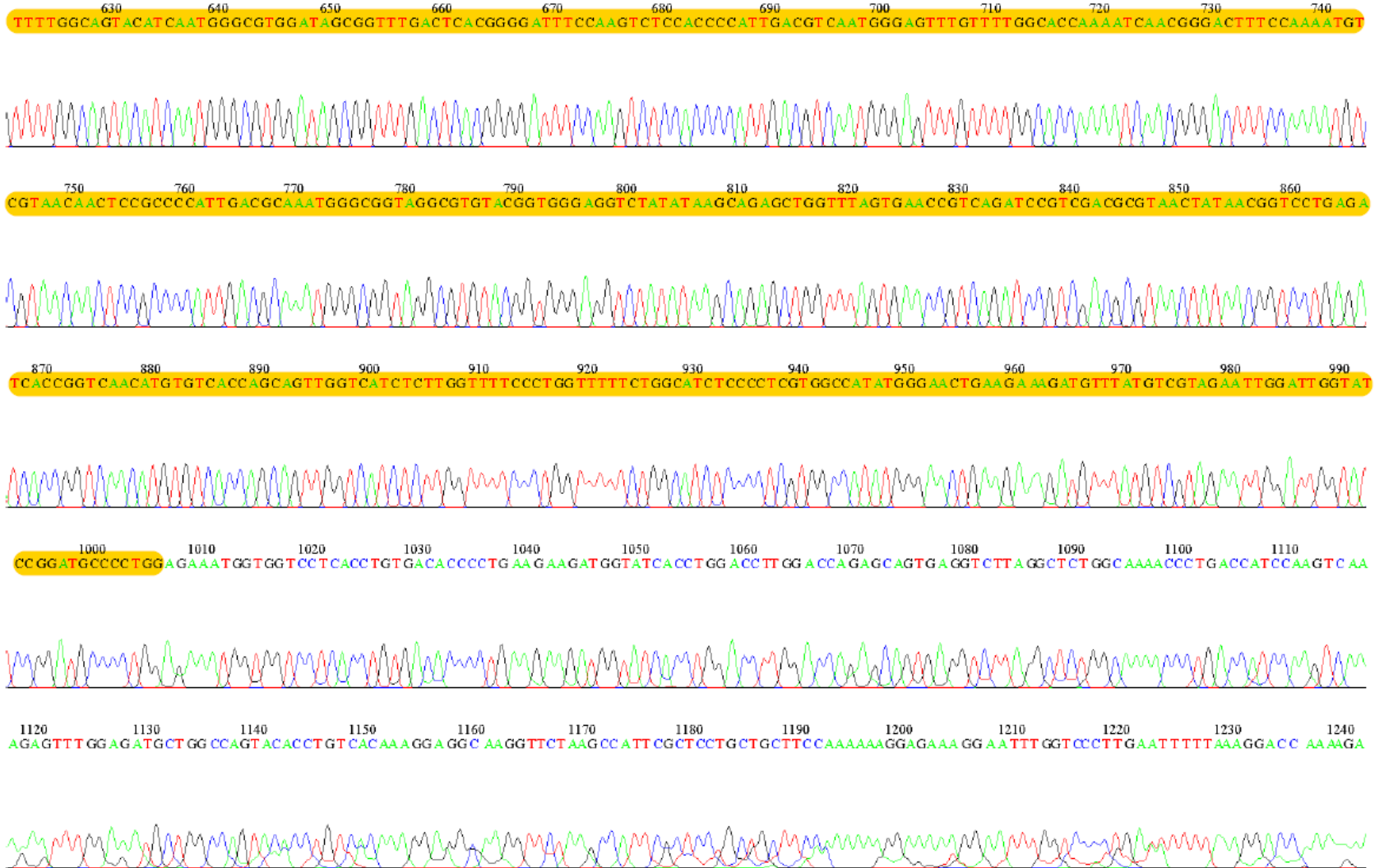
1285 bases in 15432 scans

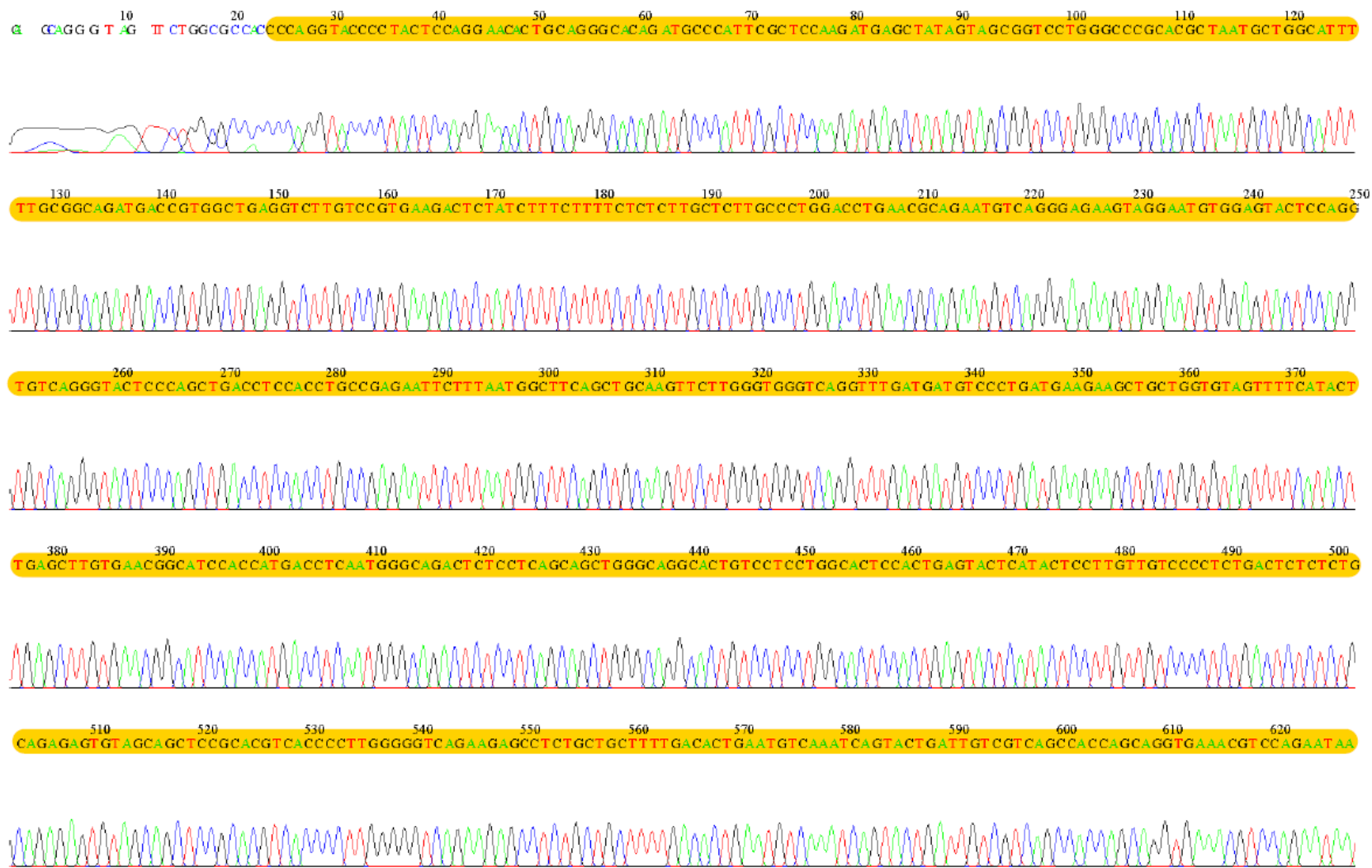
Page 2 of 2



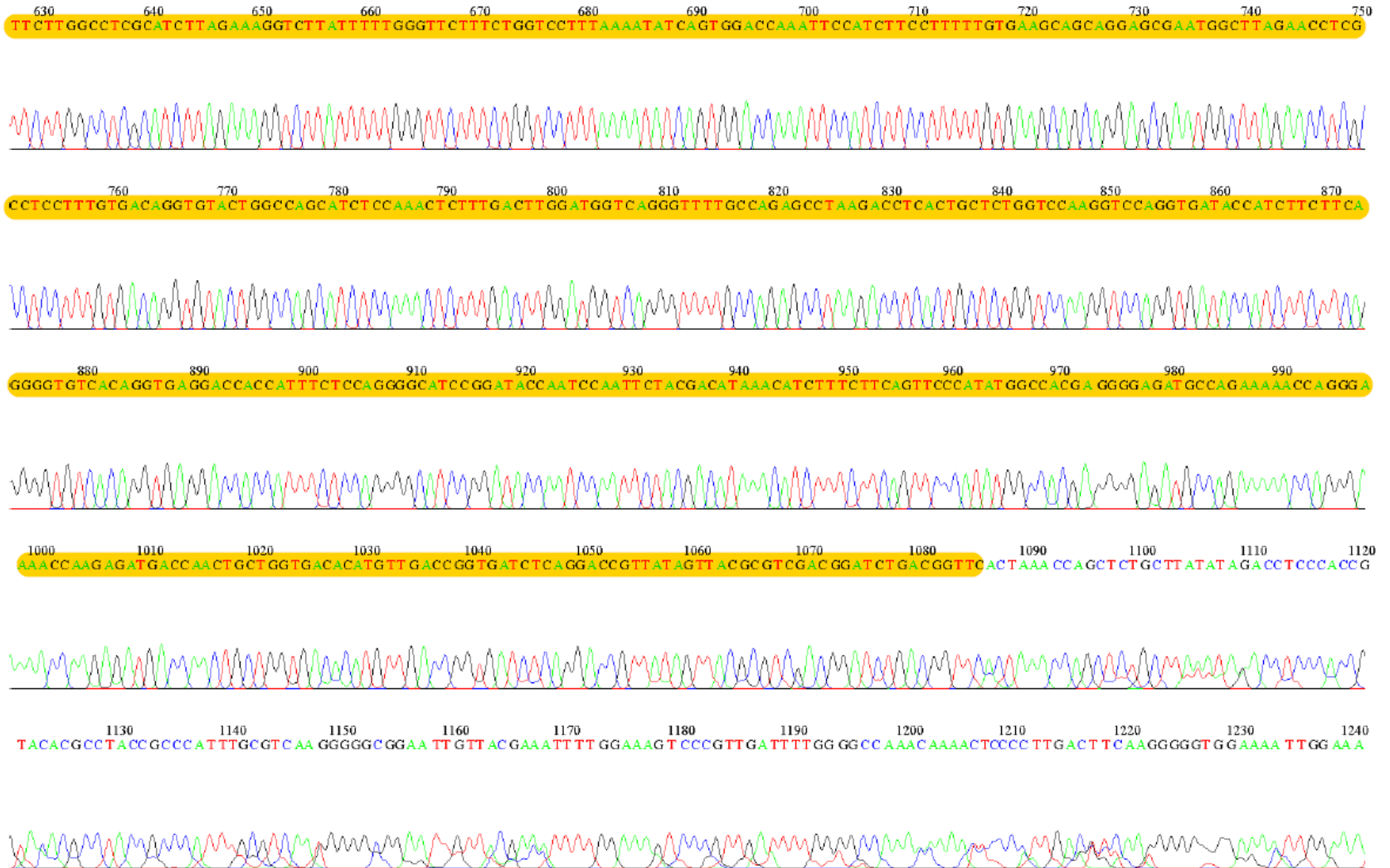


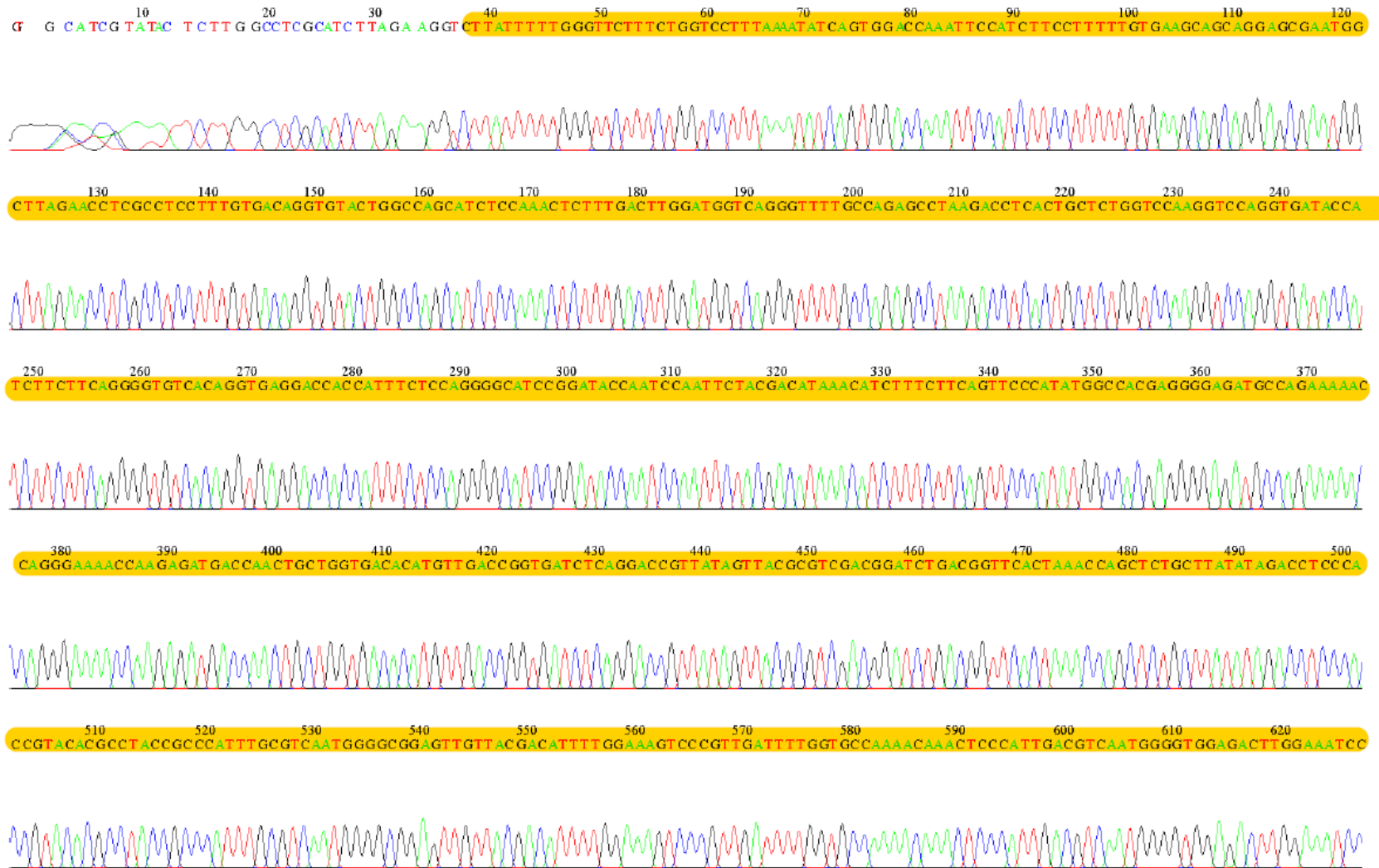
File: pIL12_12-6-20_Pcmv_5_cloning_site.ab1 Run Ended: 2020/7/18 4:51:30 Signal G:1396 A:1816 C:2010 T:1964
Sample: pIL12_12-6-20_Pcmv_5_cloning_site Lane: 85 Base spacing: 15.689623 1285 bases in 15493 scans Page 2 of 2



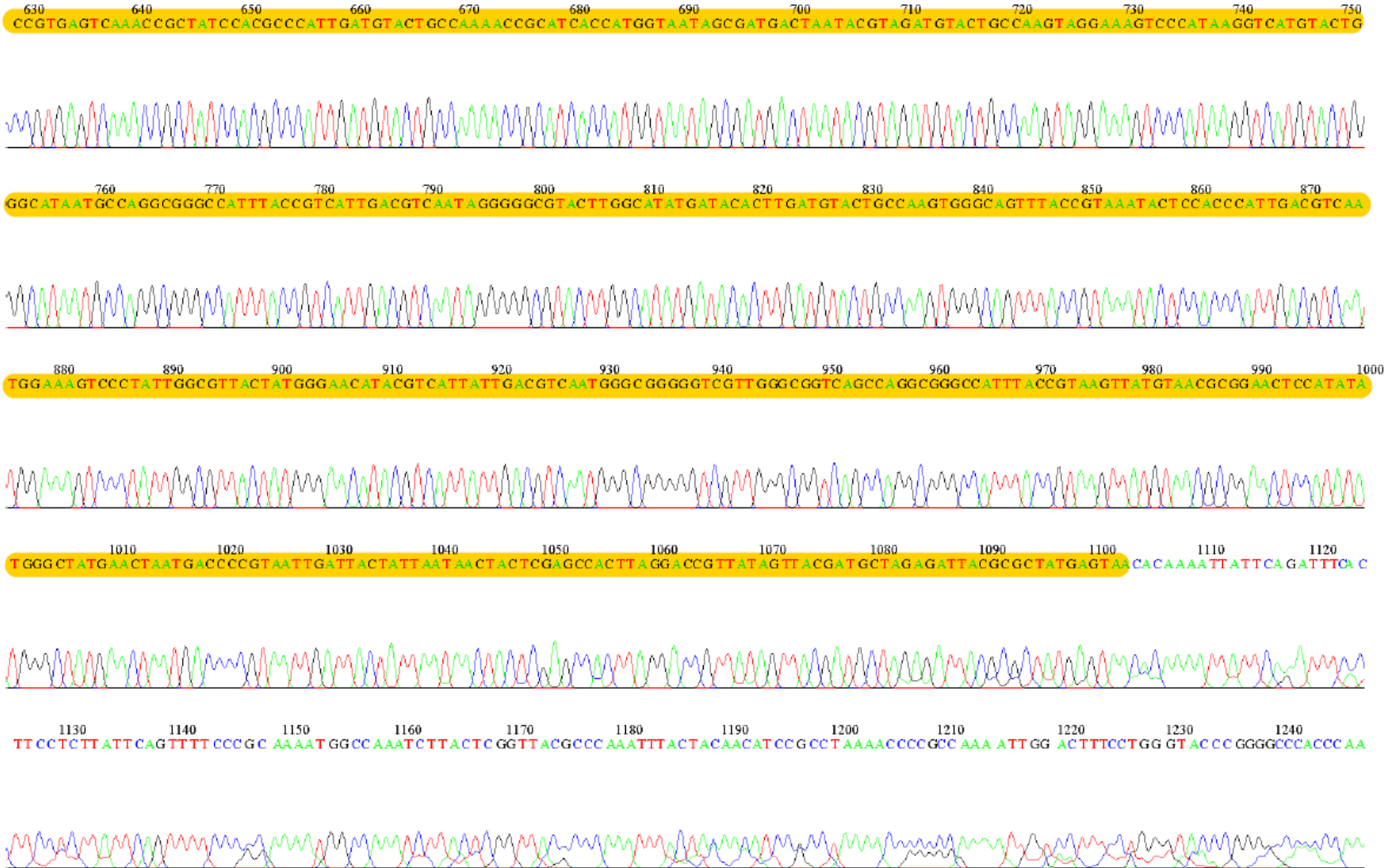


File: pIL12_12-6-20_Primer_1-IL12-3_ab1 Run Ended: 2020/7/18 4:51:30 Signal G:1663 A:2068 C:3139 T:2904
Sample: pIL12_12-6-20_Primer_1-IL12-3_ Lane: 91 Base spacing: 15.669835 1306 bases in 15771 scans Page 2 of 2





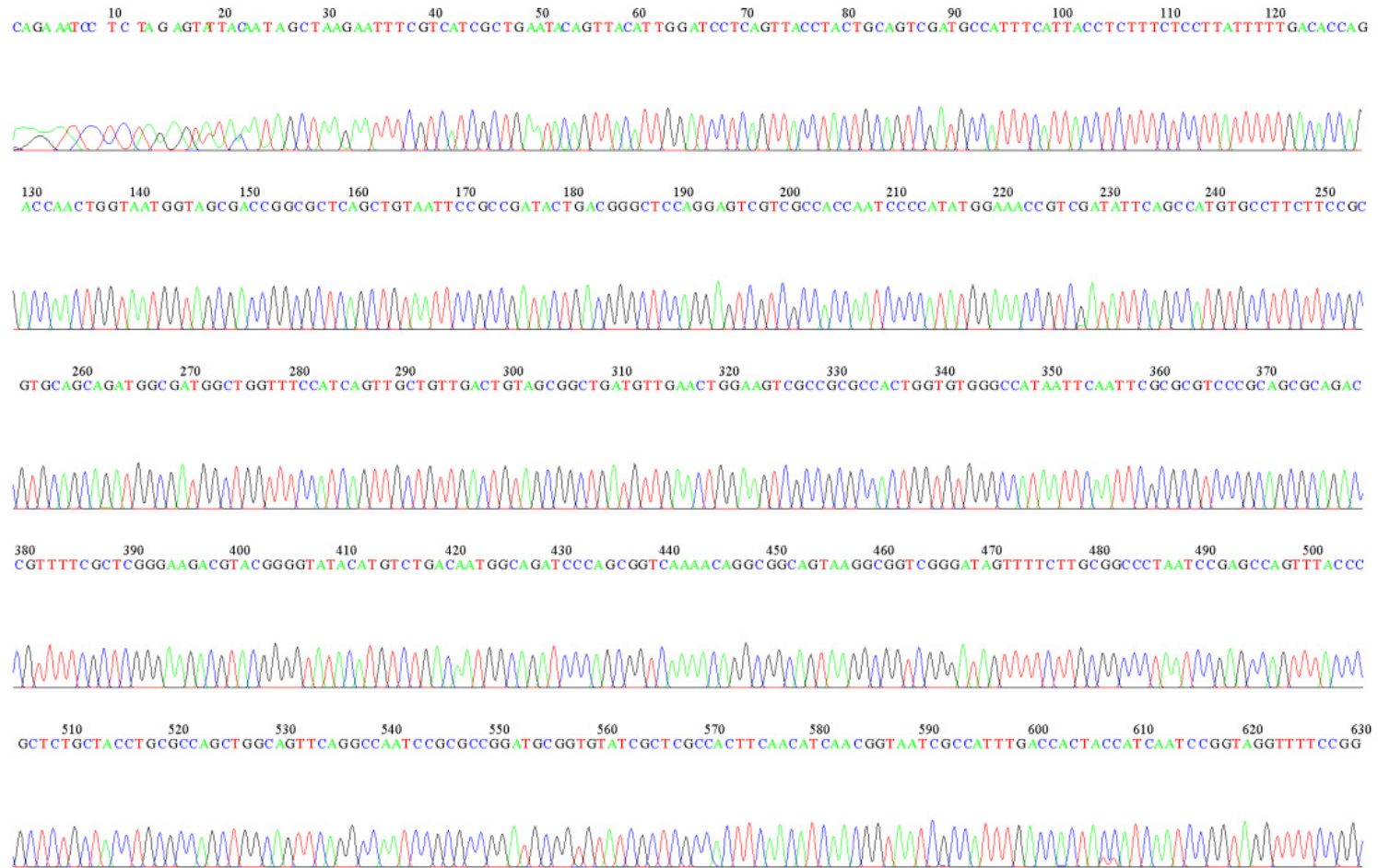
File: pIL12_12-6-20_Primer_2-IL12-3_ab1 Run Ended: 2020/7/18 4:51:30 Signal G:1467 A:2095 C:2663 T:2344
Sample: pIL12_12-6-20_Primer_2-IL12-3_ Lane: 89 Base spacing: 15.5928545 1300 bases in 15628 scans Page 2 of 2



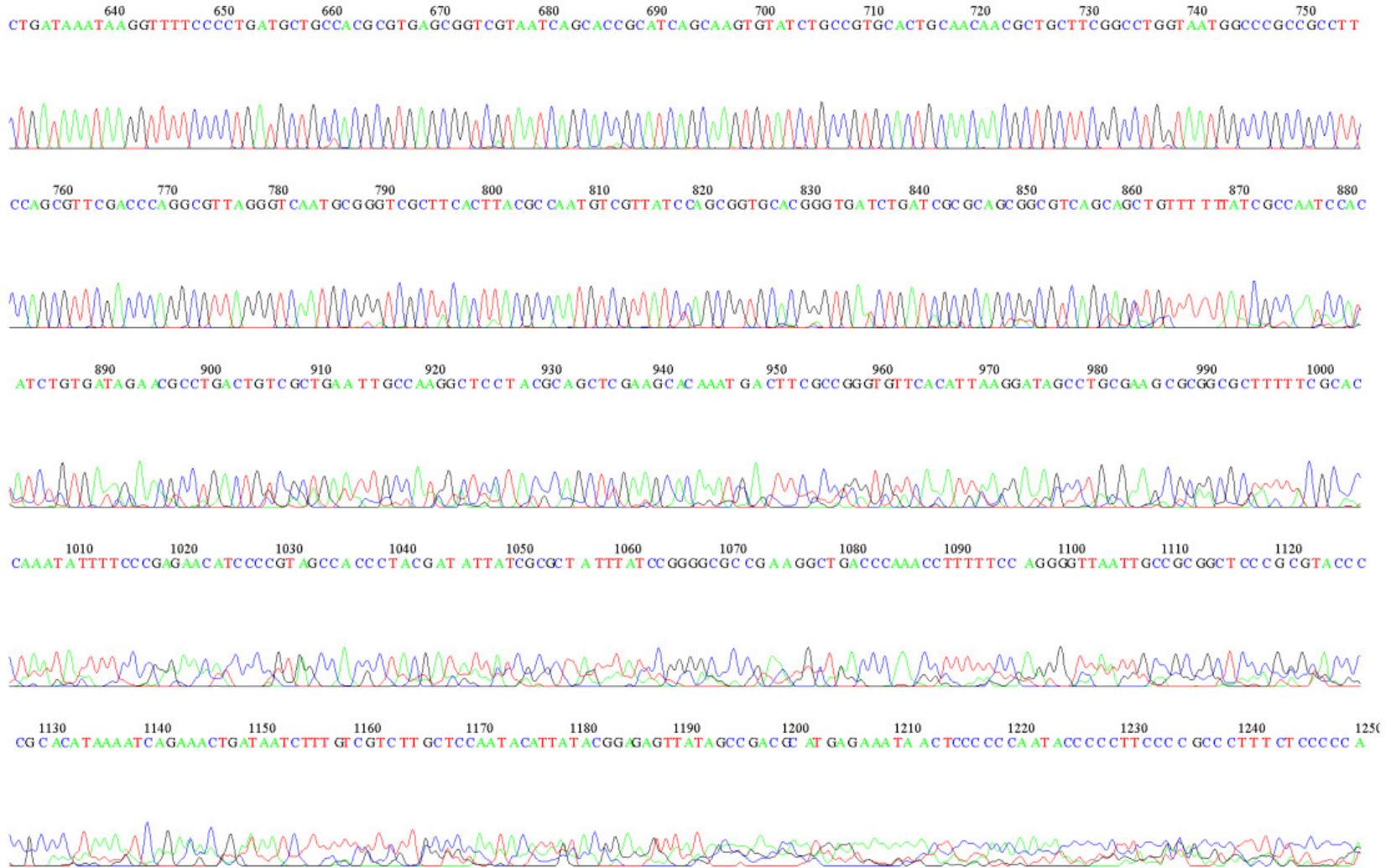
APPENDIX B: 2) Results of Sanger Sequencing of pAdenoX-lacZ recombinant plasmid



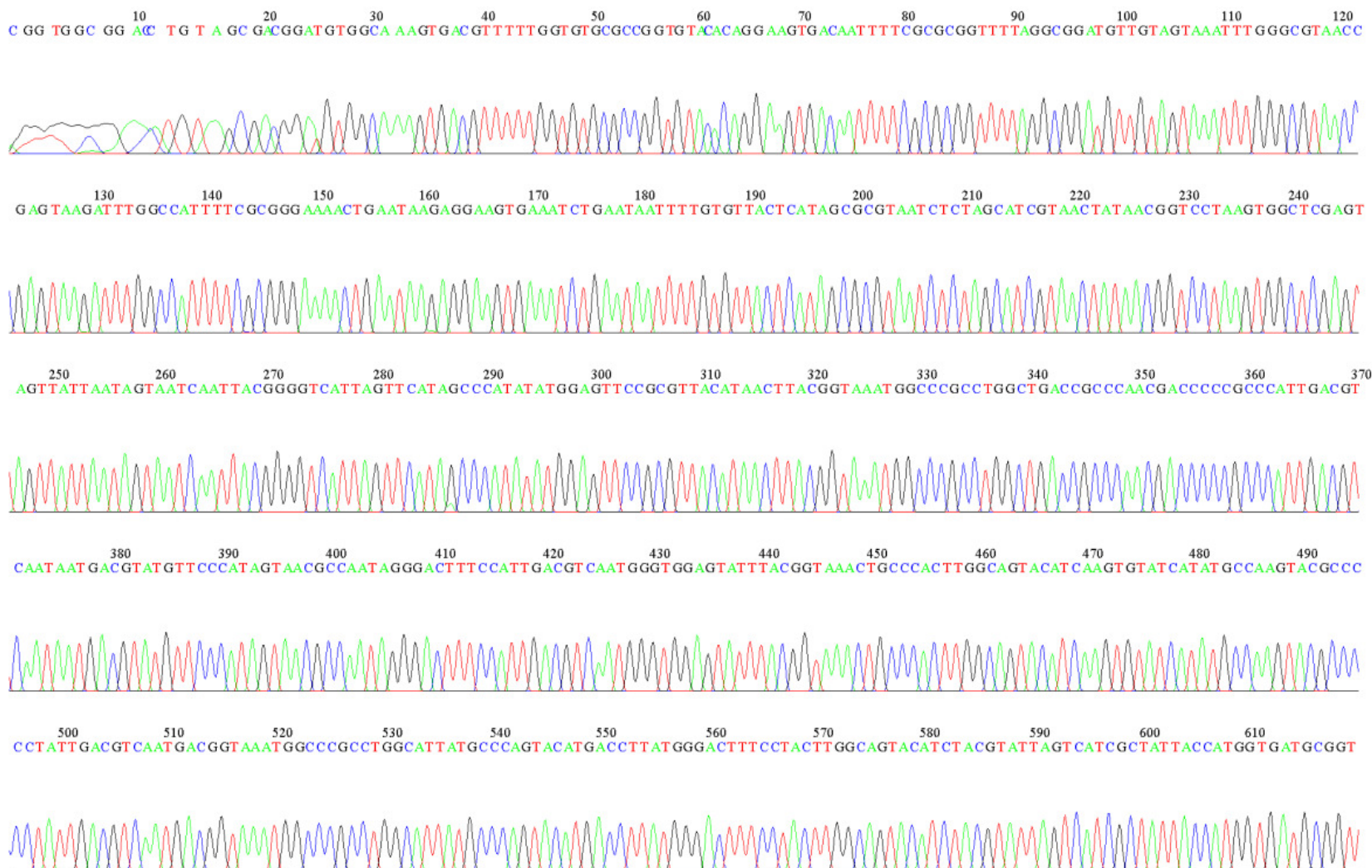
File: Ctrl_Pcmv_3_cloning_site.ab1 Run Ended: 2020/3/9 10:57:11 Signal G:1245 A:1003 C:1759 T:1368
Sample: Ctrl_Pcmv_3_cloning_site Lane: 28 Base spacing: 14.840175 1632 bases in 21025 scans Page 1 of 2



File: Ctrl_Pcmv_3_cloning_site.ab1 Run Ended: 2020/3/9 10:57:11 Signal G:1245 A:1003 C:1759 T:1368
Sample: Ctrl_Pcmv_3_cloning_site Lane: 28 Base spacing: 14.840175 1632 bases in 21025 scans Page 2 of 2

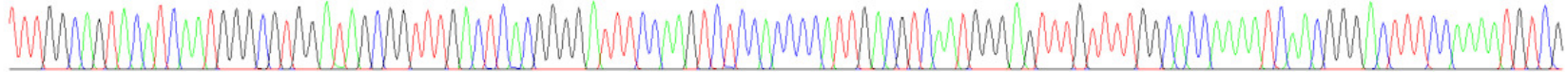


File: Ctrl_Pcmv_5_cloning_site.ab1 Run Ended: 2020/3/9 10:57:11 Signal G:1452 A:1496 C:1559 T:1708
 Sample: Ctrl_Pcmv_5_cloning_site Lane: 26 Base spacing: 15.582863 1541 bases in 18030 scans Page 1 of 2

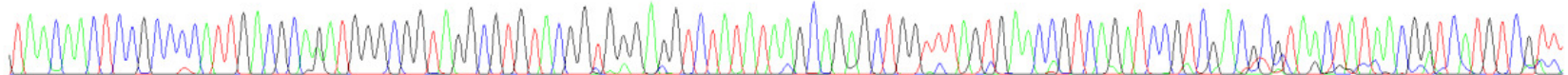


File: Ctrl_Pcmv_5_cloning_site.ab1 Run Ended: 2020/3/9 10:57:11 Signal G:1452 A:1496 C:1559 T:1708
Sample: Ctrl_Pcmv_5_cloning_site Lane: 26 Base spacing: 15.582863 1541 bases in 18030 scans Page 2 of 2

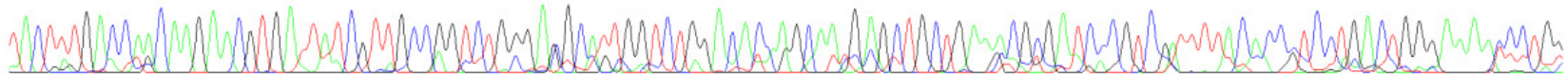
620 630 640 650 660 670 680 690 700 710 720 730 740
TTTGGCAGTACATCAATGGGCGTGGATAGCGGTTTGACTCACGGGGATTTCCAACTCTCCACCCATTGACGTCAATGGGAGTTTGTTTGGCACCAAAATCAACGGGACTTTCCAAAATGTCTG



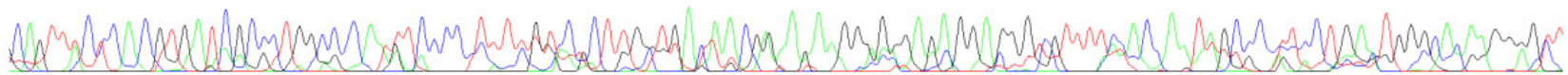
750 760 770 780 790 800 810 820 830 840 850 860
TAACAACTCCGCCTCATTGACGCAGATGGGCGGTAGGCCGTGTACGGTGAGAGGTCATATAAGCAGAGCTGGTTTAGTGAACCCGTGAGATCCGTGACGCGTAACATAACGGTCATGTCGTT



870 880 890 900 910 920 930 940 950 960 970 980
TACTTTGACCAACAAGAACGTGATTATCGTTGCCGGTCTGGAGGCATTGGTCTGGACAACGCAATGAGCTGCTGAAACGCGATCACGTCGTTTTACACCGTCCTGACTGGGAAAACCCTGG



990 1000 1010 1020 1030 1040 1050 1060 1070 1080 1090 1100 1110
CAGTTTCTCACTGATCGCCCTGGCGCAATTTCCCTTTTGTGCGCTTGCTGACAAAGAAAGGAGGGAGAGGAGGTTTCCACCATAAGCATTCTGACTGGGCACAAGGAGTT



1120 1130 1140 1150 1160 1170 1180 1190 1200 1210 1220 1230
TTTCGCGCAAAATCAGGCCAAAAAGCGGGGCATCCAAATAGTTTTGGGGTGGGGATTATCTGAAATCCATGAAATGGTTAGTTCCACCCAAAACGGGGAAAGGATAGGTACGTGTGGCCAA

